IOP Publishing Journal of Physics D: Applied Physics
J. Phys. D: Appl. Phys. **58** (2025) 133001 (40pp) https://doi.org/10.1088/1361-6463/adab7f

Topical Review

Experimental and theoretical advances in $Cu_2ZnSn(S,Se)_4$ solar cells

K G Rodriguez-Osorio[1], J A Andrade-Arvizu[2], I Montoya De Los Santos[3], J P Morán-Lázaro[1], M Ojeda-Martinez[1], F J Sánchez-Rodríguez[4], L A Sánchez-Hernández[1], L M Pérez[5], D Laroze[6], P Chandrasekar[7], S Routray[8] and Maykel Courel[1,*]

[1] Centro Universitario de los Valles (CUValles), Universidad de Guadalajara, Carretera Guadalajara—Ameca Km. 45.5, Ameca, Jalisco, C.P. 46600, Mexico
[2] Catalonia Institute for Energy Research (IREC), Jardins de les Dones de Negre 1, 08930 Barcelona, Spain
[3] Instituto de Estudios de la Energía, Universidad del Istmo, Santo Domingo Tehuantepec, Oaxaca, C.P. 70760, Mexico
[4] Facultad de Ciencias Físico-Matemáticas, Universidad Autónoma de Sinaloa, C.P. 80010 Culiacán, Sinaloa, Mexico
[5] Departamento de Ingeniería Industrial y de Sistemas, Universidad de Tarapacá, Casilla 7 D, Arica 1000000, Chile
[6] Instituto de Alta Investigación, Universidad de Tarapacá, Casilla 7 D, Arica, 1000000, Chile
[7] Department of Computer Science and Engineering, Faculty of Engineering and Technology, Parul University, Vadodara, Gujarat 391760, India
[8] Department of Electronics and Communication Engineering, SRM Institute of Science and Technology, Kattankulathur, Chennai 603203, India

E-mail: maykel.courel@academicos.udg.mx

Received 23 September 2024, revised 24 December 2024
Accepted for publication 17 January 2025
Published 30 January 2025

Abstract

$Cu_2ZnSn(SSe)_4$ (CZTSSe) semiconductor is quite promising to solar cell applications, recently achieving a new record efficiency of 14.9%. Despite theoretical works have shown that efficiencies higher than 20% are possible in this technology, there are some critical points that should be carefully solved by the scientific community. In this review, it is presented a critical analysis on the state-of-the-art of $Cu_2ZnSn(SSe)_4$ solar cells. First, we summarize advantages and disadvantages of most used vacuum and non-vacuum thin film fabrication methods, followed by the most important results in solar cell fabrication along with key factors in performance improvement. Furthermore, the future experimental outlook is also analyzed with a particular focus on kesterite material engineering and its grading band-gap engineering. Likewise, the experimental state-of-the-art of CZTSSe device fabrication, a non-typical contribution of this work to the literature it is the presentation and discussion of most important theoretical results on solar cells. A particular attention is paid to results concerning numerical and analytical approaches for the study of $Cu_2ZnSn(SSe)_4$ solar cells. Finally, theoretical results concerning the potential use of nanostructured CZTSSe solar cells for achieving efficiencies higher than that of the Shockley–Queisser limit are presented and discussed.

* Author to whom any correspondence should be addressed.

Keywords: kesterite solar cells, experimental data, theoretical data, state-of-the-art

1. Introduction

The second generation of solar cells consisting of thin films have become more and more attractive to the scientific community for its promise in reducing the cost per watt-peak of modules. In general, semiconductor materials from thin film solar cells have been described by direct band gap transitions, requiring lower material thicknesses in comparison to silicon solar cells. Within the family of thin film solar cells, kesterite-based compounds have gained significant attention. In particular, $Cu_2ZnSnSe_4$ (CZTSe), $Cu_2ZnSn(S,Se)_4$ (CZTSSe), and Cu_2ZnSnS_4 (CZTS) have been the traditional ones, whose properties have been extensively studied, with leading solar cell efficiencies of 12.5% [1], 14.9% [2], and 12.1% [3], respectively. These materials have shown properties comparable to other high-performance solar cell materials, such as $CuInGaSe_2$ (CIGS) [4], while being composed of abundant, less toxic, economical elements, and direct tunable band-gap values of 1.05–1.5 eV [5], resulting in absorption coefficients that surpass 10^4 cm^{-1} [6, 7]. These properties make them suitable for efficiently capturing solar radiation across a broad spectrum of wavelengths. The isoelectronic nature of kesterite in comparison to chalcopyrite results in various material features, such as crystal structure and tensor properties, being shared by kesterite and chalcopyrite semiconductors. This guarantees that same preparation procedures may be used, and photovoltaic devices can be successfully manufactured utilizing the same device design, structure, and processing processes as chalcopyrite solar cells [8].

Kesterite compound was identified as natural alloy in 1959 in the Këster deposit, in Russia [9, 10]. The CZTS quaternary compound was obtained by chemical transport with iodine in 1966, published by Nitsche *et al* [11]; previously, Hahn and Schulze had grown CZTSe single crystals for the first time in 1965 [12]. Nakazawa in 1988 reported the experimental process of a heterojunction diode based on CdSnO transparent conductive layer and CZTS layer, highlighting a voltage output characteristic of 165 mV for the first time, although its current output was practically null [13]. The initial *J*–*V* characteristics analysis of CZTS solar cell was reported until 1996; in this work, Katagiri *et al* demonstrated a voltage output and efficiency of 400 mV and 0.66%, respectively [14]. A similar efficiency was also reported by Friedlmeier *et al* by thermal evaporation in high vacuum, achieving 570 mV of open circuit voltage [15]. By 2001, Katagiri continued exploring distinct procedures in this material with not much progress, inside the variation of 522.4–735 mV in open circuit voltage (V_{oc}), 11.7–14.11 mA cm^{-2} in short-circuit current density (J_{sc}), 0.29–0.36 in fill factor (FF), with power conversion efficiency (PCE) values ranging 2.49%–2.62% [16, 17]. Before 2003, only these groups mentioned above had informed about the properties of CZTS photovoltaic solar cells. After that, the most relevant data was published by Katagiri in 2008, who showed J_{sc}, V_{oc}, FF, and efficiency values of 17.9 mA cm^{-2}, 610 mV, 0.62, and 6.77%, respectively [18], followed by significant advancement in the development of kesterite solar cells characterized by a new efficiency record around the 10%, reported by IBM [19]. CZTSSe solar cell efficiencies reported before 2020 had not been able to exceed the score of 12.6% in efficiency; one of these records was published by IBM and Solar Frontier for CZTSSe absorbers from hydrazine-based solution [20], with V_{oc} = 513.4 mV, J_{sc} = 35.21 mA cm^{-2}, and FF = 0.698 values. Due to the complexity involved in the study of the CZTSSe quaternary compound, multiple investigations about optical and electrical properties were necessary during next 10 years; in general, the optimization of the kesterite absorber material to enhance its light absorption and carrier transport properties has been one of the most analyzed areas [21–23]. After almost 10 years with no significant progress, the report of a new top certified efficiency of 13.8% for CZTSSe devices in 2023 renews the interest in this inorganic cell [24]. Recently, Li *et al* published the latest records [2]. In this work, a particular attention is paid to V_{oc} losses owing to abundant secondary phases and defects, resulting in a high crystalline CZTSSe material with a substantially lower defect density. The remarkable PCE of 14.9% with a V_{oc} of 576 mV in 2024 is the most actual data for kesterite devices. CZTSSe solar cell efficiencies behavior since 1996 to up to date are summarized in figure 1—data were taken from reference [25]. Figure 1 illustrates that an initial efficiency of 0.66% was promoted to 14.9%, demonstrating the potential use of this absorber compound in solar cells.

One of the principal reasons CZTSSe is deemed ideal for solar absorption lies in its capability for high efficiency alongside the utilization of earth-abundant, and non-toxic materials. This synergy effectively addresses the sustainability and environmental impact concerns associated with solar cell technologies. Moreover, CZTSSe adaptability to low-cost fabrication methods stands to significantly bolster the commercial viability of solar cells predicated on this material. Recent scholarly contributions underscore CZTSSe thin-film solar cells potentiality for heightened efficiency, focus on augmenting the material optoelectronic attributes, bolster its stability, and refine efficient fabrication methodologies. These investigations further emphasize the criticality of precise composition and property control in CZTSSe to fully leverage its capabilities for photovoltaic applications [26–28]. CZTSSe solar cells are increasingly recognized within the photovoltaic domain for their potential to achieve high efficiency while utilizing non-toxic and earth-abundant materials. This technology spans several critical areas: the specific composition and properties of the compound, diverse fabrication methodologies, performance metrics, developmental challenges, and avenues for future investigation. In this review, we present the state-of-the-art of CZTSSe solar cells from not only an experimental view but also from the theoretical perspective.

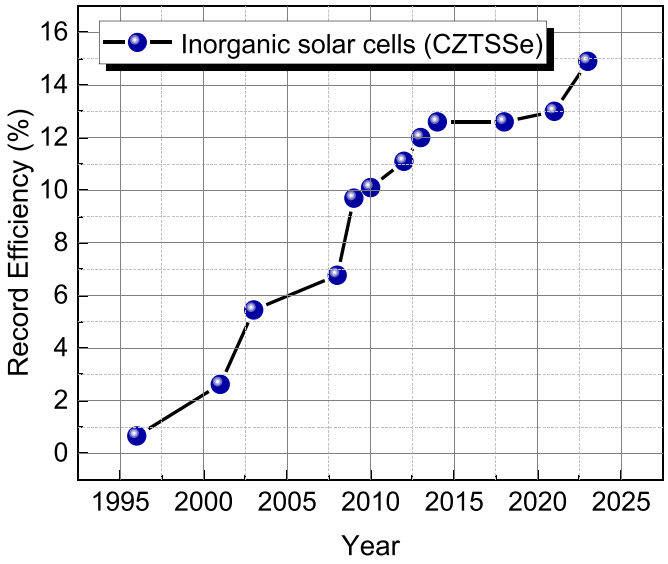

Figure 1. Record efficiencies reported for inorganic CZTSSe solar cells.

We take a glance to most important fabrication methods for kesterite material, followed by the discussion on results reported in kesterite solar cells with particular emphasis on key factors in performance improvement. Finally, numerical and analytical results on kesterite solar cell simulation are presented, where the potential application of kesterite nanostructures for achieving efficiencies higher than that of the Shockley–Queisser limit is discussed.

2. Thin film fabrication methods

The fabrication of CZTSSe thin films can be executed through various vacuum and non-vacuum methods as illustrated in figure 2, each contributing uniquely to the material final properties and the cells overall performance. Techniques such as sputtering and evaporation belong to typical vacuum processes for kesterite thin film deposition. These methods allow for precise control over the films composition and thickness but may require high capital investment for equipment. On the other hand, non-vacuum processes such as solution processing, electrodeposition and nanoparticle ink-based deposition are notable for their lower cost and potential for scalable production. They involve depositing a precursor solution on a substrate followed by annealing to achieve the desired CZTSSe phase. The advantages of both vacuum and non-vacuum processes are often considered in the called hybrid methods. Under the hybrid methods elements of both vacuum and non-vacuum processes are combined to optimize the fabrication process, i.e. sputtering a metallic precursor followed by a selenization process in a non-vacuum environment. There are several works available in the literature focused on discussing the different experimental approaches for kesterite thin film deposition. In this review, we summarized the most important ones along with their characteristics as presented below:

2.1. Vacuum processes

Vacuum co-evaporation is a pivotal fabrication technique for CZTSSe solar cells, involving the concurrent evaporation of Sn, Zn, Cu, S, and Se in a vacuum to deposit the thin film onto a substrate. This method is renowned for its precise control over the stoichiometry and composition of the thin film, a key parameter for solar cell efficiency optimization. However, the high processing cost associated with this technique is an important drawback. The potential use of co-evaporation technique for CZTS layer deposition was highlighted by Katagiri *et al* in 2009 [29]. The fabrication of kesterite solar cells by vacuum evaporation method on conducting substrates such as Cu, Ag, AZO, and FTO was also reported [30], suggesting that improvements can be obtained in solar conversion efficiencies with different substrate materials. Sputtering is also a potential technique for kesterite deposition. This technique allows the formation of uniform layers along large surfaces. It enables the deposition of intricate multicomponent films with exacting control over their composition and thickness qualities needed for optimizing CZTSSe solar cell performance. Nonetheless, sputtering encounters challenges, notably in maintaining a uniform distribution of elements. This necessitates the adoption of sophisticated strategies for fine-tuning deposition parameters and target compositions, ensuring the method effectiveness in fabricating high-efficiency CZTSSe solar cells. Gang *et al*, in 2016 achieved a 9.24% efficiency for CZTSSe solar cells fabricated via a green sputtering process without toxic gases, presenting a pathway towards the industrialization of environmentally friendly solar cells [31]. The impact of metal precursors through sputtering was evaluated by Kim *et al* in 2018, achieving significant efficiencies [32]. In the same year, it was published advancements and ongoing challenges in the synthesis of CZTS via sputtering and annealing, emphasizing the critical role of understanding material and device properties to overcome efficiency limitations [33]. A novel approach employing double-pressure sputtering technology was published in 2021, demonstrating the technique potentiality for enhancing CZTS solar cell performance through the reduction of interface state and deep level defects [34]. The advancements in sputtering technique for kesterite solar cell fabrication was recently reported [35]. These references present relevant information on the role of vacuum deposition techniques on kesterite material and solar cell properties.

2.2. Non-vacuum processes

Among the different non-vacuum processes for kesterite thin film deposition, electrodeposition stands for its cost-effectiveness and scalability. Practical issues of electrodeposition process such as controlled composition and deposit morphology were addressed by Ge & Yan, culminating in a CZTSSe device efficiency of 7.4% [36]. The role of electrolyte pH in managing hydrogen evolution during Cu–Zn–Sn co-electrodeposition was studied by Agasti *et al*, achieving dense and compact CZTS films with optimal stoichiometry [37]. An improved interface in CZTSSe solar cells has been reported

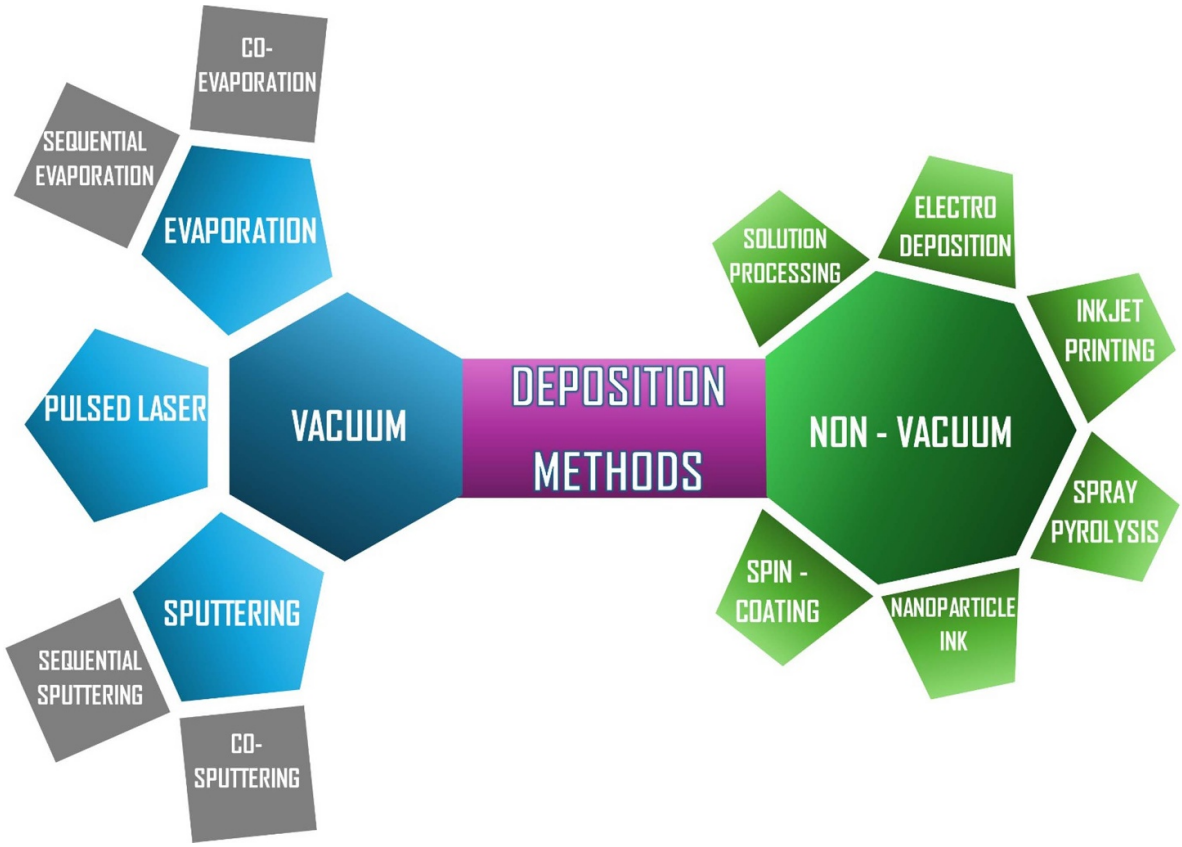

Figure 2. Deposition methods commonly used for CZTSSe thin film fabrication.

via a thermal annealing process on co-electrodeposited layers, resulting in the reduction of the voltage deficit issue caused by interface recombination (IR). Applying a thermal annealing at 200 °C significantly enhanced the device's efficiency by 32%, from 7.11% to 9.40%. This improvement is attributed to increased conductivity and reduced nonradiative recombination due to Cd ion diffusion, suggesting thermal annealing potential in advancing CZTSSe solar cell performance and its applicability to other fabrication processes [26].

Improvements in CZTSSe solar cell efficiency deposited by electrodeposition method have been reported by using cesium treatments. The incorporation of cesium into kesterite material favors grain boundary passivation and reduces non-radiative recombination losses. Recently, Hwang *et al*, discussed the effectiveness of cesium treatment during the electrodeposition process for promoting CZTSSe solar cell efficiency [38]. A detailed review on CZTSSe solar cells processed by electrochemical deposition (ED) was presented by Hwang *et al* [39], where deposition qualities such as environmental friendliness and cost-effectiveness are highlighted. However, rough morphology and phase inhomogeneity are important drawbacks, resulting in kesterite solar cell efficiencies lower than 10%. The exploration of alternative external stimuli such as ultrasonication, the continue exploration on cesium treatments, the development of advanced electrolyte compositions and the integration of real-time monitoring system are highlighted as future research directions for electrodeposited-CZTSSe solar cell improvement. The attention to these opportunity areas would push this technology to commercial viability and environmental sustainability.

Solution processes, such as spin-coating, inkjet printing, and chemical bath deposition, have gained attention for CZTSSe solar cell fabrication because of their low cost, simplicity, and potential for large-scale production. These methods involve the deposition of precursor solutions containing Cu, Zn, Sn, S, and Se onto a substrate, and a subsequent thermal annealing for CZTSSe thin film obtention. However, achieving high efficiency and reproducibility with solution processes can be challenging, and the control over the film morphology and impurity incorporation is critical for device performance. Recent research efforts have focused on optimizing the precursor solution formulations, exploring new solvent systems, and developing novel post-deposition treatments to enhance CZTSSe quality. Advancements in solution processing through bismuth doping and optimized selenization was reported by Zhao *et al* [40], improving the CZTSSe device efficiency to 7.27%, in comparison to the traditional ones with an efficiency of 5.3%. The enhancement of CZTSSe solar cell efficiency was reported by Wei *et al* in 2024, by adding HCl to the precursor solution to improve material crystallinity for better solar cell performance [41], achieving a 14% efficiency. This result constitutes an important step for obtaining superior crystallinity and fewer defects in kesterite material, emphasizing the role of chemical modulation for

high solar cell efficiency. Kesterite thin film deposition based on nanoparticle ink is a novel proposal for processing CZTSSe devices. A solar cell with 6.2% efficiency starting from CZTS nanoparticles ink and eco-friendly solvents was presented by Zhang *et al* in 2019 [42]. In this work a particular attention is given to film crystallinity and grain growth, pointing out the significance of non-toxic processes in achieving high efficiency kesterite devices. Recently, performances of 9.3% and 9.4% in CZTSSe solar cells were reported by a hydrazine-free approach [43]. By the structural and compositional studies on the nanoparticle inks and their result in solar cell processing, the authors proposed this method as suitable for obtaining scalable devices.

The key achievements and challenges in vacuum and non-vacuum approaches for kesterite thin film deposition are summarized in table 1. In particular, the precise control of film composition, stoichiometry, crystallinity and secondary phases are general key accomplishments of the vacuum techniques, while non-vacuum techniques in general are low cost, simple, and scalable. Among all vacuum and non-vacuum techniques, solution processing is leading the highest efficiencies reported for kesterite solar cells. Furthermore, table 1 also demonstrates that vacuum techniques such as co-evaporation and sputtering are heading the best efficiencies under vacuum conditions.

Properties of kesterite material such as urbach energy, defect energy, defect concentration, defect capture cross-section, carrier concentration, minority carrier lifetime, minority carrier diffusion length, carrier mobility, crystallite size and lattice strain for representative vacuum and non-vacuum techniques are summarized in table 2. The lowest urbach's energy values are found for spray pyrolysis and electrodeposition techniques while sputtering and spin-coating retain the lowest defect densities. The highest crystallite sizes, the lowest lattice strain, and the lowest defect concentrations have been reported for kesterite deposited by spin-coating, which is in general in good agreement with the highest efficiencies achieved by this technique [2, 24]. It is also observed that sputtering and electrodeposition are heading the best mobility values for vacuum and non-vacuum techniques, while thermal evaporation and spin-coating present the highest values of minority carrier diffusion length. In addition, vacuum techniques present the biggest values of minority carrier lifetime.

3. Solar cell performance

CZTSSe solar cells have made remarkable strides, achieving efficiencies over 14%, highlighting their potential in photovoltaic applications. This progress is attributed to their capability to form high-quality kesterite structures with minimal secondary phases and optimized properties for solar absorption, positioning CZTSSe as a formidable competitor to established CIGS and CdTe technologies. This advancement showcases CZTSSe growing importance in the competitive landscape of photovoltaics. Recently, Shi *et al* reported a study focused on the optimization of CZTSSe solar cells, addressing the challenges associated with deep defects that hamper efficiency [77]. By identifying the dominant deep defect exhibiting donor characteristics, the research proposes a novel elemental synergistic alloying approach. This strategy aims to facilitate the kinetics of cation exchange by weakening the metal-chalcogen bond strength, thus significantly reducing charge losses and achieving an improved cell efficiency of over 14.6%. This advancement not only enhances CZTSSe solar cell performance but also opens avenues for defect identification and regulation in multinary inorganic compounds. CZTSSe solar cells, despite having lower efficiency levels than CIGS and CdTe technologies which exceed 20%, offer significant advantages in terms of environmental impact and material availability. The use of abundant and non-toxic materials it positions CZTSSe as an alternative semiconductor with great potential to cost-effectiveness devices. The incorporation of Ge into CZTSSe was recently studied, demonstrating the role of ZnSe layer formed on the metal during selenization, resulting in a more effective interface for carrier collection, thereby increasing device efficiency [99]. It is emphasized the necessity of precise control on selenization conditions to solar cell optimization. On the other hand, a recent review paper on Cd-free solar cells highlighted the necessity of an environmentally friendly buffer material to increase device performance [100]. This review paper highlights the last progress in identifying suitable Cd-free buffer materials like $Zn_{1-x}Sn_xO$ and Zn(O,S) for CZTS and CZTSSe, respectively, and discusses promising results with TiO_2.

On the other hand, a novel strategy to enhance CZTSSe device efficiency by modifying the sequence addition of metal ion in the solution was proposed, achieving an efficiency over 12% [78]. By employing a specific sequence (S─Sn─Cu─Zn), the study enhances absorber quality, leading to large grain growth, reducing defects, and improving interface quality. This method significantly increases J_{sc} and FF, offering insights into the crystallization mechanism of kesterite materials and directions for further material quality enhancement. The incorporation of Eu ions into CZTSSe solar cells was performed, aiming to overcome the limitations of short carrier lifetimes on V_{oc} and efficiency [79]. The incorporation of Eu results in the absorber quality improvement, having larger grains and less defects, thereby increasing solar cell efficiency from 10.6% to 13.3%, as a result of the carrier lifetime promotion. This type of studies opens up new opportunities for lanthanide cation doping for achieving higher CZTSSe solar cell efficiencies.

A new review paper has critically examined CZTSSe solar cells obtained by a solution process, focused on solvent and precursor selection, device structure design, layer optimization, and defect regulation [101]. It highlights the gap between current CZTSSe cell efficiencies and their theoretical potential, stresses the importance of absorber layer quality for performance enhancement. The review culminated in proposing future directions for research to attain high-efficiency CZTSSe cells, providing deep analyses on advancements and challenges in the field. Another interesting proposal for kesterite device promotion it is Sb doping to favor growth and suppress

Table 1. Key achievements and challenges in vacuum and non-vacuum pathways for the development of CZTSSe thin-film solar cell technologies.

Route	Technique	Key accomplishments in thin film	Challenges	Key outcomes in devices	References
Vacuum	Co-evaporation	Precise control of film composition and thickness; high control of stoichiometry; crystallinity and minimal secondary phases.	High capital investment; requires precise temperature and pressure control.	Efficiencies up to 11.6% in CZTSe achieved by IBM; exploration of various uniform conducting substrates (e.g. Cu, Ag, AZO, FTO).	[29, 30]
	Sputtering	Scalable for large-area deposition; compatible with industrial setups for large-area applications; environmentally friendly options available (e.g. avoiding toxic gases).	Maintaining uniform distribution of elements; requires advanced target compositions.	Efficiencies over 9%; green methods; development of double pressure sputtering technology to reduce interface states and deep level defects.	[31, 32, 34]
	Pulsed laser deposition	Precise stoichiometric control; suitable for complex materials; allows fine-tuned deposition of ultra-thin films.	Micro-particle ejection and non-uniform film growth; requires optimization of annealing conditions.	Achieved ∼5.2% efficiency with an ultra-thin (<450 nm) absorber. Enhanced sulfurization processes and pressure control reduced surface defects, improving grain size and device performance.	[44, 45]
Non-Vacuum	Solution processing	Cost-effective and scalable; suitable for roll-to-roll production; offers flexibility in precursor composition.	Sensitive to precursor purity; challenges with impurity incorporation and reproducibility.	Efficiencies >14% achieved using cesium doping to improve grain boundaries and defect passivation.	[41]
	Electrodeposition	Low cost, scalable, and capable of fine-tuning stoichiometry through electrolyte control.	Phase purity issues; requires post-deposition annealing for crystallinity enhancement	Achieved ∼9.4% efficiency using thermal annealing and Cd diffusion for improved conductivity; optimization of electrolyte pH for managing hydrogen evolution.	[37, 39]
	Spin coating	Simple and cost-effective setup; ideal for small-scale production and prototyping.	Limited scalability; uneven film morphology at larger scales.	Optimized precursor solutions led to ∼8% efficiency; post-annealing improved film crystallinity and uniformity.	[40]
	Inkjet printing	Highly customizable; minimal material waste; ideal for research on device geometry.	Poor reproducibility; requires advancements in ink formulations to reduce roughness and defects.	Efficiency improved to ∼7% through enhanced precursor formulations and bismuth doping.	[42]
	Nanoparticle ink-based	Eco-friendly and scalable approach, avoiding hazardous solvents and minimizing environmental impact.	Challenges in film uniformity and sintering.	Efficiencies up to 9.4% achieved via hydrazine-free approaches.	[43]
	Spray pyrolysis	Eco-friendly, cost-effective, versatile, and scalable technique	Issues related to film uniformity, precursor decomposition, and the reproducibility of material properties	Efficiencies higher than 10% achieved by tuning S/(S + Se) compositional ratio	[46–49]

Table 2. Physical properties of kesterite material deposited by representative vacuum and non-vacuum techniques.

Deposition technique	Urbach energy (meV)	Defect energy (meV)	Defect concentration (cm^{-3})	Defect capture cross-section (cm^2)	Carrier concentration (cm^{-3})	Minority carrier lifetime (ns)	Minority carrier diffusion length (μm)	Mobility ($cm^2\ Vs^{-1}$)	Crystallite size (nm)	Strain	References
Sputtering	33, 37–44	38–56, 100–150, 241–244, 311	1.11×10^{15}–2.66×10^{16}	—	1×10^{15}–8.16×10^{17}	0.89–8.0	0.19–0.35	0.2–30	32–37	0.0037–0.0043	[34, 50–59]
Thermal evaporation	4–27, 34–90	20, 110–160, 177–230, 310–330	1.3×10^{17}–2.1×10^{17}	—	1×10^{13}–1.39×10^{19}	2–7.8	0.35–2.1	0.6–12.9	16–67	0.0007–0.009	[60–69]
Electrodeposition	28–33	85–87, 122–127	—	—	4×10^{15}–5.87×10^{19}	—	—	3.79–79.25	6–62	0.00381–0.0058	[38, 70–76]
Spin coating	21–27, 30–47	22, 50–99 119–177, 270–327, 362, 500–535	2.53×10^{12}–3.22×10^{16}	3.61×10^{-21}–6.92×10^{-18}	9.2×10^{14}–6.24×10^{18}	0.2–6.58	0.203–1.38	0.22–5.99	25–73	0.00049–0.00072	[40, 41, 77–90]
Spray-pyrolysis	15–22	47–85, 98–144, 148–211, 258–272, 367, 476	7.01×10^{14}–2×10^{19}	4.9×10^{-22}–9.4×10^{-19}	4.0×10^{15}–7.0×10^{18}	0.16–2.34	0.11–0.171	0.6–29	22–43	0.0032–0.0063	[46, 91–98]

defects [102]. This study introduced an Sb doping strategy to enhance CZTSSe solar cells by replacing Sn with Sb via solution treatment. Sb doping promotes grain growth, results in dense films with larger grains and reduced defects. The optimal Sb doping level increased the V_{oc} and PCE significantly, showcasing the potential of Sb to improve CZTSSe device efficiency. Despite the important advancements reported in CZTSSe solar cells, that make this technology competitive to the traditional existing ones, it is important to keep working on remaining opportunities areas—material and device challenges—for solar cell improvements by proposing innovative strategies.

Results presented in this section on recent reports on CZTSSe solar cell fabrication are summarized in table 3 for comparison. It is note that most important recent reports that present a significant efficiency enhancement in kesterite solar cells are mainly focused on improving the issue of poor crystalline quality associated with defect formation and the presence of small grains during crystal growth. In particular, the incorporation of Ag, Ge, Cd, Eu, and Sb elements is demonstrated to be attractive proposals to promote device performance. Consequently, further studies on these directions are needed.

3.1. Key factors in performance improvement

The path for boosting CZTSSe solar cell efficiency involves multifaceted research efforts. The chemical composition optimization, tailoring the stoichiometry of CZTSSe to minimize defects and non-radiative recombination losses is an important step. Zhao *et al* in 2024 have demonstrated high efficiencies in kesterite devices processed by solution method by suppressing surface and bulk defects [80]. This study presents an innovative approach to enhance CZTSSe solar cell efficiency by introducing a thin ammonium sulfide layer for simultaneous interface and bulk defect passivation. This method optimizes absorber surface quality, transforms detrimental defects into shallower beneficial ones, and significantly reduces carrier recombination, leading to increased carrier lifetimes and device efficiency. The authors demonstrated by a sulfurization annealing an efficiency increase to 13.19% in CZTSSe solar cells. Areas such as buffer/absorber interface quality and the necessity of advanced techniques such as Atomic Layer Deposition (ALD) for interface engineering, band-alignment engineering for better charge carrier transport, appropriate buffer layers, and device architecture stand for critical topics in CZTSSe solar cells for efficiency improvements. These opportunities areas for CZTSSe solar cell efficiency improvement are described below:

(a) **Absorber/buffer interface quality:** The enhancement of interface quality is a required area for promoting CZTSSe device performance. This objective could be accomplished by incorporating very thin insulating layers at the junction to reduce interface defects. On the other hand, since ALD can help in the creation of interfaces with high quality at the same time it guarantees a precise deposition of material, this technique is quite promising for improving interfaces, reducing thereby carrier recombination, and consequently increasing solar cell efficiency.

(b) **Band-alignment engineering:** Band alignment is a critical factor for carrier transport and separation. The appropriate selection of buffer layers with electron affinities and band gap that favor electrons and holes transport is crucial for the best efficiencies. It is pointed out that ALD can be also used to improve band alignment between buffer and CZTSSe layers.

(c) **Appropriate buffer layer:** Buffer layers should have relatively high band-gap to guarantee photons get absorbed at the CZTSSe material at the same time it facilitates photogenerated carriers separation and facilitating carrier transport through the appropriate band alignment, thereby minimizing non-radiative recombination losses. Zn(O,S), TiO_2 and ZnSnO have been presented as potential proposals for replacing CdS layer since these materials fulfill the required characteristics mentioned above.

(d) **Device architecture:** In order to guarantee optimal light absorption and carrier transport, attention should be paid to the layout and stacking order of layers conforming solar cells. Besides, innovative proposals that result in higher photon absorption and better carriers transport and their collection, such as the use of nanostructures and tandem structures can significantly promote device efficiency.

Although specific references from the recent search are scant, ALD is expected to enhance CZTSSe solar cell efficiency supported by its successful application in CIGS and perovskite solar cells. The application ALD to deposited buffer layers in kesterite solar cells has shown promising results. An efficiency of 8.6% was achieved in CZTSSe solar cell by using ZnSnO buffer layer deposited by ALD, reporting an accurate control over the buffer layer composition and thickness [103]. By optimizing the ALD process, the CZTSSe device performance was significantly improved, resulting in an 8.60% efficiency, surpassing the reference CdS/kesterite solar cell. This achievement is attributed to an improvement in band alignment at the buffer/absorber interface. The surface passivation of CZTS solar cells was successfully reported by the incorporation of hydrogen from Al_2O_3 layer deposition by ALD [104]. Better solar cell efficiencies were reported with higher hydrogen concentrations incorporated to the CdS/CZTS interface by changing Al_2O_3 layer thicknesses. Particularly, three ALD- Al_2O_3 cycles resulted in enhanced V_{oc} and in an increased efficiency to 8.08%, due to CZTS surface passivation by hydrogen, constituting this proposal a new opportunity area to be explored. After this work, results on semitransparent CZTSe solar cells by using V_2O_x as hole transport layer deposited by ALD were published [105], informing a solar cell efficiency of 3.9%. Hydrofluoric acid dips were used as a cleaning method to improve CZTSe surface, emphasizing the potential of V_2O_x for high efficiency in semitransparent or bifacial solar cells. The ALD technique was also introduced to depositing ZnSnO thin films to be

Table 3. Brief summarize of recent reports (challenges, issues, proposal and key outcomes) on CZTSSe solar cells.

Current challenges	Issues	Proposals to solve the problem	Key outcomes	Year	References
Defect control (Identification and regulation)	Sn_{Zn} antisite deep defect with donor characteristics is identified as responsible for charge loss in kesterite solar cells.	Ag, Ge and Cd have been added to regulate the CZTSSe fabrication, facilitating the cation exchange in the crystallization process.	PCE = 14.6% (certified at 14.2%)	2024	[77]
Precise control of selenization conditions	Negative impact of small grains, defects and the detrimental effect of grain boundaries	Incorporating Ge during the selenization process at different annealing time points	Larger grain sizes and reduced grain boundaries (PCE = 10.69%)	2024	[99]
Kesterite material quality	Unsatisfactory material quality due to poor crystallization and various defects	The use of an optimal ion addition sequence consisting of S─Sn─Cu─Zn	Enhanced absorber and interface quality, with large grains and reduced defects (PCE = 12.15%)	2024	[78]
Kesterite material quality	Poor crystalline quality (defects formation and small grains) resulting in short carrier lifetimes	Doping with Ag and Eu elements	The formation of Cu_{Zn}, Cu_{Sn} and Sn_{Zn} defects is suppressed, resulting in high-quality absorber (PCE = 13.3%)	2024	[79]
Kesterite material quality	Poor crystalline quality (defects formation and small grains)	Doping with Sb element	Sb doping promotes grain growth, it results in dense films with larger grains and reduced Sn_{Zn} defects and $[2Cu_{Zn} + Sn_{Zn}]$ defect clusters (PCE = 6.82%)	2023	[102]

used as n-type buffer material of CZTSSe devices [106]. The Zn/(Zn + Sn) composition ratio impact on device performance was studied. An optimal ratio of 0.76 led to a cell efficiency of 8.54%, demonstrating significant improvements in device parameters over conventional CdS buffers. The uniform ALD process enhanced cell-to-cell uniformity, indicating ZnSnO potential for CZTSSe device processing. In a recent report, a novel dual treatment strategy is presented to overcome recombination limitations associated to Cu_{Zn} and Sn_{Zn} defects [91]. This approach combines Ag-alloying within the absorber's bulk to significantly mitigate deep defects and employs Al_2O_3-ALD to achieve defect passivation and a well-defined heterojunction. This synergistic method not only enhanced all device parameters but notably increased the FF, attributed to the minimized element intermixing at the heterojunction, culminating in a remarkable efficiency of 13.33% without requiring an antireflection coating. This work pointed out the need for addressing simultaneous improvements at kesterite/buffer interface and kesterite bulk for achieving high solar cell efficiency.

The most important results concerning the application of ALD in kesterite solar cells are summarized in table 4. So far, it has been demonstrated that ALD technique can provide better absorber/buffer band alignment at the same time it can contribute to surface passivation. Therefore, this technique should be further explored in the kesterite solar cell processing.

3.1.1. Material and interface quality issues. Producing consistent and high-quality CZTSSe thin films remains a prominent challenge, mostly due to the material's sensitivity to processing conditions and its tendency to form undesired secondary phases. SnS phase impact on CZTS was analyzed by Ren *et al* in 2017 [107]. The authors demonstrated by different techniques that SnS accumulates at surfaces of CZTS layers after thermal annealing under non-stoichiometric conditions. However, SnS formation at the rear was identified as beneficial, likely due to the interface passivation. This insightful analysis not only deepens understanding the secondary phases impact on kesterite devices, but also opens new avenues for interface engineering to enhance photovoltaic performance. Later, Gao *et al* delved into the critical role of interfaces in CZTSe solar cells, which, despite being a potential proposal, lags behind CIGS solar cell efficiency, primarily because of recombination at interfaces [108]. The paper summarizes the state of research focused on understanding and improving interfacial properties through various methodologies. Key areas of progress include optimizing buffer/absorber interface band alignment, and managing the thickness of $MoS(e)_2$ layer formed at the Mo/absorber interface, employing strategies for the passivation of both rear and front interfaces. Additionally, it discusses the importance of etching secondary phases to enhance device performance. The review highlights the comprehensive efforts and strategies employed to tackle interfacial challenges, offering insights into advancing CZTS(e) solar cell efficiency closer to their theoretical potential. The progress and challenges in the CZTSSe solar cell fabrication were presented in a review paper [109], where phase instability, secondary phases formation and material defects were pointed out as factors limiting efficiency. In this review, an in-depth analysis on CZTSSe processing techniques, buffer layer, device structure, secondary phases, and defects was presented. On the other hand, in 2021 a comprehensive review on defects at interfaces and bulk in CZTSe material was presented [110], pointing out the dominant role of bulk defects, back interface voids, and dislocation defects at the front interface on solar cell degradation. The crucial role of composition in reducing defects in CZTSSe devices was discussed in the same year [81]. A particular attention is paid to secondary phases, IR and bulk defects to mitigate V_{oc} deficit of CZTSSe devices. A methodology for thin film quality optimization was presented, resulting in an absorber free of secondary phases and with low concentration of band tailing and interface defects, thereby enhancing photovoltaic performance. A PCE of 11.5% was reported for such optimized CZTSSe device. The CZTSSe solar cell improvement by a thermal annealing process was analyzed by Pakštas *et al* in 2022 [111]. The authors were able to obtain CZTSSe films with low structural disorder and defect density when annealed at 420 °C. These results remarked the relevancy of the annealing temperature in achieving good crystallinity in CZTSSe thin films.

3.1.1.1. Voltage deficits. Voltage deficit is among the main critical challenges for boosting CZTSSe device efficiency. Figure 3 summarizes the most important factors contributing to the V_{oc}-deficit. In particular, kesterite material and absorber/buffer interface quality constitute the most important V_{oc} limiting factors. Experimental conditions for materials deposition and their subsequent thermal annealing are directly associated with the quality of materials and interfaces, determining the formation of bulk and interface defects, and material grain quality. The presence of bulk defects negatively impacts the electrical properties of carriers such as their mobility, diffusion length and lifetime, thereby reducing device efficiency. On the other hand, the use of buffer layers with different material structure and lattice parameters to the ones of the absorber it results in the formation of defects at the interface that act as recombination centers. In addition, absorber/buffer band alignment is crucial to the transport of carriers through the p–n junction. Therefore, particular attention should be paid to all these parameters for achieving the best solar cell efficiency.

In 2016, Hao *et al* [112] tackled a reduction of the voltage deficit in pure sulfide kesterite CZTS devices by employing innovative engineering at the absorber/buffer interface, resulting in a PCE of 9.2% with a V_{oc} of 0.762 V. The main source of voltage losses was associated to kesterite/CdS IR, because of the cliff-like alignment. The authors reported that reduced voltage deficit was due to a more favorable spike-like band alignment formation along with a lower formation of interface defects. By utilizing an optimized (Zn,Cd)(O,S) buffer layer, the team significantly improved the buffer/CZTS interface quality. This work not only elucidates the mechanisms

Table 4. Results on the application of ALD in kesterite solar cells for different material deposition.

Structure	Material deposited by ALD	Key outcomes	J_{sc} (mA cm^{-2})	V_{oc} (mV)	FF (%)	PCE (%)	Year	References
Mo/CZTSSe/ZnSnO/ ZnO/ZnO:Al	ZnSnO	An appropriate band alignment between the CZTSSe and the ZnSnO buffer was achieved, with an optimal conduction band offset of 0.03 eV for a Sn/(Zn + Sn) buffer compositional ratio of 0.167.	34.1	414	60.8	8.6	2016	[103]
Mo/CZTS/Al_2O_3/ CdS/ZnO/ITO	Al_2O_3	ALD-Al_2O_3 layers were deposited on CZTS absorbers prior to CdS deposition, achieving an interface passivation, as a result of the hydrogen accumulation from the ALD process.	19.65	630	65.3	8.08	2018	[104]
FTO/V_2O_x/CZTSe/ CdS/ZnO/ITO	V_2O_x	The use of V_2O_5 as a hole transport layer increases the FF parameter and consequently reduces the series resistance of the solar cell. The use of ALD results in a higher V_{oc} associated to rear surface passivation.	25.4	375	41.8	3.9	2021	[105]
Mo/CZTSSe/ZnSnO/ ZnO/ZnO:Al	ZnSnO	Solar cell exhibited bigger J_{sc} values than the ones of CdS reference cell because of a lower photon parasitic loss.	32.98	436	59	8.54	2022	[106]
Mo/ACZTSSe/Al_2O_3/ CdS/ZnO/ITO	Al_2O_3	Improvements in both the bulk absorber and the heterojunction are reported (by using Ag-alloying and Al_2O_3-ALD, a reduction in deep defects and the formation of a well-defined p–n junction is obtained)	36.81	514.2	70.4	13.33	2023	[91]

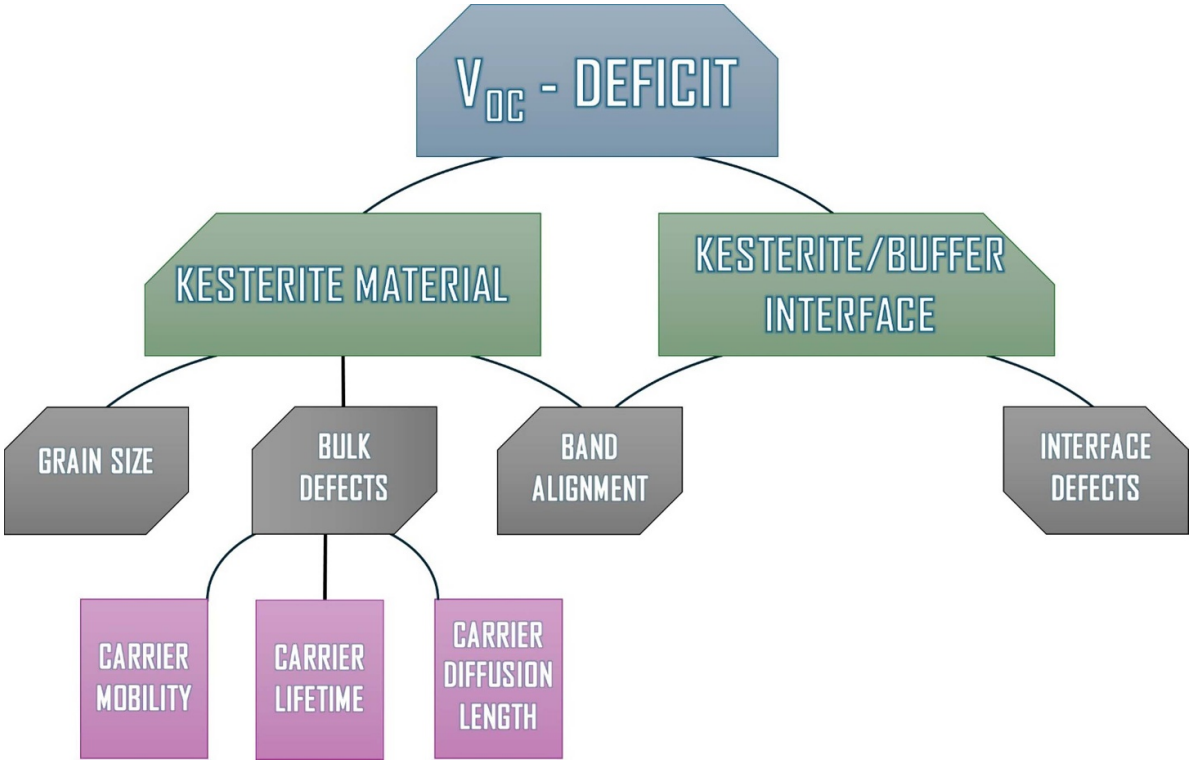

Figure 3. Main causes of V_{oc}-deficit in kesterite solar cells.

behind V_{oc} and efficiency enhancements but also introduces a viable approach to mitigate the open-circuit voltage deficit in CZTS devices, marking a significant stride towards advancing kesterite-based photovoltaic technology. Grenet *et al* presented a comprehensive exploration to understand the bottlenecks hindering the kesterite solar cell efficiency [113]. The authors presented a deep review into the existing literature, conducting a unique survey involving feedback from a consortium of more than 15-expert leading universities, institutes and laboratories which studies were partially dedicated to the kesterite thin film technologies, a fieldwork in a research project aimed to discern and evaluate different causes of performance degradation in devices collectively with a focus on the major issue being the open circuit voltage deficit. This study utilized a Design Failure Mode and Effects Analysis to not only document these issues but also rank them in order of significance providing valuable insights, for future studies aimed at systematically addressing these obstacles. Also, this study highlighted the significance of looking at particular failure modes to increase the effectiveness of devices for commercial use, representing an advancement towards creating more eco-friendly solar technologies without relying on essential raw materials and harmful elements such as cadmium. In 2020, a detailed analysis was published on how to manipulate the CdS/CZTSSe interface to reduce the V_{oc} deficit [114]. This study looked into the problem of high V_{oc} deficit in CZTSSe devices, which is a key obstacle preventing them from becoming a cost-effective alternative to mature technologies. Furthermore, it was observed that while CZTSSe shows promise as a material for photovoltaics, its performance is controlled by the V_{oc} deficit. The review highlights the importance of charge separation and extraction to reduce voltage losses and increase PCE of sunlight into energy. The authors pinpoint IR spurred by the poor quality of the p–n junction, defects, and secondary phases as key culprits for the technology inefficiency. They discussed the detrimental impact of structural inhomogeneities, non-ideal band alignment, and a high interface defect density, which foster dominant recombination pathways at the interface. Addressing these issues, the review focuses on interface engineering and modification strategies aimed at improving the absorber–buffer heterojunction quality. By examining various approaches to develop favorable interface characteristics, the work underscores the interface role in bridging the performance gap between CZTSSe and the more mature CIGS solar cell technology, providing a pathway to increase efficiency in kesterite photovoltaics. In another work, the integration of In_2S_3 passivation layer at the CdS/CZTSSe interface was proposed to increase solar cell efficiency by addressing the significant V_{oc} deficit, attributed to severe interfacial recombination owing to a high defect concentration and rough CZTSSe surface [70]. The introduction of In_2S_3 layer allowed an efficiency increase from 7.3% to 9.2%, attributed to more uniform CdS growth along with reduced interface defects. A combined post-deposition treatment considering LiF and AgF was proposed by Liu *et al* in the same year to reduce V_{oc} deficit in CZTSSe solar cells [82]. These combined treatments suppressed the Sn_{Zn} defect formation and reduce band tailing defects, thereby improving carrier lifetime. Under this proposal, a PCE of 12.58% with a V_{oc} of 0.507 V was informed. More recently, Cao *et al*, explored an innovative approach to enhancing CZTSSe device efficiency through the grain boundaries (GBs) passivation, which are known to significantly impede efficiency due to severe non-radiative recombination [83]. By incorporating a two-dimensional graphene additive into the CZTSSe precursor solution, the authors successfully integrate single-layer graphene into the GBs of the CZTSSe absorbing layer. This incorporation of graphene, characterized by its high carrier mobility and electrical conductivity, transforms the GBs into electrically benign zones, thus mitigating their role as high recombination sites for carriers. This graphene passivation resulted in a remarkable improvement in PCE, increasing from 10.40% to 12.90%, marking one of the highest efficiencies achieved for this type of solar cell. This study not only shows graphene's effectiveness in passivating GBs but also paves the way for boosting CZTSSe device efficiency through an additive engineering process.

Table 5 summarizes the main causes of V_{oc}-deficit in kesterite solar cells as well as the research directions proposed to reduce it. Both bulk absorber and buffer/absorber interface have been identified as critical points accounting for V_{oc}-deficit. On one hand, the consensus is that CdS/CZTSSe interface is more detrimental due to the presence of interface defects and non-ideal band alignment between the absorber and buffer layer, while on the other hand a more important role is given to kesterite material quality associated with GBs recombination, bulk defects and band tails resulting in short minority carrier lifetime, the formation of secondary phases due to the narrow phase stability, structural inhomogeneities, insufficient quasi-fermi level splitting, low carrier mobility, etc. In order to solve these problems, interesting proposals that go from the use of optimized buffer layers, the integration of passivation layers, to innovative thermal annealing have been discussed with promising results. Considering the advancements achieved by these research directions, further studies on these topics are encouraged to minimize the V_{oc}-deficit.

3.1.1.2. Reproducibility issues. CZTSSe solar cells face up reproducibility challenges due to differences in deposition techniques, in addition to variation in experimental conditions concerning material processing and their subsequent chemical and/or thermal treatment, limiting their large-scale commercialization as presented in figure 4. Furthermore, the presence of secondary phases, non-uniform element distribution and defect formation at bulk and interfaces are limiting the results reproducibility of kesterite solar cells.

A multiple selenization process for CZTSSe devices was studied by Neuwirth *et al* in 2016, reporting uniform, compact and defect free CZTSSe layer that resulted in stabilized values of series resistance and J_{sc}, as well as a reproducible CZTSSe conversion efficiency of 7.2% [115]. This type of study points

Table 5. Main causes of V_{oc}-deficit in kesterite solar cells and research directions proposed to reduce it.

Kesterite type	Main causes of V_{oc}-deficit	Research directions to reduce V_{oc} deficit	Year	References
CZTS	CZTS/CdS interface recombination, because of the cliff-like band alignment.	The use of an optimized (Zn,Cd) (O,S) buffer layer, resulting in a spike-like band alignment and a lower formation of interface defects	2016	[112]
CZTSSe	Bulk absorber instead of interfaces	Research priority on bulk absorber issues such as short minority carrier lifetime, band tails, insufficient quasi Fermi level splitting and low carrier mobility	2018	[113]
CZTSSe	CdS/CZTSSe interface recombination due to interface (non-ideal band alignment, high interface defect density) and material (bulk defects, secondary phases, structural inhomogeneities, narrow phase stability) issues	More attention to charge separation and extraction at the absorber/buffer junction (interface engineering of absorber-buffer heterojunction)	2020	[114]
CZTSSe	Interfacial recombination induced by the rough surface of CZTSSe and numerous physical defects.	The incorporation of In_2S_3 between the CZTSSe and CdS as a passivation layer, suppressing defects and improving surface morphology	2022	[70]
CZTSSe	Defects such as Sn_{Zn} in the bulk absorber	A combined post-deposition treatment considering LiF and AgF to suppress the Sn_{Zn} defect formation, resulting in the reduction of band tailing defects, and an improved carrier lifetime	2022	[82]
CZTSSe	Non-radiative recombination at grain boundaries	Grain boundary passivation by incorporating a two-dimensional graphene additive into the CZTSSe precursor solution, turning grain boundaries into benign zones	2024	[83]

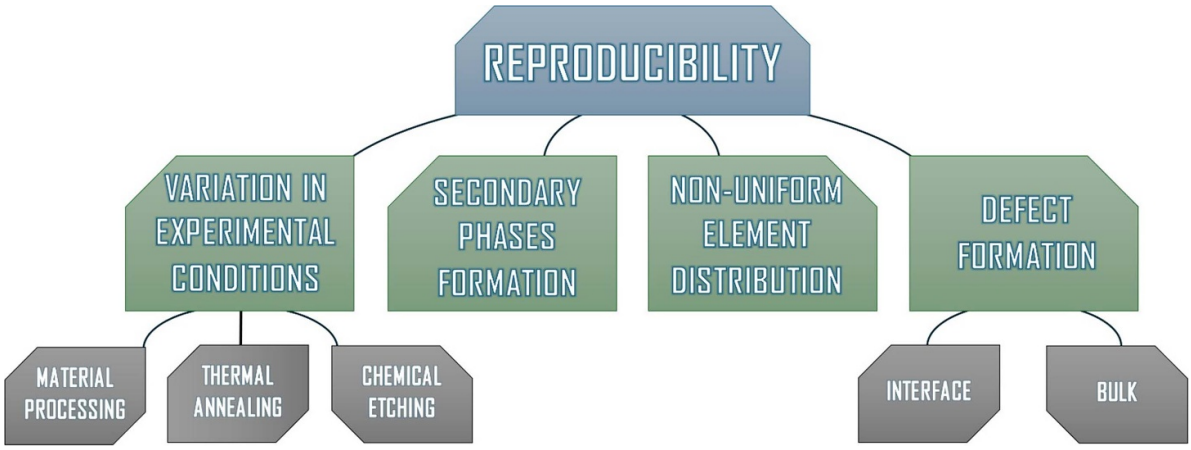

Figure 4. Main issues limiting the results reproducibility in kesterite solar cells.

out the potential of multiple selenization process for achieving consistent device characteristics in views of its scalability. The correlation between CZTSSe chemical purity and solar cell performance was studied in 2019 [84]. Utilizing high and low purity chemical precursors for the absorber layers, the research elucidates the material quality impact on kesterite solar cell efficiency. Through comprehensive photoluminescence spectroscopy and deep level transient spectroscopy analyses, the study reveals significant insights into the presence of shallow and deep defects, highlighting the role of quaternary acceptor-pair defects in radiative recombination processes. Notably, the research uncovers that despite improvements in film quality with higher grade chemicals, the PCE remained similar, around 5%, suggesting that factors beyond bulk absorber defects may be limiting solar cell efficiency. This pivotal work underscores the complexity of optimizing kesterite-based photovoltaics and sets the stage for further exploration of device architecture and surface recombination pathways to enhance solar cell efficiency. A subsequent article tackled the efficiency problems of CZTSSe devices, specifically addressing the issues of Sn volatilization loss and thick $MoSe_2$ interfacial layer formation during selenization, which have hindered the achievement of high PCE [116]. By employing a novel approach that utilizes $SnSe_2$ vapor in selenization processes, the team successfully demonstrated the surface and back contact stabilization in CZTSSe devices. The use of $SnSe_2$ vapor not only mitigates Sn loss by adjusting the partial pressure in the selenization atmosphere, but also

optimizes Mo/absorber interface by preventing the formation of a thick $MoSe_2$ layer. This methodological innovation leads to a notable solar cell efficiency of 10.85%. In another work, Yixiong *et al* in 2024 reported a notable efficiency over 10% without the use of anti-reflective coating [117]. The research introduces a novel ZnO/AgNW/ZnO/AgNW (ZAZA) window structure as an alternative to traditional indium tin oxide (ITO) layers, addressing the challenge of V_{oc} deficit owing to high-density interface states. This proposal allows shorter carrier collection paths as well as a homogeneous carrier lifetime in the device. The proposed procedure for ITO replacement is also a significant step for fabricating sustainable devices.

3.1.2. Challenges faced by CZTSSe solar cells. The main challenges in kesterite devices should be addressed to improve their efficiency, making them commercially viable. In a review work, the role of alkali doping for defect passivation, thermal annealing and band gap grading in solar cell efficiency promotion was discussed [118]. This work also presented the importance of band gap grading considering cation and anion alloying to optimize device performance, offering valuable insights for the future research. In 2016, the importance of critically controlling ZnS thickness during the sputtering deposition of CZTSSe solar cells starting from ZnS, SnS and Cu sequential growth followed by a thermal annealing in Se atmosphere was discussed by Kim *et al* [119]. The authors found a PCE of 9.1% for an optimal ZnS thickness. In addition, they concluded that a careful control of ZnS thickness is essential for reducing secondary phases formation, therefore advancing PCE of CZTSSe devices. CZTSSe decomposition during device processing is another important problem that results in high V_{oc} deficit and low FF as discussed by Xu *et al* [85]. The authors proposed adding Sn vapor during the synthesis process, resulting in reduced densities of Zn_{Sn} and Cu_{Zn} defects as well as in high quality CZTSSe thin films free from secondary phases. In addition, this proposal inhibited CZTSSe decomposition and favors a reduction in bulk and IR, achieving an efficiency of 12.03%. A research paper aimed at enhancing stability and efficiency of CZTSSe devices was presented by Campbell *et al* [120]. Improvements in CdS/CZTSSe interface and charge extraction were obtained by utilizing a thermal annealing under low temperature, demonstrating the important role of thermal annealing in promoting lifespan and efficiency of devices. The progress of CZTSSe solar cells was recently discussed in a review paper [121]. Opportunity areas for solar cell efficiency promotion such as Kesterite absorber and interface were discussed. Despite an efficiency of 14.9% has been recently reported, this record is still far behind that of CIGS mainly due to defects. Significant advance in the processing of kesterite devices was reported in 2023, resulting in a certified PCE of 13.8% [24]. By controlling the chamber pressure, the team expertly managed the selenium concentration during the early stages of annealing, which reduced the chances of collisions between kesterite precursors and selenium atoms. As a result, high quality CZTSSe layers with fewer defects were informed, emphasizing the need of accurate control of selenization process for the kesterite phase formation. The exciting potential of kesterite application into building-integrated photovoltaics was demonstrated by Zhou *et al* by developing CZTSSe solar cells on FTO [122]. An efficiency enhancement from 7.02% to 9.56% was shown by adding a MoO_3 interlayer that improved crystallization, being this latter value further improved to a certified value of 11.43% by Na and Ag doping. Results of this work stand for a milestone for transparent kesterite solar cells. In short, important factors such as material quality, defect formation, phase control, V_{oc} deficit and reproducibility must be addressed in order to push forward CZTSSe solar cell technology for its future commercialization. Further studies are required for a deep understanding of these important challenges and the proposal of innovative solutions.

3.2. Future outlook and potentiality

Nowadays, research works on CZTSSe technology are mainly focused on achieving efficiencies similar to the ones reported for CIGS and CdTe devices. By overcoming the actual material and fabrication challenges, along with creative engineering solutions, researchers aim to significantly boost performance. The goal is to make CZTSSe a key player in the renewable energy market, offering a sustainable and environmentally friendly alternative. The future research directions for achieving higher kesterite solar cell efficiencies are depicted in figure 5. In particular, the optimization of the thermal annealing process and material composition, joined with further research on material and interface engineering are necessary to take advantage of the promising potential of the kesterite absorber material. In addition, the cation substitution, material doping and innovative proposals such as the use of graded, tandem, flexible and nanostructured solar cells are opportunity areas for device promotion.

A recent article [123] emphasized both the promise and challenges of CZTSSe technology, highlighting its highest recorded efficiency of 14.9%. Strategies like interface engineering, cation substitution, and annealing processes show promise for enhancing performance. The paper emphasizes the importance of understanding these mechanisms for future development in kesterite solar cells. In another recent review, the ED technique for fabricating CZTSSe devices was discussed [39], highlighting its cost-effectiveness and environmental friendliness. Despite the industrial appeal, electrodeposited CZTSSe cells currently exhibit lower efficiency ($\sim$10%) due to phase inhomogeneity and rough morphology. Strategies for intrinsic film control and extrinsic treatments to enhance film quality and device performance are needed. Future prospects of ED CZTSSe cells in applications like tandem, flexible, and solar water-splitting devices are outlined, offering insights into technical challenges and development directions for high PCE in CZTSSe devices.

3.2.1. Material engineering. Developing new material compositions, treatments for surface improvements, and doping strategies are required to improve efficiency and stability. For CZTSSe technology, it is pivotal improving their performance

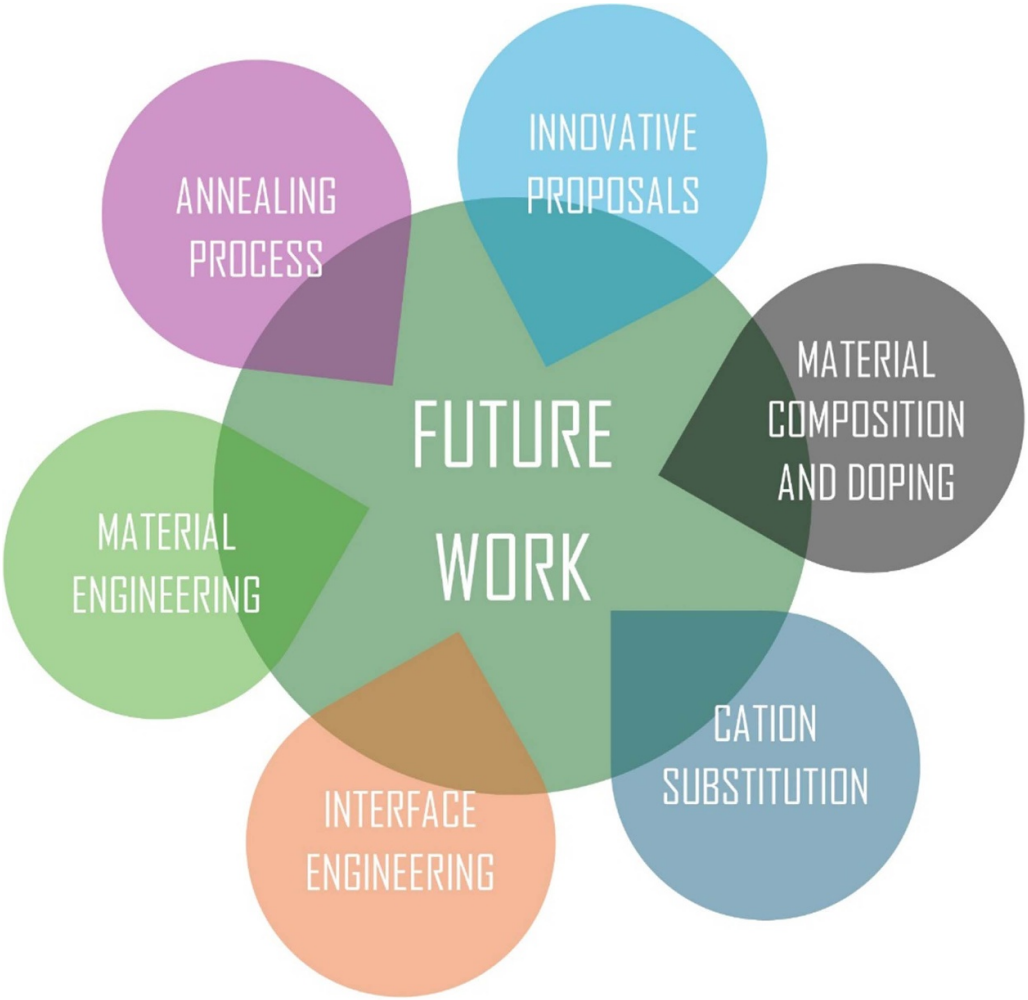

Figure 5. Future research directions for a further kesterite solar cell efficiency promotion.

and stability through the development of new material compositions and doping strategies. The germanium incorporation into kesterite layers to address the V_{oc} deficit issue in CZTSSe photovoltaics is an interesting proposal [124]. By substituting Sn with Ge, they were able to control the CZTSSe band gap, enhancing their photovoltaic application potential. The optimal Ge doping level was determined to be 30%, resulting in 4.8% of PCE, without using antireflection coating. Adding Ge not only widened the absorber band gap but also improved the crystallinity and grain structure of the films, especially when the Ge content was between 20% and 40%. However, at higher Ge doping levels, cracks and discontinuities in the film emerged due to thermal expansion mismatch. The study demonstrated that Ge doping is a viable strategy to enhance the photovoltaic performance of CZTSSe-based solar cells by adjusting the band gap and improving the material electrical properties. A novel back contact engineering method was proposed to increase CZTSSe device efficiency [125]. The study revealed that applying mechanical exfoliation to devices with absorber thickness around or below 1 μm, it results in significant V_{oc} improvements, with increases up to 49 mV observed for a 1 μm thick absorber and up to 61 mV when etching the back CZTSSe surface with bromine-methanol. This strategy offers a route to circumvent the V_{oc} limitations of CZTSSe devices by focusing on back contact optimization. In other work, a novel surface modification strategy for CZTSSe solar cells was developed by the Ag_2ZnSnS_4 layer integration to achieve front gradient distribution and surface inversion [126]. This approach significantly improves the carrier transport and separation, reducing electron-hole recombination. Moreover, these enhancements lead to increased V_{oc} and J_{sc}, resulting in a PCE of 12.55%. The innovation also reduces the V_{oc} deficit to 306 mV. This progress in CZTSSe band engineering paves the way for promising future solar technologies that are more efficient and cost-effective. On the other hand, by 2022, researchers explored the impact of ex situ germanium (Ge) doping to decrease the open-circuit voltage deficit, a key efficiency-limiting factor. By incorporating Ge into Cu_2ZnSnS_4 nanocrystals before selenization, this study improved grain structure and crystallinity without changing the bandgap, leading to better V_{oc} and overall conversion efficiency [127]. The study demonstrated a more uniform electronic landscape, suggesting a reduction in low work function Sn(II) chalcogenide phase segregation. Ge doping proves to stabilize CZTSSe

structures, suggesting a suppression of Cu_{Sn} antisite defects and associated recombination pathways, potentially via a Ge-induced flux during selenization that promotes grain growth. This research opens new avenues for optimizing CZTSSe solar cells through doping strategies, focusing on interface and bulk improvements to overcome the V_{oc} deficit challenge. These studies underscore the ongoing efforts and innovative strategies in material engineering to overcome present limitations in CZTSSe devices, aiming to unlock their full potential for high-efficiency and stable photovoltaic applications.

3.2.2. Gradient band gap engineering. CZTSSe band gap grading stands for a potential proposal for optimizing absorption of the solar spectrum and enhancing carrier transport and separation, thereby increasing PCE. The partial replacement of Cu^+ by Li^+ ions in CZTSSe was proposed in 2016 for band gap tuning to improve CZTSSe/CdS interface band alignment [128]. The impact of different Li/Cu ratios on lattice parameters, carrier concentration, and solar cell performance was analyzed. This breakthrough suggests a promising route for optimizing kesterite-based solar cell efficiency through alkali metal doping. In the same year, a method using SeS_2 for chalcogenization in CZTSSe solar cells to control S and Se contents was introduced, obtaining a graded band gap [129]. This approach increased V_{oc} through band gap grading and suggested mechanisms for J_{sc} enhancement. The introduction of SeS_2 during annealing resulted in a CZTSSe record PCE of 12.3%, showcasing a significant improvement in V_{oc} deficit to 576 mV. The selenium annealing of CZTS to introduce sulfur-selenium gradients was investigated [130]. Annealing CZTS in selenium atmosphere aimed to substitute sulfur with selenium, potentially forming gradients. However, practical challenges arose due to selenium incorporation correlation with sodium distribution and its effect on CZTSSe grain growth. Findings suggest sodium-assisted recrystallization limits the practicality of achieving desired sulfur–selenium gradients, highlighting the complexity of manipulating CZTSSe material properties for improved solar cell efficiency. A theoretical work focused on kesterite PCE enhancement through graded band-gap was reported [131]. By simulating various grading models, they found that modifying the inside graded model could significantly enhance device performance, leading to a PCE of 15.6%. This efficiency boost is a result of optimized recombination rates and current density enhancements achieved by the graded band-gap profiles. The research highlights the potential of band-gap engineering in enhancing CZTSSe device efficiency. The incorporation of selenium (Se) into CZTS was explored at temperatures higher and lower than that of CZTSSe nucleation temperature [132]. It was found that at 337 °C and 360 °C, Se diffusion is primarily through GBs, with increased Se near the CZTS/Mo interface suggesting grain boundary diffusion. At 409 °C, nucleation and recrystallization of CZTSSe occur, facilitated by sodium diffusion from the back contact. The research demonstrates the challenges in achieving graded band gap by controlling Se diffusion into CZTS, due to recrystallization dominating Se incorporation. The effects of incorporating selenium into CZTS precursors through compound co-sputtering, followed by a thermal annealing in a mixed atmosphere of Ar, S, and Se was studied [133]. The research found that selenium inclusion allows for more rapid recrystallization at lower temperatures and that precursors consisting of sulfur and selenium stacking alternation can influence the absorber's morphology and the segregation of Zn(S,Se) secondary phase. Devices fabricated from these absorbers showed a PCE ranging 2.0%–9.0%. The study demonstrated the potential for selenium-containing precursors to produce superior devices under certain conditions. CZTSSe devices with enhanced PCE (10.04%) were developed by optimizing the S/(S + Se) ratio through water-based spray pyrolysis [46]. This adjustment improved solar cell efficiency by the V_{oc} deficit reduction, and the FF increase. They observed increased surface compactness and shunt resistance with a moderate S/(S + Se) ratio, but excessive S-alloying negatively affected performance. Sharp S–Se profiles were successfully obtained in kesterite devices with a significant improvement in material quality by a new chalcogenization process in 2019 [134]. This approach led to devices with up to 9% efficiency and improved voltage performance, highlighting the potential of band gap grading profiles for enhancing kesterite solar cell performance. This work constitutes an important step for enhancing CZTSSe solar cell efficiency through anionic band gap grading. In a subsequent work, the same research group proposed the partial replacement of Sn by Ge for band gap engineering, obtaining an improved efficiency without the use of antireflection coatings or metallic grids [135]. The impact of CZTSSe grading in solar cell efficiency was explored in 2020, finding that a sinusoidal band gap grading can result in an efficiency enhancement from 12.6% to 21.74% [136]. In another work, a two-step annealing process was introduced to create a graded band gap, achieving a solar cell improvement from 7.62% to 10.11% [86]. This study not only proposes a simple and reproducible method to enhance CZTSSe solar cell efficiency but also contributes to the understanding of the effects of sulfur content gradation within the thin-film structure on its electrical performance. A sharp surface bandgap gradient was created through sputtering a very thin CZTS layer on CZTSSe absorber for boosting CZTSSe device efficiency [58]. Improvements in V_{oc} and overall PCE were reported by modifying band alignment and reducing carrier recombination. A proposal for increasing CZTSSe device efficiency by creating a bandgap-graded structure through an annealing strategy during ZnO:Al deposition was presented [137]. This approach promotes an ion exchange reaction, modifying the p–n junction and forming a graded bandgap that improves electron transport and reduces carrier recombination. This method marks a significant advancement in kesterite devices, with a certified PCE of 12.25%. A review work published in 2022 delves into bandgap tailoring in kesterite devices to enhance their performance, focusing on graded absorber layers [138]. They discussed the impact of different types of gradings on Sb_2S_3, CdTe, CZTS, and CIGS solar cell performance, emphasizing the importance of band gap tuning to improve V_{oc}, J_{sc}, and PCE. The article also outlines future directions and challenges in graded devices, highlighting the potential for significant advancements in solar

cell efficiency through absorber layer bandgap optimization. In another work, a proposal to control the anionic ratio and gradient within kesterite technologies, specifically focusing on CZTSSe and CZGSSe materials was discussed [139]. This work, aimed at enhancing the physicochemical properties of chalcogenide solid solutions, involves the sequential synthesis of pure sulfide and selenide layers to achieve desired compositional profiles. By controlling the thickness of different layers and fine-tuning processing conditions, this research shows how the anionic composition in the absorber can be controlled, creating either a uniform or graded distribution. This control is a key factor for optimizing band gap engineering, improving interface quality, and forming carrier-selective contacts. This method offers a step toward more efficient and reproducible CZTSSe solar cell fabrication. The enhancement of CZTS solar cells was also reported by replacing Sn by Ge for band gap tunning [140], by means of sol–gel technique and a subsequent thermal annealing. In particular, the addition of KCl as a reactive chemical etching improved kesterite crystalline quality and favored the formation of compact grains. A band gap grading was successfully created in CZTSSe by sputtering technique in 2023, offering a promising method for fine-tuning the kesterite device properties [59]. A double graded CZTSSe band gap was introduced by incorporating K_2S during the preparation of the precursor film, achieving a maximum efficiency of 13.7%, because of enhanced carriers generation and collection [87]. A recent work explored Ge doping effect into CZTSSe devices, having this element a crucial role in controlling defect formation and grain growth [99], offering relevant information on Ge role in the promotion of CZTSSe device properties, and establishing new ways to optimize its performance.

The main results on kesterite band-gap graded solar cells are summarized in table 6. Different strategies including changing Li/Cu, S/Se, and Cu/Cd ratios have been used to obtain the band gap grading in the kesterite absorber material. In particular, S/Se ratio changing it is presented as the most popular one as observed in table 6. The application of kesterite band-gap graded solar cells has shown promising results, where efficiencies in the range of 2%–13.7%, with J_{sc}, V_{oc} and FF values in the ranges of 15–37.37 mA cm^{-2}, 330–544 mV, and 45%–68.48%, respectively have been reported. Therefore, considering the experimental state of the art in kesterite solar cells, strategies such as the use of kesterite graded solar cells joined with ALD technique for surface passivation, along with the presence of passivation layers, an optimized buffer layer and last but not least an innovative thermal annealing should be further explored since their combination are expected to provide a kesterite solar cell efficiency higher than the current record one of 14.9%.

4. The theoretical viewpoint: past, present, and future

While characterization techniques of solar cells provide important information on device performances in dependence on experimental conditions, theoretical studies are also required in order to achieve complete understanding of physical principles that govern the analyzed solar cells. The use of modeling and simulation tools allows a deep knowledge on mechanisms limiting solar cell efficiency, which results in the material utilization reduction. In this sense, modeling and simulation tools are powerful to reinforce the complete understanding of the working principles of device and helps finding routes for efficiency promotion. For this purpose, the accurate selection of model that reproduces the experimental data, along with the justified choice of the input parameters for simulations are key points that guarantee the quality of simulation results.

For CZTSSe solar cell simulation, different analytical and numerical approaches have been used. While for the numerical simulations typical semiconductor equations are solved numerically considering boundary conditions, for analytical methods certain useful conditions are proposed that allow exact solutions to these equations. For numerical simulation softwares like wxAMPS, Sentaurus, and SCAPS have been considered. More information on numerical and analytical simulations are presented below:

4.1. Numerical simulations

One of the first attempt to simulate CZTS solar cells by SCAPS software was presented in 2012 [141]. The authors mainly focused on the role of acceptor concentration, work function of back contact, and CZTS absorber thickness on solar cell behavior. Despite this report opened the door for further simulation works on kesterite solar cells, ideal mechanisms were assumed for calculations, being radiative and Auger recombination overestimated for calculations. A more accurate numerical study on CZTSSe solar cells was presented in 2014 by wxAMPS software [142]. In this paper, the authors simulated kesterite-based device with a PCE of 12.6%, being able to replicate the experimental observations. A particular attention was paid to CZTSSe bulk defects rather than CZTSSe/CdS interface, thereby suggesting that CZTSSe/CdS interface defects could be neglected. Furthermore, band tailing was presented as the main cause of V_{oc} losses. The CZTSSe band tailing impact on devices has been also discussed [143, 144]. Under the authors experimental conditions, interface defects neglection is acceptable since appropriate band alignment between CZTSSe and CdS (transition from cliff-type band alignment to spike-type band alignment) that reduce IR is achieved, as will be explained later by analytical approaches. However, in most CZTSSe solar cells the consideration of interface defects is necessary to achieve the accurate experimental data reproduction. Numerical simulations on CZTS, CZTSe and CZTSSe solar cell performances were presented by Simya *et al* in 2015 [145], with a particular focus on the optimization of resistances, metallic work function and thickness properties under radiative and Auger recombination mechanisms. A theoretical study on CZTS photovoltaics was proposed by Firsk *et al* in 2016, where IR and diffusion length were assumed as important; calculations were performed by SCAPS [146]. The authors concluded that IR has the dominant role followed by the bulk recombination.

Table 6. Main results on kesterite graded solar cells.

Structure	Proposal to realize the band gap grading	J_{sc} (mA cm^{-2})	V_{oc} (mV)	FF (%)	PCE (%)	Year	References
Mo/$Li_xCu_{2-x}ZnSn(S,Se)_4$/CdS/i-ZnO/ITO/Al	Li/Cu ratio	25.86	408	63.5	6.7	2016	[128]
Mo/CZTSSe/CdS/i-ZnO/ZnO:Al	SeS_2/Se weight ratio	34.98	521	67.2	12.3	2016	[129]
Mo/CZTSSe/CdS/i-ZnO/ZnO:Al	S/Se ratio	15–32	330–500	45–65	2–9	2018	[133]
Mo/CZTSSe/CdS/i-ZnO/ITO	S/Se ratio	30.69	524	62.38	10.04	2019	[46]
Mo/CZTSSe/CdS/i-ZnO/ITO	S/Se ratio	31.6	444	65. 8	9.23	2019	[134]
Mo/CZTGSe/CdS/i-ZnO/ITO	Sn/Ge ratio	29.9	471	65.1	9.2	2020	[135]
Mo/CZTSSe/CdS/i-ZnO/ITO	S/Se ratio	32.41	531.25	58.73	10.11	2022	[86]
Mo/CZTSSe/CZTS/CdS/i-ZnO/ITO	S/Se ratio	35.26	450	62.73	9.9	2022	[58]
Mo/CZTSSe/ CdS/i-ZnO/ZnO:Al	Cu and Cd interchange	37.37	484.75	67.69	12.25	2022	[137]
Mo/CZTSSe/ CdS/i-ZnO/ITO	S/Se ratio	25.59	509	56	7.30	2023	[59]
Mo/CZTSSe/ CdS/ITO	S/Se ratio	36.73	544	68.48	13.70	2024	[87]

At the same time, Meher *et al* studied the effect of inhomogeneity in CZTS solar cells from a randomly graded absorber layer [147]. The role of secondary phases and material properties on open-circuit voltage deficit was evaluated by Kanevcen *et al* [148]. The authors validated the model by comparing its results with the experimental data, and were able to conclude that despite IR and carrier lifetime are the main sources of V_{oc} deficit, the presence of secondary phases could be another factor for V_{oc} deficit, depending on their location and type. That is, secondary phases at the heterojunction interface are more detrimental since might increase IR. In addition, the authors found that experimental data can only be explained by 2D models when incorporating secondary phases. In 2020 Minbashi *et al* deepen into the CZTSSe solar cell efficiency enhancement by meticulously examining various potential defects within the absorber layer using a combination of electrical and optical approaches via the Finite Element Method [149]. By validating their simulation results against experimental data, the researchers established clear guidelines for enhancing cell performance. They highlighted the critical role of defect management and secondary phase control in performance improvement. The study underscores that synthesis techniques adjusting Na-doping, Zn/Sn, Cu/(Zn + Sn), and S/(S + Se) ratios significantly mitigate trap-assisted recombination, thereby boosting efficiency. By categorizing defects into benign ($Nt < 10^{16}$ cm^{-3}) and detrimental ($Nt > 10^{16}$ cm^{-3}) based on their energy positions, the research identifies detrimental defects as the primary efficiency detractors in kesterite solar cells. By reducing these detrimental defects and overall defect densities, a PCE of 19.06% was achieved, positioning kesterite devices as a promising technology for industrial application, especially considering their non-toxic, environmentally friendly, and cost-effective attributes.

An important research direction for kesterite solar cell efficiency improvement is the replacement of CdS as buffer layer. Alternative buffer layers to CdS have been experimentally studied to mitigate IR. Traditional CdS presents the inconvenient of Cd toxicity and on the other hand it forms non-ideal band alignment with CZTS material (cliff-like alignment) and also participates in photon parasitic losses due to its low band-gap. These mentioned points have been the most important ones considered when proposing alternative buffer layer materials. In particular, ZnSnO and Zn(O,S) have been highlighted in a review work as promising low-cost nontoxic alternative buffer layers [150], where ZnSnO/CZTS heterojunction has demonstrated efficiencies comparable to the ones of CdS/CZTS. The potential of replacing the traditionally used CdS in kesterite devices with a ZnSnO (ZTO) layer deposited via sputtering was also evaluated [151]. This approach is motivated by the dual benefits of avoiding toxic cadmium and improving device performance through a better-suited buffer layer for CZTS absorbers. The research demonstrates that adjusting the sputtering deposition power it allows for the manipulation of ZTO's metallic composition, thereby enhancing the optoelectronic properties. Experiments with reactive sputtering using either Ar:O_2 or Ar:SF_6 mixtures were conducted to further optimize the ZTO layers' characteristics. The integration of optimized ZTO buffer layers into Mo/CZTS/ZTO/ZnO:Al solar cell configurations, followed by thermal treatment and deposition condition adjustments, resulted in a notable promotion of PCE to 5.2%, surpassing the reference CdS-based solar cells by 0.6%. This improvement is attributed to minimized absorber damage through low deposition power and a two-stage sputtering process. The study underscores the significance of buffer layer composition and deposition techniques in enhancing CZTSSe device efficiency, showcasing a promising direction to developing Cd-free photovoltaic devices. On the other hand, among the different proposals, experimental and numerical results have presented TiO_2 buffer layer as a suite candidate for CZTS solar cells [152–156]. Theoretical calculations performed by Bencherif *et al* have demonstrated that an increase in V_{oc} for TiO_2/CZTS solar cells is expected in comparison to typical CdS/CZTS solar cells, being able the optimal device to achieve an efficiency of 14.5% [155]. A spike-like alignment between amorphous-TiO_2 and CZTS described by a conduction band offset of 0.17 eV was reported [153]. Among the nontoxic proposals, zinc-based buffer layers such as ZnMgO have been studied for its wider and adjustable band-gap that reduce optical losses at short-wavelengths [157]. The author showed that a spike-like alignment with nearly flat-band is formed by controlling Zn/Mg compositional ratio, favoring carrier transport at the interface. CdZnS buffer has been also proposed as alternative layer to replace CdS, which is able to reduce the Cd concentration and parasitic losses [158]. Efficiencies around 11.2% were obtained for CdZnS with 60% Zn, while the use of ZnS results in poor device efficiencies. In other work, GaSe was proposed as an alternative buffer layer, reporting a better band alignment and therefore the absence of Cd-toxic element [159]. Other interesting experimental and theoretical proposals are the use of bi-layers such as CdS/Zn(O,S), CdS/In_2S_3, and CdS/ZnS as buffer in kesterite solar cells [160–162]. Authors have shown better performances in kesterite devices by using bilayers, since this proposal reduces cadmium amount in layers, while improving interface quality, however, further theoretical works are required to understand their impact on kesterite solar cells. A recent review work on alternative Cd-free buffer layers analyzes with detail buffer layers effect on CZTSSe devices [100]. Among the different proposals, the authors paid particular attention to Zn(O,S), ZnSnO, In_2S_3, and TiO_2 buffer layers as potential candidates for CZTSSe devices.

Aside from the problem of kesterite/buffer interface, kesterite bulk defects have been identified as dominant in this type of technology. In 2021 Sravani *et al* performed an analysis on CZTS and CZTSe loss mechanism effect on devices from numerical simulations [163]. In particular, different traps and defects forming band tails with Gaussian distribution were analyzed, observing an efficiency degradation due to defects. In another work, the same authors studied CZTS and CZTSe GBs effect on devices by numerical simulations [164], highlighting their role in carrier losses. The critical challenge for enhancing CZTSSe device efficiency by the control and minimization of secondary phases and lattice defects was experimentally and theoretically analyzed [165]. The findings underscore the potential of achieving a maximum efficiency of 18.47% by strategically reducing defects, particularly those

near the electron Fermi level and the band gap midpoint. This work not only advances the understanding of defect engineering in solar cell materials but also sets a foundation for developing more cost-effective and efficient CZTSSe solar cells suitable for larger-scale applications. The use of a back surface field (BSF) layer (p+ layer) based on kesterite and SnS in kesterite solar cells have been also analyzed by numerical simulations [166–168], demonstrating the potential use of these layers as BSF for reducing carrier recombination. A recent work presents theoretical results on CZTSSe device efficiency enhancement using SCAPS-1D software by incorporating a SnS-BSF layer [169]. The SnS-BSF layer increased PCE from 12.54% to 15.84%, with a further optimization to 20.17% by changing doping concentration and absorber thickness. Efficiency was further increased to 24.10% under 10 suns concentration. Experimental validation confirmed the simulation predictions, highlighting the potential of kesterite devices with BSF layers under concentrator applications. The use of kesterite-graded for improving carrier transport in solar cells is also an interesting proposal. Despite some experimental works have performed the fabrication of kesterite graded solar cells as mentioned earlier, only few works can be found in the literature regarding theoretical proposals for graded solar cells [131, 136, 170–172]. This topic is still open research. Another interesting proposition for kesterite application is tandem solar cells, which have been mainly studied by numerical simulations. A CZTS/CZTSe tandem solar cell was proposed in 2017, showing that under optimized bandgap an efficiency of 21.4% is expected by replacing CdS by ZnS as buffer layer [173]. Another work demonstrated that efficiencies of 20% can be achieved in kesterite tandem solar cells by using CZTSSe in the bottom cell and CZTS as the top cell [174]. Figure 6 presents a typical two-junction solar cell based on CZTS and CZTSSe absorber materials, where photons with energies higher than 1.4 eV are expected to be absorbed in the CZTS, while photons with energies between 1.0–1.4 eV can be absorbed in the CZTSSe—depending on the anionic composition. In general, some theoretical works on tandem devices based on kesterite/kesterite [175–179], perovskite/kesterite [180–182] and kesterite/silicon [183, 184] have been studied, achieving promising results, thereby the exploration on the application of kesterites to different types of tandem solar cells is an emerging field.

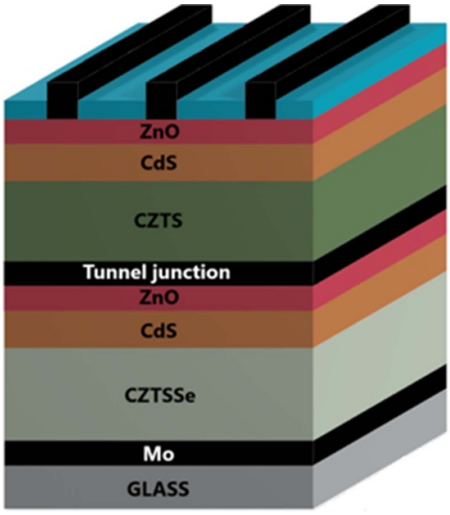

Figure 6. Tandem solar cell based on CZTSSe materials.

4.2. Analytical simulations

The analytical procedures are very useful for a better understanding of device physics. In a very brief explanation, for analytical calculations the current density–voltage dependence (*J*–*V* characteristics), which is expressed by an equation based on double or more diodes with the superposition of the term of photo-current density given by the absorption of the incident light is commonly assumed as a good approximation [185–192]. In this equation, the diode terms accounts to losses owing to the different ideal and non-ideal carrier loss mechanisms like radiative recombination, diffusion, thermionic emission, and non-radiative recombination, being the latter due to interface defects or bulk defects. Non-radiative recombination is based on the Shockley-Read-Hall (SRH) theory. Under certain conditions, recombination through defects (non-radiative recombination) can be enhanced with the assistance of an electric field, being this mechanism often called as trap-assisted tunneling recombination (TATR) or simply tunneling enhanced recombination. Another important part is photocurrent density calculation, being necessary in a first step to calculate external quantum efficiency (EQE) dependence on wavelength for quasi-neutral and depletion zones of the device [185–192]. In this way, *J*–*V* and EQE characteristics can be obtained from calculations and compared to the experimental data to conclude on the dominant loss mechanisms, thereby validating the model. Analytical approaches are less available for kesterite solar cells in comparison to numerical procedures. This can be understood from the point that there are some available softwares for numerical simulations while analytical calculations require to state the adequate model to continue with the programing of equations, variables, and constants in chosen platforms such as Wolfram Mathematica, Matlab etc. The first proposals to study analytically CZTSe and CZTS devices were presented by Courel *et al* [186–188, 190]. In fact, these works are the first reports presenting a deep analysis on each loss mechanism effect on kesterite devices. The schematic representation of CZTS and CZTSe devices band diagram is presented in figure 7, where each carrier loss mechanism is presented.

In the diffusion mechanisms, majority carriers (holes in p-type semiconductor and electrons in the n-type semiconductor) are injected over the potential barrier into n-type and p-type semiconductors, respectively, due to a gradient of concentration, diffusing away from the junction until they recombine in bulk or at interface. In heterojunctions such as CZTSe and CZTS devices, in addition to potential barrier at the junction, the band offsets prevent carriers diffusion, making this mechanism less likely in comparison to homojunction such as typical silicon solar cells [185–187]. Under the thermionic

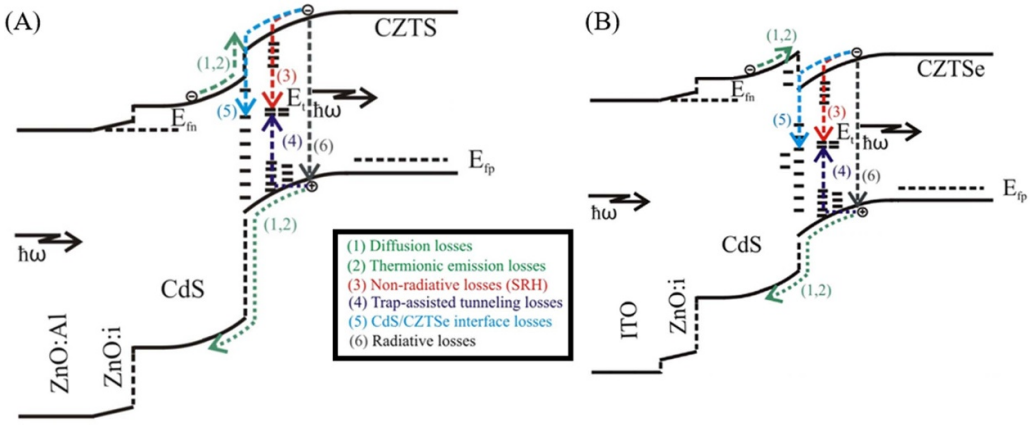

Figure 7. Carrier loss mechanisms in CZTS (a) and CZTSe (b) solar cells. Reprinted from [187], with the permission of AIP Publishing. Reprinted from [190], Copyright (2016), with permission from Elsevier.

emission, majority carriers are more likely to overcome the potential barrier due to thermal energy. However, the band-offset in addition to built-in potential make this loss mechanism less likely on kesterite solar cells when comparing model results with the experimental data [185–187]. Since radiative recombination is an ideal mechanism where only losses through band-to-band transitions take place, the best solar cell performances are expected under this mechanism as published before [185–187]. On the other hand, it has been shown that recombination due to bulk defects (non-radiative recombination) is a more realistic proposal since mid-gap state defects such as Cu_{Sn} and Sn_{Zn} for kesterite and V_{Cd} for CdS have been predicted [193, 194]. In fact, simulations based on non-radiative recombination have resulted in solar cell performances near to the experimental reported ones [185–187, 190]. Recombination through bulk defects in the depletion zone can be increased via tunneling process, that is, majority carriers might tunnel to energy states within the band gap under forward-biased junctions, where they partially loss their energy until completing the non-radiative recombination process with the opposite charge as originally proposed by Hurkx *et al* [195, 196]; this process in shown in figure 7. TATR presented by Hurkx and collaborators is mainly based on the traditional SRH theory, with a small perturbation added to SRH equation, which mainly depends on electric field intensity, consequently, higher recombination losses are obtained under high electric field, while for low electric field it turns into SRH theory. In kesterite devices, tunneling enhanced recombination was highlighted as dominant, being able to explain the experimental data [185–187, 190]. Shallow traps such as V_{Zn}, Zn_{Sn}, V_{Cu}, and Cu_{Zn} have been reported for kesterite material [193] while for CdS shallow traps such as Cd_i and Cd_S have been identified [194], making likely tunneling recombination of majority carriers thereby increasing non-radiative recombination. An important advantage from the analytical approaches is that mechanisms such as tunneling enhanced recombination can be studied in detail, while often used numerical softwares do not facilitate this type of study. In addition to the previously mentioned loss mechanisms, interfaces often play a dominant role in carrier recombination due to lattice and thermal expansion mismatches along with band alignment. Figure 7 shows a cliff-like band alignment for CZTS devices, while a spike-like alignment is observed for CZTSe devices. The cliff-like band alignment is the most harmful since carriers at the interface require an energy shorten than band gap to recombine. IR at CdS/kesterite was also demonstrated to be dominant in these types of solar cells [185–187]. However, losses at CdS/CZTSe interface are quite shorter than the ones of CdS/CZTS interface [185–188, 190]. Previous analytical analyses have introduced IR and TATR as the most important mechanisms to explain the experimental data [185–188, 190]. The effect of tunneling mechanism can vary from cell to cell depending on electric field at the junction, this result is in good agreement with other works that emphasize bulk and interface defects as the dominant ones. Interface losses and tunneling enhanced recombination were also identified as dominant in CZTS processed devices [94].

Reverse dark current density (J_0) is also an important parameter. For most numerical approaches, this parameter is not available as an output result, this explains why most theoretical studies performed by numerical analysis do not provide results on J_0. On the contrary, another advantage of analytical procedures in comparison to the numerical ones is that J_0 can be straightforward evaluated. The role of minority carrier lifetime and CdS/CZTS IR on PCE, V_{oc} and J_0 was evaluated [188], results are presented in figure 8. It is important to increase minority carrier lifetime along with reducing CdS/CZTS IR for boosting CZTS device performance, being these mechanisms detrimental for V_{oc}. It was also pointed out that maximum efficiency reported were under the effect of IR and TATR. Despite TATR is presented as dominant, figure 8(c) shows that the increase of minority carrier lifetime to values higher than 10 ns results in the reduction of TATR, turning IR as the dominant loss mechanisms. In the case of CZTSe solar cells, this occurs for minority carrier lifetime higher than 100 ns [188], thereby indicating lower losses at CdS/CZTSe interface and consequently higher efficiency can be obtained only focusing on reducing the effect of CZTSe bulk defects.

The effect of minority carrier lifetime and IR on PCE and V_{oc} of CZTS and CZTSe is shown in figure 9. CdS/CZTSe

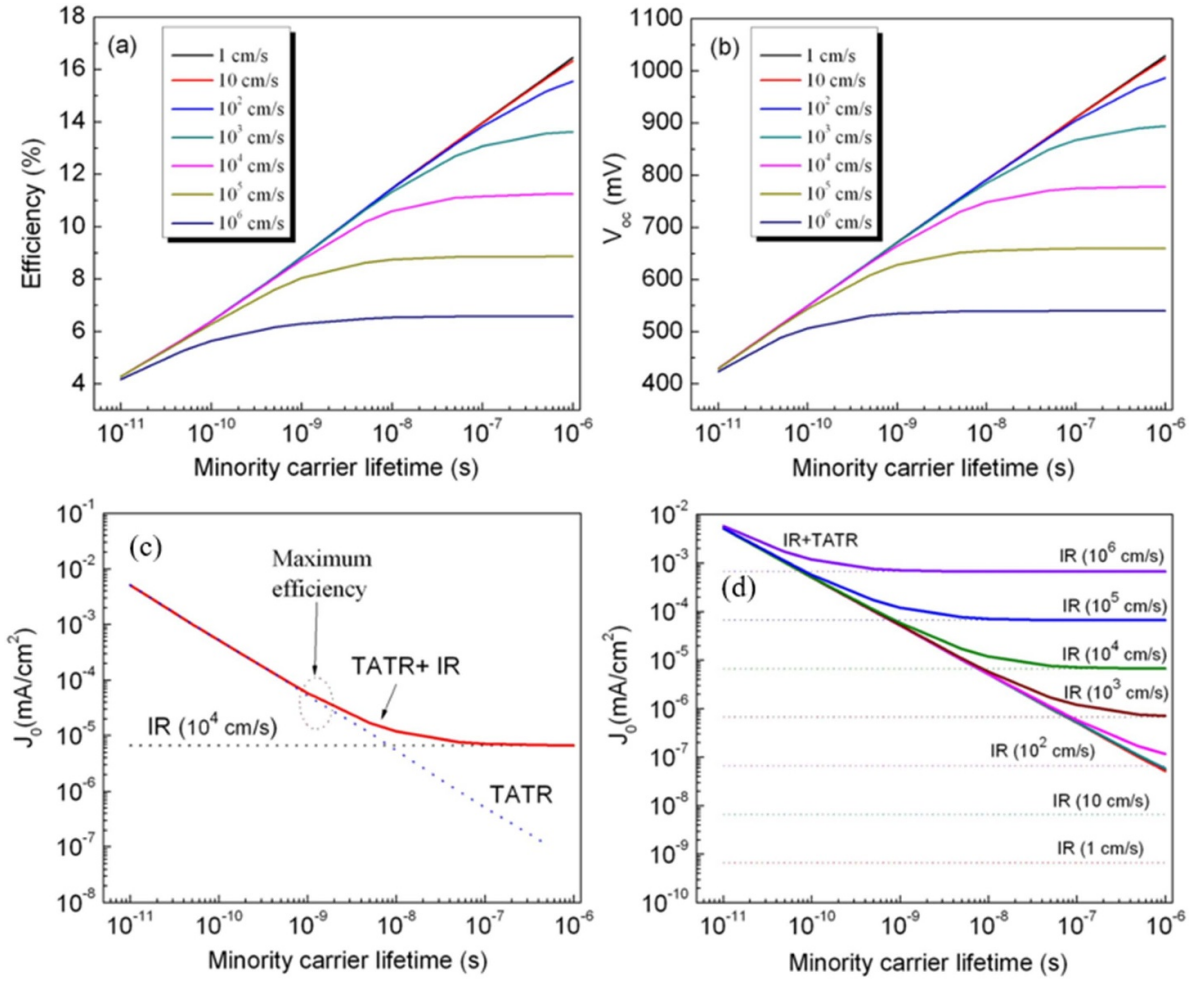

Figure 8. Efficiency dependence on interface recombination speed and minority carrier lifetime (a), V_{oc} dependence on interface recombination speed and minority carrier lifetime (b), J_0 dependence on minority carrier lifetime (c), and J_0 dependence on interface recombination speed and minority carrier lifetime (d) for CZTS solar cells. Reproduced from [188].

IR is almost negligible for CZTSe minority carrier lifetimes shorten than 5 ns. The analytical results have shown that an efficiency of 18% is expected for both technologies, however, these results point out that bulk defects and CdS/kesterite interface are still one of the main problems of V_{oc} deficit, which is in good correspondence with the experimental information discussed before [34, 37, 70, 77, 79–82, 85, 108, 110, 112, 114].

The identification of trap assisted tunneling recombination as dominant mechanism allows explaining an interesting experimental result concerning CZTSe solar cells, working as a Metal-Insulator-Semiconductor (MIS) structure rather than traditional p–n junction [197]. Solar cells under traditional p–n junction theory support that higher solar cell efficiencies are obtained when increasing CdS donor concentration and thereby its conductivity, since it results in higher depletion region width in the absorber material, thereby increasing carrier separation and recollection. However, the opposite results were reported experimentally for CZTSe solar cells [197], where the authors found that very resistive layers are obtained for CdS films doped with Cu, which result in a V_{oc} increase higher than J_{sc} reduction, and consequently in bigger CZTSe solar cell efficiencies. A very thin and resistive CdS layer behaves as an insulator material, while TCO and CZTSe films stand for conducting (metal) and semiconductor, respectively, thereby having device a MIS structure. Under the dominant role of TATR, for higher CdS layer resistivity values, lower electric field intensities are obtained, consequently reducing losses through tunneling mechanism. Therefore, higher V_{oc} and efficiency values are expected despite the reduction in J_{sc}. In fact, a CZTSe solar cell efficiency near 20% is expected by reducing CdS thickness and increasing its resistivity, without paying attention to CZTSe bulk defects and CdS/CZTSe interface defects [190]. The use of more resistive CdS layers have also resulted in enhanced efficiencies in CdTe solar cells by the V_{oc} enlargement [198–200]. In this sense, depositing very thin and resistive CdS layers it could be an attractive solution to achieve higher experimental efficiencies in kesterite solar cells.

Numerical and analytical results on kesterite solar cells are summarized in table 7. An increased interest in theoretical studies on kesterite solar cells are clearly observed in

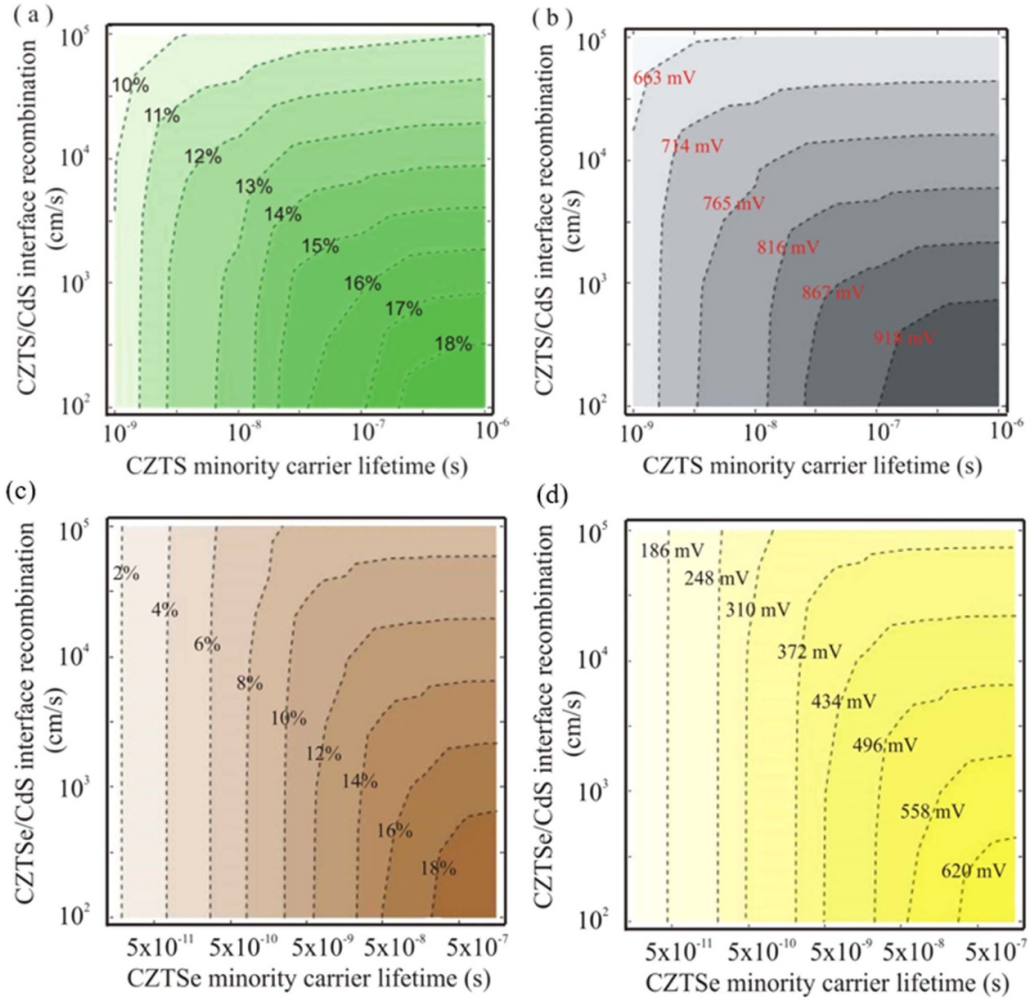

Figure 9. Efficiency and V_{oc} dependence on interface recombination speed and minority carrier lifetime for CZTS and CZTSe solar cells. Reproduced from [188]. © IOP Publishing Ltd. All rights reserved.

the recent years. In general, interesting proposals such as the use of different buffer layers, BSF layers, cationic alloying, graded devices, and tandem structures have been studied, showing promising device results. These works demonstrate that numerical and analytical simulations are powerful tools helping in identifying the main issues limiting kesterite solar cells at the same time they provide interesting routes for the device promotion to be implemented at laboratories.

4.3. Nanostructured solar cells based on kesterite compound

Using nanostructures in photovoltaics is an attractive proposal for high efficiency devices. By controlling nanostructure size, electrical and optical properties can be tailored through the discretization of energy states due to quantum confinement (QC), which is translated into better tunning of incident light utilization. The term "quantum confinement" describes the occurrence in which the characteristics of particles, specifically electrons, are restricted and impacted by their confinement within structures at the nanoscale. This confinement allows energy discretization and modifies physical properties in comparison to larger-scale materials. The observed phenomenon is attributed to characteristics exhibited by quantum systems like nano wires, quantum dots (QDs) and quantum wells (QWs), which possess dimensions on the nanometer scale. Confinement induces discrete energy states rather than continuous energy bands, giving rise to distinct optical, electrical, and chemical properties that play a critical role in diverse applications within the fields of nanotechnology and quantum physics [243]. Quantum confined (QC) structures are categorized into 1D, 2D and 0D material based on the degree of freedom for particle movement in different directions. A 1D material refers to a structure that is constrained, allowing particles to move in only one direction. In other words, the confinement of the particles is imposed in the remaining two directions.

4.3.1. Quantum well solar cells. QWs stand for the most proposed nanostructures in kesterite solar cells. QW solar cells consist of p–i–n structures where QWs are embedded withing the intrinsic region. Since a type-I heterojunction is formed at CZTS/CZTSe with 70% of conduction band offset, by changing S/(S + Se) compositional ratio it is possible to have a continue variation of well depth and barrier height as a

Table 7. Numerical and analytical simulation results on kesterite solar cells.

DEVICE STRUCTURE	SOFTWARE/METHOD	J_{sc} (mA cm^{-2})	V_{oc} (V)	FF (%)	PCE (%)	Year	References
Mo/CZTS/CdS/ZnO:Al	SCAPS	19.31	1.002	75.81	14.7	2012	[141]
Mo/CZTS/CdS/ZnO	AMPS-ID	23.04	0.87	83.0	16.38	2012	[201]
Mo/CZTSSe/CdS/ZnO/TCO	wxAMPS	35	0.54	70	13.23	2014	[142]
Mo/CZTS/CdS/ZnO/ZnO:Al	ANALYTICAL METHOD	20.3	0.661	62.7	8.4	2014	[187]
Mo/CZTSSe/CdS/ZnO	SCAPS	31.98	0.7615	64.73	15.77	2015	[145]
Mo/CZTSe/CdS/ZnO/ZnO:Al	SENTAURUS	37.4	0.377	64.9	9.15	2015	[148]
Mo/CZTS/CdS/ZnO/ZnO:Al	ANALYTICAL METHOD	22.4	0.633	58.3	8.26	2015	[186]
Mo/CZTSSe/CdS/ZnO/TCO	ADEPT	35.6	0.4	68	9.68	2016	[143]
Mo/CZTSe/CdS/ZnO/TCO/ MgF_2	ADEPT	35.2	0.4	66.2	9.3	2016	[144]
Mo/CZTS/CdS/ZnO/ZnO:Al	SCAPS	23.1	1.114	82.5	21.3	2016	[146]
Mo/CZTS/CdS/ZnO/ZnO:Al	SCAPS	18.68	1.009	77.29	14.57	2016	[147]
Mo/CZTS/CdS/ZnO/ZnO:Al	ANALYTICAL METHOD	22.7	0.775	63.8	11.2	2016	[188]
Mo/CZTSe/CdS/ZnO/ITO	ANALYTICAL METHOD	40.9	0.733	75.4	22.6	2016	[190]
Mo/CZTSSe/ZnS/ZnO	SCAPS	23.96	0.64	65.2	10.0	2017	[202]
Mo/CZTSSe/CdS/ZnO/ZnO:Al	SCAPS	38.81	0.67	60.48	15.60	2017	[131]
Mo/CZTSe/ZnS/ZnO/TJ*/CZTS/ZnS/ZnO/AZO	ANSYS LUMERICAL FDTD	19.59	1.492	73.4	21.44	2017	[173]
Mo/CZTSe(p+)/ACZTSe/ZnS/ZnO/ITO/CZTS/ZnS/ ZnO/FTO/CBTSSe/ ZnS/ZnO/ZnO:Al	ANSYS LUMERICAL FDTD	17.88	2.73	73.7	36.04	2017	[203]
Mo/CZTS/CdS/ZnO	SCAPS	44.87	0.64	82.54	23.72	2018	[204]
Mo/CZTS/CdS/ZnO/ZnO:Al	SCAPS	21.88	0.921	71.6	14.4	2018	[167]
Mo/$MoS(e)_2$/CZTSSe/SnS_2/ZnO/ZnO:Al	SCAPS	27.98	0.5230	67.34	12.57	2018	[205]
Mo/ CZTSe/CdS/ZnO/ZnO:Al/CZTS/CdS/ZnO/ZnO:Al	SCAPS	20.98	1.324	78.2	21.7	2018	[206]
Mo/CZTS/CdS/ZnO/TCO	ANALYTICAL METHOD	28.5	0.889	65.9	16.9	2018	[207]
ITO/CZTS/ACZTS/ZnS/ZnO/ZnO:Al/MgF2	ANSYS LUMERICAL FDTD	26.57	0.975	76.70	19.86	2018	[208]
Mo/CZTSSe/CdS/ZnO/ITO	ANALYTICAL METHOD	41.2	0.59	72	17.5	2018	[185]
Mo/ CZGS/CdS/ZnO/ZnO:Al	ANALYTICAL METHOD	17.98	1.619	91.91	12.08	2018	[61]
Mo/MoS_2/CZTS/CdZnS/ZnO/ITO	SCAPS	28.25	0.54	70	10.69	2019	[158]
Mo/CZTSSe/CdS/ZnO/CZTS/CdS/ZnO/TCO	ANALYTICAL METHOD	19.8	1.42	71.5	20.03	2019	[174]

(Continued.)

Table 7. (Continued.)

Mo/ACZTSe/CdS/ZnO/ZnO:Al	SCAPS	28.1	0.619	64.5	11.2	2019	[209]
Mo/CZTSe/CdS/ZnO/ITO	ANALYTICAL METHOD	34	1.0	88	29.9	2019	[210]
Mo/MoSSe/CZTSSe/CdS/ZnO/ZnO:Al/MgF2	FINITE ELEMENT METHOD	35.34	0.501	65.62	11.62	2020	[149]
Mo/CZTS/CdS/ZnO	SCAPS	22.91	0.78	78.8	16.28	2020	[211]
Mo/MoSSe/CZT(S,Se)/CdS/ZnO/AZO/MgF_2	SCAPS	38.1	0.631	76.8	18.47	2020	[165]
Mo/CZTSSe/CZTS/CdS/ZnO/ZnO:Al	SCAPS	25.84	0.986	69.87	17.81	2020	[168]
Mo/MoSSe/CZTSSe/CdS/ZnO/AZO/MgF_2	DIFERENCIAL EVOLUTION ALGORITHM (DEA)	37.39	0.772	75.2	21.74	2020	[136]
Mo/SnS/CZTSe/CdS/ZnO/TJ*/SnS/CZTS/CdS/ZnO	FINITE ELEMENT METHOD	23	1.72	72.69	28.86	2020	[212]
Mo/CZTSSe/CdS/ZnO/ZnO:Al	SCAPS	42.64	0.724	74.96	23.16	2020	[213]
Mo/SnS/CBTSSe/CdS/ZnO/ITO	SCAPS	16.986	0.867	49.63	7.31	2020	[214]
Ni/SnS/CZTS/TiO_2/ITO/Al	SCAPS	31.89	1.099	87.85	30.79	2021	[154]
Mo/CZT(S,Se)/CdS/ZnO/ZnO:Al	SILVACO ATLAS (TCAD)	13.32	0.998	85.28	11.34	2021	[163]
Mo/CZT(S,Se)/CdS/ZnO/ZnO:Al	SILVACO ATLAS (TCAD)	40.66	0.640	81.17	21.15	2021	[164]
Glass/ITO/CZTSe(p+)/ACZTSe/ CdS/AZO/MgF_2	ANSYS LUMERICAL FDTD	38.99	0.6467	73.89	18.63	2021	[166]
Mo/CZTSe/CZTS/CdS/ZnO/ZnO:Al	wxAMPs	21.58	0.883	89.02	21.1	2021	[170]
Mo/CZTS/CdS/ZnO/ZnO:Al	wxAMPS	29.18	0.8514	63.41	15.04	2021	[172]
Mo/CZTSSe/CdS/TCO/CZTS/CdS/ZnO	SCAPS	18.6	1.21	66	15.12	2021	[175]
Si(p+)/Si/Si(n+)/CZTS/ZnMgO/ZnO/ZnO:Al	SCAPS	19.38	1.4	83.5	22.9	2021	[215]
Mo/CZTSSe/CdS/ZnO/ZnO:Al/TJ*/CZTS/ CdS/ZnO/ZnO:Al	SCAPS	20.40	1.10	81.30	19.25	2021	[216]
ITO/CZTS(p+)/CZTS/ZnOS/ZnMgO:Ga	SCAPS	27.74	1.040	71.40	20.6	2021	[217]
Mo/CZTS/MoS_2/ZnO:Al	SCAPS	28.96	0.84	85	23.69	2021	[218]
Mo/CZTSe/CZTS/CdS/ZnO/FTO	SCAPS	35.18	1.01	83.86	29.86	2021	[219]
Ni/SnSe/CZT($S_{0.4}Se_{0.6}$)$_4$/ Zn($O_{0.3}S_{0.7}$)/i-ZnO/AZO	SCAPS	35.25	0.640	77.52	17.55	2021	[220]
Mo/$MoSe_2$/CZTSe/CdS/ZnO:Al	SCAPS	42.44	0.745	79.31	25.40	2021	[221]
Mo/CZTSSe/CdS/ZnO/ZnO:Al	SCAPS	30.03	0.73	69.17	15.35	2021	[222]
Mo/CZTSe/CZTS/ZnSe/ZnO/ZnO:Al	SCAPS	22.26	1.14	83.28	21.17	2021	[223]
Mo/CZTSSe/CdS/ZnO/ITO	SILVACO ATLAS	44	0.45	62.7	12.2	2021	[224]
Mo/MoS_2/CZTS/TiO_2/ITO	AMPS-1D	18.75	0.87	85.85	14.5	2022	[155]

(Continued.)

Table 7. (Continued.)

DEVICE STRUCTURE	SOFTWARE/METHOD	J_{sc} (mA cm^{-2})	V_{oc} (V)	FF (%)	PCE (%)	Year	References
Mo/CZTSSe/GaSe/n-ZnO	SCAPS	36.45	0.685	81.7	20.4	2022	[159]
Mo/ACZTSe/ZnSe/ZnO/TJ*/CZTS/ZnOS/ZnMgO:Ga	SCAPS	17.3	1.37	68.3	16.2	2022	[176]
Mo/CZTSe/CdS/ZnO/ZnO:Al /CZTS/CdS/ZnO/ZnO:Al	SCAPS	20.33	1.48	75.94	22.91	2022	[177]
Mo/CZTSe/CdS/ZnO/ITO /CZTS/CdS/ZnO/ZnO:Al	SCAPS	16.67	1.28	78	23.83	2022	[178]
Mo/CZTSSe/CdS/ITO/Spiro/$CsPbI_3$/ZnS/ZnO/ITO	COMSOL	—	—	—	32.35	2022	[182]
Ni/Zn_3P_2/CZTSSe/ZTO/ ZnO/ZnO:Al/Zn_3P_2/CZTS/ZMO/ ZnO/ZnO:Al	SCAPS	21.09	1.52	74	23.99	2022	[225]
Mo/ACZTS/CZTS/CdS/ZnO/ZnO:Al	SCAPS	37.17	0.93	68.15	23.50	2022	[226]
Au/CuI/CZTS/ZnS/ZnO/ZnO:Al	SCAPS	23.89	0.93	69.6	15.53	2022	[227]
Mo/CZTS-II/CZTS-I/ZnS/ZnO/ZnO:Al	SCAPS	26.44	1.04	74	20.34	2022	[228]
Mo/CMTS/SnS_2/ZnO/ZnO:Al	SCAPS	26.44	1.12	68.33	20.26	2022	[229]
Pt/CZTSe/CZTS/ SnS_2/ZnO:Al/FTO	SCAPS	50.76	0.9926	64.59	32.55	2022	[230]
Mo/CZTS(p+)/CZTS/CdS/GZO	SCAPS	21.12	0.756	66.87	10. 68	2022	[231]
Mo/CZTS/ZrS_2/ZnO:Al	SCAPS	27.75	0.776	84.75	17.61	2022	[232]
Mo/AMTSSe/ZnSe/ZnO/ZnO:Al	SCAPS	36.20	0.774	76.20	21.35	2022	[233]
Mo/$MoSe_2$/CNGS/CdS/ZnO/ZnO:Al	SCAPS	29.039	0.648	58.07	10.94	2022	[234]
Mo/CCTS/CdS/ZnO:Al	SILVACO TCAD	26.3	0.988	81.6	21.2	2022	[235]
Mo/CZTSSe/CdZnS/ZnO	SCAPS	35.60	0.6700	77.61	14.59	2023	[236]
Mo/CZTSSe/In(O,S)/ZnO/ITO	TCAD simulator	43.43	0.574	66.08	16.48	2023	[237]
Sn_2S_3/CZTSSe/CdS/ZnO/ZnO:Al	SCAPS	14.9	1.7	65.3	16.58	2023	[180]
NiO/$Cs_2AgBi_{0.75}Sb_{0.25}Br_6$/PCBM/ SnO_2							
Mo/CZTSSe/ZnSe/ZnO/ZnO:Al/Cu_2O/ $Cs_2AgBi_{0.75}Sb_{0.25}Br_6$/ZnS	SCAPS	17.90	2.31	69	28.42	2023	[181]
Al/Si(p+)/Si/Si(n+)/CZGSSe(p+)/CZGSSe/ CdS/ZnO/ITO/Al_2O_3	SCAPS	17.32	1.961	84.3	28.63	2023	[183]
Al/Si(p+)/Si/Si(n+)/CFTS/CdS/ITO	SCAPS	22.22	1.81	87.61	35.23	2023	[184]
Mo/(ACC)ZTSSe/CdS/ZnO/ZnO:Al	SCAPS	32.6	0.75	79	19.3	2023	[238]
Mo/$MoSe_2$/CCGS/CdS/ZnO/ZnO:Al	SCAPS	25.09	0.93	64.06	15.1	2023	[239]
Mo/MoSe2/CNGS/CdZnS/ZnO/ZnO:Al	SCAPS	29.67	0.983	66.77	20.05	2023	[240]
Mo/CZTS/ZMO/ZnO/ITO	SCAPS	27.25	1.115	64	22.5	2024	[157]
Mo/SnS/CZTSSe/CdS/ZnO/ZnO:Al	SCAPS	38.287	0.847	74.50	24.1	2024	[169]
$MoSe_2$/CZTSSe/WS_2/i-ZnO/ZnO:Al	SCAPS	24.96	0.6920	83.28	14.38	2024	[171]
Mo/CZTSe/ACZTSe/ZnSe/ZnO/ ZnO:Al/ACZTS/CZTS/ ZnMnO/$SnMnO_2$	SCAPS	20.29	1.64	72.05	23.96	2024	[179]
Mo/CZTSe/CZTS/ZnS/ZnO:Al	SCAPS	28.2	1.05	85.4	24.7	2024	[241]
Ni/CNTS/CZTS/WS_2/FTO/Al	SCAPS	31.75	1.08	88.04	30.26	2025	[242]

TJ* tunneling junction.

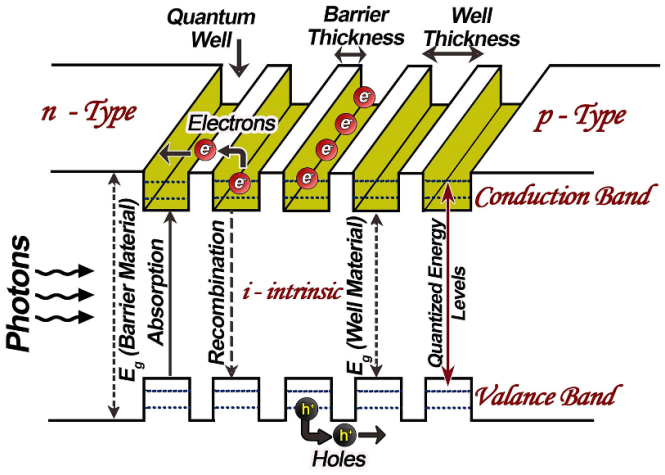

Figure 10. Energy band diagram of multiple quantum well solar cells. © [2021] IEEE. Reprinted, with permission, from [246].

function of composition [4]. In particular, barriers based on CZTS are desirable to keep the highest V_{oc} reported for CZTSSe compound [118, 121], while the incorporation of QWs based on CZTSSe would guarantee an extra photon absorption in comparison to traditional CZTS solar cells, that could result in higher efficiencies. The selection of the QW material is typically based on its narrower bandgap energy in comparison to the barrier layers that surround it. This feature facilitates discrete energy levels formation at QWs, thereby improving absorption and emission processes [244–246]. Figure 10 illustrates the schematic representation of energy band diagram and the carrier separation mechanism in Multiple QWs (MQWs).

In order to minimize carrier recombination, it is imperative that the QW material possesses favorable electronic properties. The barrier material must have a bandgap energy that is greater than that of the QW material. The purpose of this mechanism is to establish an energy barrier that effectively restricts the charge carrier movement in QWs. The barrier material is essential for preventing carrier leakage and ensuring effective confinement [247]. In instances where electron and hole incoming energy exceeds the barrier bandgap, the QWSC operates similarly to a conventional p–i–n device. Within this specified range, the material exhibits conventional behavior by effectively absorbing photons and subsequently converting their energy into electricity through standard processes [247, 248]. Photons within the energy range spanning from the barrier bandgap to the QW bandgap undergo absorption by the QWs. The enhancement of photon absorption is attributed to the quantized energy levels present within the QW (figure 10). When photons are absorbed, they have the ability to stimulate the creation of excitons within the QWs by exciting electron–hole pairs [248]. The carrier in an excited state will experience escape mechanisms, such as thermionic emission and tunneling through the barrier, assisted by the junction electric field [248].

The first proposal on QWSC was presented by Barnham and Duggan in 1990 [249] followed by some scientific pivotal works concerning the implementation of MQWs based on different materials in solar cells. In the first work of Barnham and Duggan [249] they introduced a novel method for enhancing the efficiency of multiband gap solar cells through the use of MQW or superlattice (SL) systems. By modifying the QW thickness, it is possible to tune band gap to achieve the best efficiencies. This method enables the fine-tuning of current and voltage production factors individually, which could result in increased efficiencies. According to the study, structures utilizing the AlGaAs/GaAs/InGaAs system have the potential to achieve efficiencies that go beyond current single-band-gap limits, with maximum values surpassing 40%. Challenges involve maintaining resonant conditions for electrons and ensuring efficient charge separation and collection. This study emphasizes the possibility of utilizing QWs as the main absorber system in photovoltaics, specifically in InGaAs/GaAs and AlGaAs/GaAs MQW or SL. Anderson [245] devised and compared a suitable framework for QW solar cells with a framework tailored for bulk homojunction cells. The investigation examined the influence of terminal properties on both cell and QW parameters. The model used the QW and barrier band gaps as inputs to determine V_{oc}, J_{sc}, and PCE. The model's conclusions were congruent with the actual data, yielding a full comprehension of the functioning of QW solar cells. The research presented a model that especially focuses on carrier creation and recombination within QWs. In another work, Barnham *et al* [250] examined both theoretical and practical aspects of QW solar cells to offer context for the more detailed pieces in these proceedings. This article explores the role that QWs play in enhancing efficiency in fully realized lattice-matched material systems. It also dives into the basic studies of radiative recombination that are relevant to figuring out whether comparable improvements may be attained in perfect cells. Bushnell *et al* [251] presented the effect of adding more QWs in strain-compensated, multiquantum-well solar cells, using GaInP for the upper cell and GaAs for the lower cell. The study showed a steady increase in the dark current level as the number of wells increased near the operating point. Besides, J_{sc} in the AM0 spectrum increased in a linear fashion with the addition of more QWs, allowing the device to keep a steady V_{oc} regardless of the well number. This adjustability could be advantageous for replacing the GaAs junction in tandem and triple-junction cells, helping to align current levels with the upper junction without sacrificing voltage performance. The study suggested that incorporating rear surface distributed Bragg reflectors could improve current levels and efficiency. The influence of electric field on absorption and tunneling processes in QWSCs was studied by Jani and Honsberg [252]. It was found that electric field favors tunneling mechanism of photogenerated carriers being carrier transport improved.

Creating semiconductor structures for MQWSC requires using various advanced methods, each with unique benefits for managing material characteristics and device efficiency. With its precise deposition of atoms or molecules onto a substrate in ultrahigh vacuum conditions, Molecular Beam Epitaxy (MBE) is a standout technique [253, 254]. With this method, researcher have exceptional control over layer thickness and

composition, making it perfect for growing the alternating semiconductor layers needed for MQWSC structures [255, 256]. Through meticulous manipulation of these layers, engineers can customize the bandgap and other characteristics to enhance PCE [257]. Utilized in the production of epitaxial layers of semiconductor materials, Metalorganic Chemical Vapor Deposition (MOCVD) is a commonly employed technique [258, 259]. Through the use of metalorganic precursors and gases on a heated substrate, MOCVD allows for the creation of thin layers of semiconductor material with exceptional uniformity and consistency [260, 261]. This technique is ideal for the large-scale production of semiconductor devices such as MQWSC, ensuring consistent performance throughout extensive production cycles [262]. Utilizing hydrogen chloride as a carrier gas, hydride vapor phase epitaxy (HVPE) is another growth technique [263]. HVPE is ideal for growing III–V semiconductor compounds and forming QW structures in solar cells [264]. This technique provides benefits like rapid growth rates and accurate regulation of layer thickness, which are valuable for effectively producing MQWSC [265]. Metalorganic vapor phase epitaxy (MOVPE), also referred to as organometallic vapor phase epitaxy [266, 267], is akin to MOCVD but employs distinct precursors [268]. With this method, one can create advanced semiconductor layers while maintaining precise control over doping levels and material characteristics [269].

4.3.2. QC solar cells based on kesterite material. Kesterite material has garnered global interest due to its potential use in solar cells for high efficiency. Currently, there is a strong focus on researching high-performance CZTSSe solar cells in the realms of material engineering and architectural design. The CZTSSe devices have achieved a maximum PCE of 14.9% [2]. Although the PCE is low, higher values could be even achieved by incorporating kesterite QC structures because of its band gap tuning and strong absorption capabilities [270]. This section delves into the latest research findings on implementing QC structure using kesterite material among researchers. In order to increase efficiency via improved photon absorption, especially for photons with energy lower than the corresponding band gaps, theoretical research suggests integrating QCs into Kesterite solar cells. In a research conducted by Arul *et al* [271], they detailed the synthesis and analysis of kesterite phase CZTS nanospheres using a solvothermal technique. Several analytical methods such as XPS, XRD, SEM, HRTEM, and UV-vis absorption spectroscopy were utilized to validate the structure and properties of the nanospheres. The CZTS nanospheres displayed QC effects, featuring a band gap of 1.84 eV. By integrating them into organic photovoltaic cells, there was a substantial boost in PCE to 0.952%, surpassing the PCE of cells lacking CZTS nanospheres (0.120%). Indications point to CZTS nanospheres showing potential for advanced third-generation photovoltaic devices. The first proposal on the QWs incorporation into kesterite devices was presented by Courel [272]. The theoretical results showed significant progress in efficiency, with an expected increase of 45.8%, along with enhancements in current density by 30.5% and voltage by 10.7% compared to devices without nanostructures. In this work, it was suggested utilizing 50 wells with varying thicknesses from 20 to 80 nm. When QWs are added to Kesterite cells, there is potential for efficiency gains of 45.8%. In particular, by adding 50 wells, keeping barrier and well thicknesses of 5 and 90 nm, respectively, the best solar cell efficiency was achieved. Despite this first proposal was based on QWs, this work opened up opportunity areas for other type of nanostructures for higher PCE compared to devices without nanostructures. The incorporation of QWs to improve kesterite devices was also evaluated by Sravani *et al* [273], obtaining a substantial increase in carrier photogeneration when using 100 wells. An efficiency of 24.8%, a FF of 79.8%, and an EQE higher than 80% were reported for kesterite devices with 50 wells, corroborating the effectiveness of nanostructures such as QWs in promoting solar cell efficiency. These works set a new research direction on nanostructured kesterite solar cell with a particular focus on device design and its processing. Another interesting proposal to increase kesterite solar cell efficiency was presented by Sahoo *et al*, by incorporating CZTSe QDs into CZTS barrier material [274]. This research studied the optical and electrical performance, focusing on carrier quantization effects and trap-assisted recombination. An efficiency of 11.27% was demonstrated for kesterite solar cells with CZTS/CZTSe QDs under IR losses, making this proposal attractive for experimental applications. The use of quantum engineering in CZTSSe devices was explored by Chandrasekar *et al* [246]. In this study the incorporation of QWs was proposed, adjusting Se and S content with the purpose of achieving the device efficiency improvement. By fine tuning the S/(S + Se) composition, a solar cell efficiency of 38% was found, with a FF value of 88%. This work also highlights that the increase of well number has a negative impact on V_{oc}. On the other hand, in order to solve typical issues of kesterite solar cells—absorber/buffer interface, poor absorption of photons with long wavelengths, and non-ohmic contact—a study focused on the incorporation of Cd-free buffer layer consisting of Zn(O,S), multiple QWs based on CZTSSe to enhance photon absorption, and the use of SnSe as BSF to reduce contact resistance effect from the theoretical point of view was presented [275]. Through the optimization of the device, it was pointed out that solar cell efficiency over 20% can be achieved.

A detailed study on the influence of CZTSSe QW incorporation into CZTSSe devices was recently reported by Rodriguez–Osorio *et al* in 2023 under the radiative limit [276]. The authors evaluated in a first step the highest PCE of CZTSSe bulk solar cells, followed by the estimation of device efficiency when incorporating QWs under different conditions. The influence of well thickness and number on PCE, V_{oc} and J_{sc} is shown in figure 11. While a maximum PCE of 29.7% is expected in kesterite devices without nanostructures [272], the QW incorporation allows a high PCE value of 36.3% (figure 11(a)), which is a consequence of the high J_{sc} observed (48 mA cm^{-2}) due to the extra photon absorption by wells (figures 11(b)) and a V_{oc} about 867 mV, dominated by bulk CZTS material (figure 11(c)). An important result from figure 11 is that well thickness plays a dominant role rather

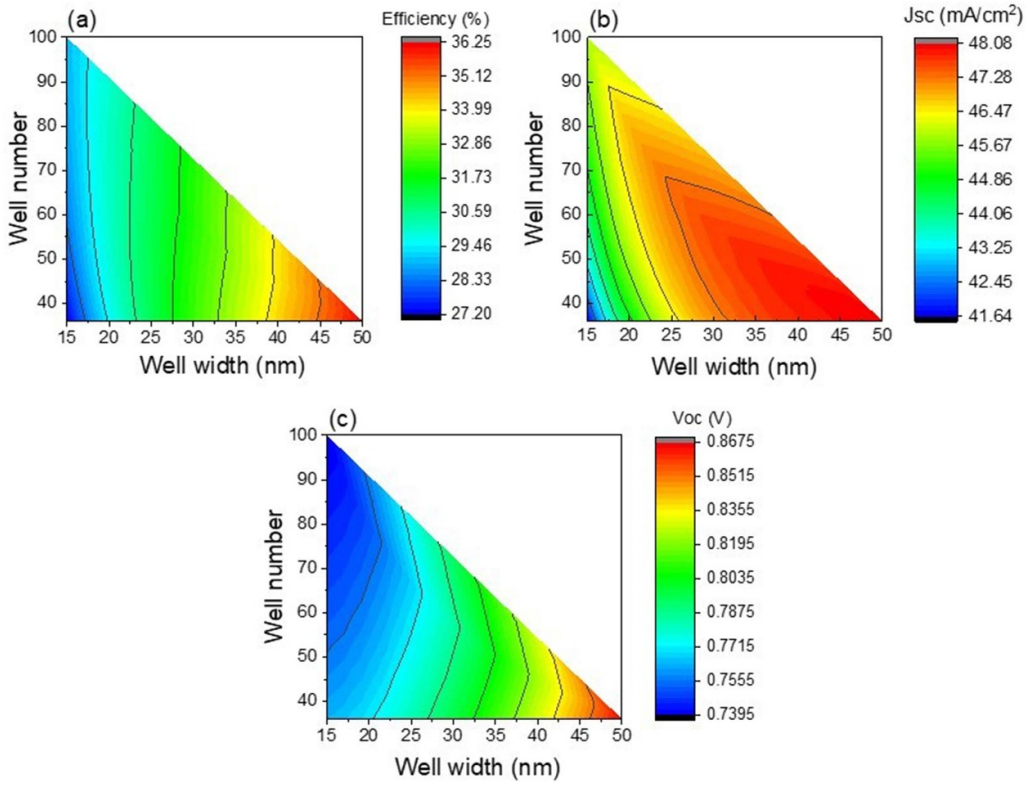

Figure 11. Contour plots of PCE (a), J_{sc} (b), and V_{oc} (c) as functions of well number and thickness. Reproduced from [276]. CC BY 4.0.

than well number, since higher well thicknesses imply higher discrete energy formations and consequently bigger absorption. This work also points out that a thickness bigger than 20 nm is required to achieve performances higher than that of devices without nanostructures. In particular, a 36.3% is expected when 36 wells of 50 nm are used.

The study on the role of well and barrier compositions was also performed by Rodriguez–Osorio *et al* under the radiative limit; results are presented in figure 12 [276]. A change in S/(S + Se) composition from 0 to 1 implies changing from CZTSe to CZTS properties. Consequently, the lowest well compositions are translated into the highest J_{sc} due to the presence of deep wells favoring photon absorption, while the highest barrier composition results in the biggest V_{oc} due to higher separation of quasi-fermi levels. This mentioned trade-off between J_{sc} and V_{oc} yields to a maximum efficiency of 37.5% for well composition about 0.25 and a barrier of CZTS (composition of 1) as shown in figure 12. In this sense, it is corroborated the hypothesis for CZTSSe nanostructured solar cells, where the use of CZTS as barrier material would guarantee keeping the highest reported V_{oc} for this technology while increasing photon absorption due to the use of CZTSSe well material, thereby promoting solar cell efficiency.

Most important results on the use of nanostructured kesterite for its application into photovoltaics are presented in table 8. Efficiencies reported refers to either absolute values or relative values when compared to solar cells without nanostructures. Furthermore, information on the type of QC (0D and 2D), the material, and the nature of the study (experimental or theoretical) are also given in table 8. Cited experimental and theoretical works remark the potential use of nanostructures in kesterite solar cells for efficiency promotion. Therefore, this emerging field is an open research, being necessary further experimental and theoretical studies that provide conditions for efficiency enlargement.

The utilization of kesterite materials in QWSCs is a highly fascinating avenue for researchers. Although the potential of QWSCs is clear, the use of kesterite materials brings about new challenges and possibilities for further research in fabrication techniques. Compounds like Kesterite, such as CZTS, CZTSSe, or similar alloys, have several benefits including their abundance, non-toxic nature, and compatibility with affordable processing techniques. The insight knowledge on material properties, phase purity, defect engineering and interface control it is a first important step to achieve the goal of optimizing the fabrication process for kesterite QW solar cells. The scientific community is currently studying different methods such as solution-based techniques, vacuum deposition, and hybrid approaches in search for the fine control of structure, composition and morphology of kesterite thin films. The goal is to enhance carrier transport and light absorption in QWSCs. In addition, researchers are investigating various strategies to reduce recombination losses and improve the performance of devices. These include bandgap engineering, interface passivation, and surface modification. This ongoing research highlights the promising potential of kesterite-based

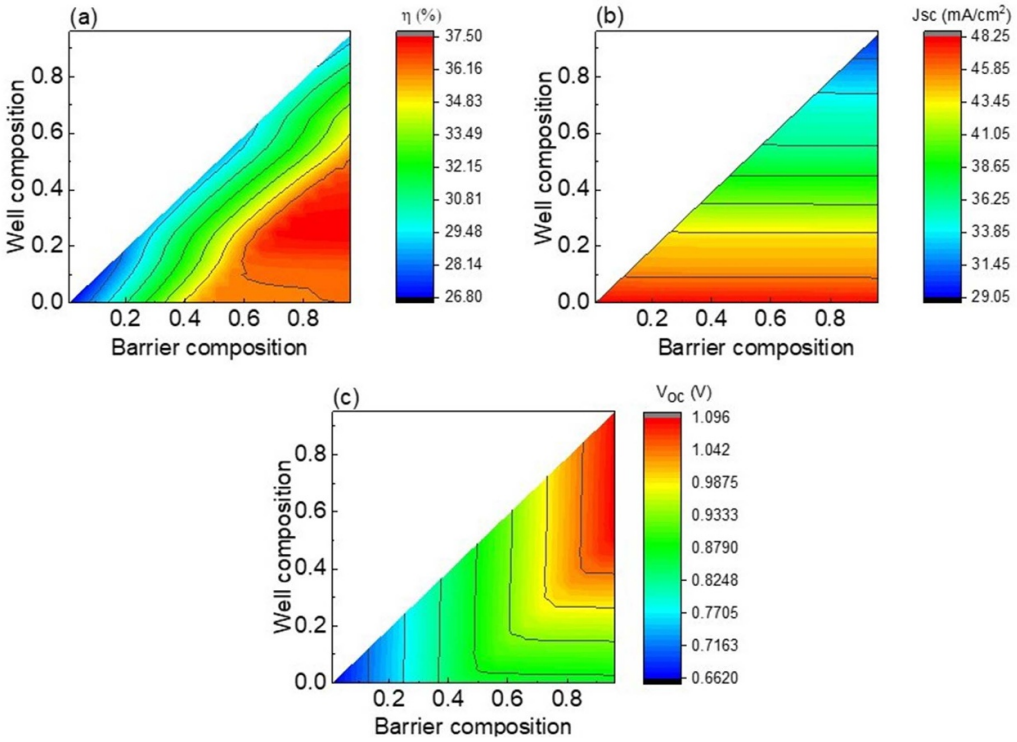

Figure 12. Contour plots of PCE (a), J_{sc} (b), and V_{oc} (c) as functions of barrier and well compositions. Reproduced from [276]. CC BY 4.0.

Table 8. Comparing kesterite-based QC structures in terms of their achieved efficiency, materials, and confinement methods.

Authors	Year	Materials	η (%)	QC	Study
Xu *et al* [277]	2012	CZTS	3.73	0D	Experimental
Cao *et al* [278]	2013	CZTSSe	3.01	0D	Experimental
Arul *et al* [271].	2013	CZTS	0.95	0D	Experimental
Gu *et al* [279]	2014	CZTS	0.27	0D	Experimental
Mahajan *et al* [280]	2018	CZTS	2.08	0D	Experimental
He *et al* [281]	2019	CZTSSe	3.54	0D	Experimental
Das *et al* [282]	2019	CZTS	—	0D	Experimental
Das *et al* [283]	2019	CZTS	—	0D	Experimental
Courel [272]	2019	CZTSSe	45.8	2D	Theoretical
Zhou *et al* [284]	2019	CZTS	4.84	0D	Experimental
Das *et al* [285]	2020	CZTS	4.12	0D	Experimental
Sravani *et al* [273]	2020	CZTSe	24.8	2D	Theoretical
Sahoo *et al* [274]	2021	CZTSe	11.27	0D	Theoretical
Chandrasekar *et al* [246]	2021	CZTSSe	38	2D	Theoretical
Das and Mahanandia [286]	2022	AZTS	6.28	0D	Experimental
Das *et al* [287]	2022	CZTS	6.11	0D	Experimental
Palanisamy *et al* [288]	2023	CZTSSe	9.6	2D	Theoretical
Chandrasekar *et al* [289]	2023	CZTSSe	21	0D/2D	Theoretical
Rodriguez–Osorio *et al* [276]	2023	CZTSSe	37.5	2D	Theoretical
Chris *et al* [290]	2023	CZGSSe	29	2D	Theoretical

QWSCs as a viable solution for sustainable and cost-effective solar energy conversion. In general, QC-based kesterite solar cells have shown great potential for enhancing kesterite solar cell efficiency. However, there is still a need for technological advancements in the fabrication of QWSCs using kesterite materials. Although there has been significant advancement in QD-based configurations, the fabrication techniques for QWSCs still pose challenges. To guarantee the control of very thin thickness and composition of kesterite materials in QWs, a precise deposition technique such as MBE is required. So far, there is only few experimental works reported on the fabrication of kesterite material by MBE [291–297]. However, very low deposition rates of 1 Å s^{-1} reported for CZTSSe growth [292, 293], open the way for future fabrication of very thin kesterite layers with the precise composition control for well and barriers materials.

5. Conclusions and perspectives

In short, the ongoing research on CZTSSe photovoltaics is focused on several key areas that aim to enhance performance and viability of this technology. One of the primary research areas is material engineering, where efforts are being made for enhancing CZTSSe composition and properties to optimize device efficiency. Recent studies have shown promising results in tailoring the bandgap of CZTSSe to better match the solar spectrum, thereby improving light absorption and overall efficiency. Interface and bulk defect passivation are crucial for improving CZTSSe solar cell performance and stability. In particular, advanced interface materials and passivation layers have shown promising results in reducing recombination losses. The optimization of CZTSSe solar cells is also an opportunity area for further efficiency enhancement, with particular emphasis on material designs, interface engineering, and innovative proposals that boost photon absorption, carriers recollection and reduce parasitic losses. Recent results have shown the potential of advanced device architectures to enhancing solar cell efficiency and stability. Particularly, the use of band gap gradings is potentially attractive for improving photon absorption and carrier transport, however, more works are needed to the complete understanding of the potential and challenges of this proposal. Recently, the application of CZTSSe material into tandem solar cells has been presented as an emerging field. The combination of CZTSSe subcells with other such as perovskite or silicon are quite promising for boosting solar cell efficiency. Furthermore, the use of nanostructured kesterite material into solar cells is also an interesting area for the next generation of solar cells. By controlling nanostructure properties such as size and composition it is possible to achieve higher photon absorption that could result in bigger solar cell efficiency. In particular, experimental and theoretical works on the use of QWs and QDs into solar cells have demonstrated not only higher efficiency than devices without nanostructures but also the potential to overcome the Shockley–Queisser limit. However, for achieving efficiency higher than 30% with the use of this type of nanostructures, future experimental works should be focused not only on mitigating bulk and interface defects but also on the fine control of MBE technique that result in very thin layers with the required compositions. With the effective development of nanostructured devices such as QWSCs and tandem, it would be possible to make a step forwards the fabrication of tandem devices with the incorporation of nanostructures, which are expected to result in efficiency values higher than 50%. Overall, the future research directions for CZTSSe photovoltaics are characterized by a multidisciplinary approach that encompasses material engineering, defect passivation, device architecture optimization, and the exploration of novel proposals such as nanostructured and tandem solar cells. Recent technological advancements and research findings provide a strong foundation for continued progress in these research areas, positioning CZTSSe devices as a promising photovoltaic technology with the potential for high efficiency and widespread commercialization.

Data availability statement

All data that support the findings of this study are included within the article (and any supplementary files).

Acknowledgment

K.G Rodriguez-Osorio acknowledges fellowship support received from Conahcyt for PhD studies. J. A. A.-A. acknowledges that this publication is part of the JDC2023-051452-I grant, funded by MICIU/AEI/10.13039/501100011033 and by the FSE+. M. Courel thanks support from pro-SNI of University of Guadalajara. L.M.P. acknowledges financial support from the ANID through Convocatoria Nacional Subvención a Instalación en la Academia Convocatoria Año 2021, Grant SA77210040. LMP and DL acknowledge partial financial support from FONDECYT 1240985.

ORCID iDs

K G Rodriguez-Osorio https://orcid.org/0009-0001-3464-1354
J A Andrade-Arvizu https://orcid.org/0000-0001-6643-7270
I Montoya De Los Santos https://orcid.org/0000-0003-3664-1881
F J Sánchez-Rodríguez https://orcid.org/0000-0003-2503-1586
L A Sánchez-Hernández https://orcid.org/0009-0004-6123-2849
D Laroze https://orcid.org/0000-0002-6487-8096
S Routray https://orcid.org/0000-0001-7217-3515
Maykel Courel https://orcid.org/0000-0001-9149-3506

References

[1] Li J *et al* 2020 Defect control for 12.5% efficiency $Cu_2ZnSnSe_4$ kesterite thin-film solar cells by engineering of local chemical environment *Adv. Mater.* **32** 2005268
[2] Li Y, Cui C, Wei H, Shao Z, Wu Z, Zhang S, Wang X, Pang S and Cui G 2024 Suppressing element inhomogeneity enables 14.9% efficiency CZTSSe solar cells *Adv. Mater.* **36** 2400138
[3] Green M A, Dunlop E D, Yoshita M, Kopidakis N, Bothe K, Siefer G, Hinken D, Rauer M, Hohl-Ebinger J and Hao X 2024 Solar cell efficiency tables (Version 64) *Prog. Photovolt., Res. Appl.* **32** 425–41
[4] Chen S, Walsh A, Yang J-H, Gong X G, Sun L, Yang P-X, Chu J-H and Wei S-H 2011 Compositional dependence of structural and electronic properties of $Cu_2ZnSn(S,Se)_4$ alloys for thin film solar cells *Phys. Rev.* B **83** 125201
[5] Li J, Sun K, Yuan X, Huang J, Green M A and Hao X 2023 Emergence of flexible kesterite solar cells: progress and perspectives *npj Flex. Electron.* **7** 16
[6] Ito K 2014 *Copper Zinc Tin Sulfide-based Thin-film Solar Cells* (Wiley) 10.1002/9781118437865
[7] Benisha C A and Routray S 2022 Performance enhancement of kesterite solar cell with doped-silicon back surface field layer *Silicon* **14** 8045–54
[8] Adachi S 2015 *Earth-abundant Materials for Solar Cells: Cu2-II-IV-VI4 Semiconductors* (Wiley) (https://doi.org/10.1002/9781119052814)

[9] Craig J R 2009 The ore minerals under the microscope: an optical guide. Bernhard Pracejus, Editor. Atlases in Geo-sciences, 3. 2008. Elsevier, Amsterdam. Pp. 894 *Econ. Geol.* **104** 759–60

[10] Ivanov V V and Pyatenko Y 1959 On so-called kesterite *Zap Vses. Miner. Obshch.* **88** 165–8 (in Russian)

[11] Nitsche R, Sargent D F and Wild P 1967 Crystal growth of quaternary 122464 chalcogenides by iodine vapor transport *J. Cryst. Growth* **1** 52–3

[12] Hahn H and Schulze H 1965 Über quaternäre Chalkogenide des Germaniums und Zinns *Naturwissenschaften* **52** 426

[13] Nakazawa K I 1988 Electrical and optical properties of stannite-type quaternary semiconductor thin films *Jpn. J. Appl. Phys.* **27** 2094

[14] Katagiri H, Sasaguchi N, Hando S, Hoshino S, Ohashi J and Yokota T 1997 Preparation and evaluation of Cu_2ZnSnS_4 thin films by sulfurization of E-B evaporated precursors *Sol. Energy Mater. Sol. Cells* **49** 407–14

[15] Friedlmeier T M, Wieser N, Walter T, Dittrich H and Schock H W 1997 Heterojunctions based on Cu_2ZnSnS_4 and $Cu_2ZnSnSe_4$ thin films *Proc. 14th European Conf. Photovoltaic Science and Engineering and Exhibition* vol 1242 (available at: www.tib.eu/en/search/id/BLCP:CN023425275/Heterojunctions-Based-on-Cu∼2ZnSnS∼4-and-Cu∼2ZnSnSe∼4?cHash=85fa1f2d94f7dd48648a1b8a11f22e16)

[16] Katagiri H, Saitoh K, Washio T, Shinohara H, Kurumadani T and Miyajima S 2001 Development of thin film solar cell based on Cu_2ZnSnS_4 thin films *Sol. Energy Mater. Sol. Cells* **65** 141–8

[17] Katagiri H, Ishigaki N, Ishida T and Saito K 2001 Characterization of Cu_2ZnSnS_4 thin films prepared by vapor phase sulfurization *Jpn. J. Appl. Phys.* **40** 500

[18] Katagiri H 2008 Development of a new type of thin-film solar cell using a multi-component compound Cu_2ZnSnS_4 light absorption layer *Appl. Phys.* **77** 831–5 (available at: https://ndlsearch.ndl.go.jp/books/R000000004-I9571325) (in Japanese)

[19] Barkhouse D A R, Gunawan O, Gokmen T, Todorov T K and Mitzi D B 2012 Device characteristics of a 10.1% hydrazine-processed $Cu_2ZnSn(Se,S)_4$ solar cell *Prog. Photovolt., Res. Appl.* **20** 6–11

[20] Wang W, Winkler M T, Gunawan O, Gokmen T, Todorov T K, Zhu Y and Mitzi D B 2014 Device characteristics of CZTSSe thin-film solar cells with 12.6% efficiency *Adv. Energy Mater.* **4** 1301465

[21] Hages C J, Redinger A, Levcenko S, Hempel H, Koeper M J, Agrawal R, Greiner D, Kaufmann C A and Unold T 2017 Identifying the real minority carrier lifetime in nonideal semiconductors: a case study of kesterite materials *Adv. Energy Mater.* **7** 1700167

[22] Hempel H, Redinger A, Repins I, Moisan C, Larramona G, Dennler G, Handwerg M, Fischer S F, Eichberger R and Unold T 2016 Intragrain charge transport in kesterite thin films—Limits arising from carrier localization *J. Appl. Phys.* **120** 175302

[23] Liu X, Feng Y, Cui H, Liu F, Hao X, Conibeer G, Mitzi D B and Green M 2016 The current status and future prospects of kesterite solar cells: a brief review *Prog. Photovolt., Res. Appl.* **24** 879–98

[24] Zhou J *et al* 2023 Control of the phase evolution of kesterite by tuning of the selenium partial pressure for solar cells with 13.8% certified efficiency *Nat. Energy* **8** 526–35

[25] NREL Best Research-Cell Efficiency Chart (available at: www.nrel.gov/pv/cell-efficiency.html)

[26] Hwang S K, Park J-H, Cheon K B, Seo S W, Song J E, Park I J, Ji S G, Park M-A and Kim J Y 2020 Improved interfacial properties of electrodeposited $Cu_2ZnSn(S,Se)_4$ thin-film solar cells by a facile post-heat treatment process *Prog. Photovolt., Res. Appl.* **28** 1345–54

[27] Min J-H, Jeong W-L, Kim K, Lee J-S, Kim K-P, Kim J, Gang M G, Hong C W, Kim J H and Lee D-S 2020 Flexible high-efficiency CZTSSe solar cells on diverse flexible substrates via an adhesive-bonding transfer method *ACS Appl. Mater. Interfaces* **12** 7

[28] Refantero G, Cahya Prima E, Setiawan A, Panatarani C, Cahyadi D and Yuliarto B 2020 Etching process optimization of non-vacuum fabricated Cu_2ZnSnS_4 solar cell *J. Mater. Sci., Mater. Electron.* **31** 3674–80

[29] Katagiri H, Jimbo K, Maw W S, Oishi K, Yamazaki M, Araki H and Takeuchi A 2009 Development of CZTS-based thin film solar cells *Thin Solid Films* **517** 2455–60

[30] Henry J, Mohanraj K and Sivakumar G 2020 Fabrication of novel $CuAgZnSnSe_4$–$Cu_2ZnSnSe_4$ thin film solar cells by the vacuum evaporation method *New J. Chem.* **44** 15270–80

[31] Gang M G, Shin S W, Hong C W, Gurav K V, Gwak J H, J H. Y, Lee J Y and Kim J H 2016 Sputtering processed highly efficient $Cu_2ZnSn(S,Se)_4$ solar cells by a low-cost, simple, environmentally friendly, and up-scalable strategy *Green Chem.* **18** 700–11

[32] Kim J, Kim G Y, Son D-H, Yang K-J, Kim D-H, Kang J-K and Jo W 2018 High photo-conversion efficiency $Cu_2ZnSn(S,Se)_4$ thin-film solar cells prepared by compound-precursors and metal-precursors *Sol. Energy Mater. Sol. Cells* **183** 129–36

[33] Englund S, Saini N and Platzer-Björkman C 2018 $Cu_2ZnSn(S,Se)_4$ from annealing of compound co-sputtered precursors—recent results and open questions *Sol. Energy* **175** 84–93

[34] Fan P *et al* 2021 High-efficiency ultra-thin Cu_2ZnSnS_4 solar cells by double-pressure sputtering with spark plasma sintered quaternary target *J. Energy Chem.* **61** 186–94

[35] Catana D-S, Zaki M Y, Simandan I-D, Buruiana A-T, Sava F and Velea A 2023 Understanding the effects of post-deposition sequential annealing on the physical and chemical properties of $Cu_2ZnSnSe_4$ thin films *Surfaces* **6** 466–79

[36] Ge J and Yan Y 2018 Controllable multinary alloy electrodeposition for thin-film solar cell fabrication: a case study of kesterite Cu_2ZnSnS_4 *IScience* **1** 55–71

[37] Agasti A, Mallick S and Bhargava P 2018 Electrolyte pH dependent controlled growth of co-electrodeposited CZT films for application in CZTS based thin film solar cells *J. Mater. Sci., Mater. Electron.* **29** 4065–74

[38] Hwang S K *et al* 2024 Cs-treatments in kesterite thin-film solar cells for efficient perovskite tandems *Nano-Micro Small* **20** 2307175

[39] Hwang S K, Yoon J H and Kim J Y 2024 Current status and future prospects of kesterite $Cu_2ZnSn(S,Se)_4$ (CZTSSe) thin film solar cells prepared via electrochemical deposition *ChemElectroChem* **11** e202300729

[40] Zhao N, Sui Y, Ma M, Wang T, Miao C, Wang Z, Yang L, Wang F and Yao B 2024 Optimized grain growth for efficient solution-processed Bi-doped Cu_2ZnSn (S, Se)$_4$ thin film solar cells via spin-coated layers adjustment and two-step selenization *Ceram. Int.* **50** 11085–93

[41] Wei H *et al* 2024 Regulating hetero-nucleation enabling over 14% efficient kesterite solar cells *Nano-Micro Small* **20** 2308266

[42] Zhang X, Fu E, Wang Y and Zhang C 2019 Fabrication of Cu_2ZnSnS_4 (CZTS) nanoparticle inks for growth of CZTS films for solar cells *Nanomaterials* **9** 336

[43] Sharma R 2024 Kesterite thin-film solar cell absorbers derived using inhomogeneous Cu_2ZnSnS_4 nanoparticle

inks (available at: www.nist.gov/news-events/events/2014/12/kesterite-thin-film-solar-cell-absorbers-derived-using-inhomogeneous)
[44] Cazzaniga A *et al* 2017 Ultra-thin Cu_2ZnSnS_4 solar cell by pulsed laser deposition *Sol. Energy Mater. Sol. Cells* **166** 91–9
[45] Gansukh M *et al* 2020 Oxide route for production of Cu_2ZnSnS_4 solar cells by pulsed laser deposition *Sol. Energy Mater. Sol. Cells* **215** 110605
[46] Enkhbat T, Kim S and Kim J 2019 Device characteristics of band gap tailored 10.04% efficient CZTSSe solar cells sprayed from water-based solution *ACS Appl. Mater. Interfaces* **11** 36735–41
[47] Vigil-Galan O, Courel M, Espindola-Rodriguez M, Izquierdo-Roca V, Saucedo E and Fairbrother A 2013 Toward a high Cu_2ZnSnS_4 solar cell efficiency processed by spray pyrolysis method *J. Renew. Sustain. Energy* **5** 053137
[48] Vigil-Galán O, Espíndola-Rodríguez M, Courel M, Fontané X, Sylla D, Izquierdo-Roca V, Fairbrother A, Saucedob E and Pérez-Rodríguez A 2013 Secondary phases dependence on composition ratio in sprayed Cu_2ZnSnS_4 thin films and its impact on the high power conversion efficiency *Sol. Energy Mater. Sol. Cells* **117** 246–50
[49] Vigil-Galán O, Courel M, Espindola-Rodriguez M, Jiménez-Olarte D, Aguilar-Frutis M and Saucedo E 2015 Electrical properties of sprayed Cu_2ZnSnS_4 thin films and its relation with secondary phase formation and solar cell performance *Sol. Energy Mater. Sol. Cells* **132** 557–62
[50] He M *et al* 2021 Systematic efficiency improvement for $Cu_2ZnSn(S,Se)_4$ solar cells by double cation incorporation with Cd and Ge *Adv. Funct. Mater.* **31** 2104528
[51] Li J, Kim S, Nam D, Liu X, Kim J, Cheong H, Liu W, Li H, Sun Y and Zhang Y 2017 Tailoring the defects and carrier density for beyond 10% efficient CZTSe thin film solar cells *Sol. Energy Mater. Sol. Cells* **159** 447–55
[52] Sanchez M F, Sanchez T G, Courel M, Reyes-Vallejo O, Sanchez Y, Saucedoe E and Sebastian P J 2022 Effect of post annealing thermal heating on Cu_2ZnSnS_4 solar cells processed by sputtering technique *Sol. Energy* **237** 196–202
[53] Vigil-Galán O, Courel M, Andrade-Arvizu J A, Sánchez Y, Espíndola-Rodríguez M, Saucedo E, Seuret-Jiménez D and González R 2017 Processing pathways of $Cu_2Zn(SnGe)Se_4$ based solar cells: the role of CdS buffer layer *Mater. Sci. Semicond. Process.* **67** 14–9
[54] Vigil-Galán O *et al* 2017 Study of CBD-CdS/CZTGSe solar cells using different Cd sources: behavior of devices as a MIS structure *J. Mater. Sci., Mater. Electron.* **28** 18706–14
[55] Jiang J, Zhang L, Wang W and Hong R 2018 The role of sulphur in the sulfurization of CZTS layer prepared by DC magnetron sputtering from a single quaternary ceramic target *Ceram. Int.* **44** 11597–602
[56] Tanaka T, Nagatomo T, Kawasaki D, Nishio M, Guo Q, Wakahara A, Yoshida A and Ogawa H 2005 Preparation of Cu_2ZnSnS_4 thin films by hybrid sputtering *J. Phys. Chem. Solids* **66** 1978–81
[57] Dhakala T P, Peng C, Tobias R R, Dasharathy R and Westgate C R 2014 Characterization of a CZTS thin film solar cell grown by sputtering method *Sol. Energy* **100** 23–30
[58] Zhang Z, Qi Y, Zhao W, Liu J, Liu X, Cheng K and du Z 2022 Nanoscale sharp bandgap gradient for efficiency improvement of $Cu_2ZnSn(S, Se)_4$ thin film solar cells *J. Alloys Compd.* **910** 164665
[59] Zeng C, Li D, Lin R, Yuan M, Xin W, Gao P and Hong R 2023 Gradient band gap CZTSSe prepared via sputtering from quaternary ceramic targets followed with annealing under different atmospheres *Sol. Energy* **259** 328–37
[60] Shin B, Gunawan O, Zhu Y, Bojarczuk N A, Chey S J and Guha S 2013 Thin film solar cell with 8.4% power conversion efficiency using an earth-abundant Cu_2ZnSnS_4 absorber *Prog. Photovolt., Res. Appl.* **21** 72–6
[61] Courel M, Sanchez T G, Mathews N R and Mathew X 2018 Cu_2ZnGeS_4 thin films deposited by thermal evaporation: the impact of Ge concentration on physical properties *J. Phys. D: Appl. Phys.* **51** 095107
[62] Maykel Courel A M-A, Sanchez T G, Regalado-Perez E, De Los Santos I M, Mathews N R and Mathew X 2018 Impact of Cd concentrations on the physical properties of $Cu_2(Cd_xZn_{1-x})SnS_4$ thin films *Superlattices Microstruct.* **122** 324–35
[63] Lee Y S, Gershon T, Gunawan O, Todorov T K, Gokmen T, Virgus Y and Guha S 2014 $Cu_2ZnSnSe_4$ thin-film solar cells by thermal co evaporation with 11.6% efficiency and improved minority carrier diffusion length *Adv. Energy Mater.* **5** 1401372
[64] Wu X, Liu W, Cheng S, Lai Y and Jia H 2012 Photoelectric properties of Cu_2ZnSnS_4 thin films deposited by thermal evaporation *J. Semicond.* **33** 022002
[65] Touati R, Ben Rabeh M B and Kanzari M 2015 Effect of post-sulfurization on the structural and optical properties of Cu_2ZnSnS_4 thin films deposited by vacuum evaporation method *Thin Solid Films* **582** 198–202
[66] Sánchez T G, Mathew X and Mathews N R 2016 Obtaining phase-pure CZTS thin films by annealing vacuum evaporated CuS/SnS/ZnS stack *J. Cryst. Growth* **445** 15–23
[67] Henry J, Mohanraj K and Sivakumar G 2019 Vacuum evaporated FTO/$(Cu,Ag)_2ZnSnSe_4$ thin films and its electrochemical analysis *Vacuum* **160** 347–54
[68] Choudhari N J, Raviprakash Y, Bellarmine F, Rao M S R and Pinto R 2020 Investigation on the sulfurization temperature dependent phase and defect formation of sequentially evaporated Cu-rich CZTS thin films *Sol. Energy* **201** 348–61
[69] Kim Y and Choi I-H 2016 Defect characterization in co-evaporated $Cu_2ZnSnSe_4$ thin film solar cell *Curr. Appl. Phys.* **16** 944e948
[70] Song J E, Hwang S K, Park J H and Kim J Y 2022 A thin In_2S_3 interfacial layer for reducing defects and roughness of $Cu_2ZnSn(S,Se)_4$ thin-film solar cells *ChemSusChem* **15** e202102350
[71] Chan C P, Lam H and Surya C 2010 Preparation of Cu_2ZnSnS_4 films by electrodeposition using ionic liquids *Sol. Energy Mater. Sol. Cells* **94** 207–11
[72] Wang Y, Ma J, Liu P, Chen Y, Li R, Gu J, Lu J, Yang S-E and Gao X 2012 Cu_2ZnSnS_4 films deposited by a co-electrodeposition-annealing route *Mater. Lett.* **77** 13–6
[73] Mkawi E M, Ibrahim K, Ali M K M and Mohamed A S 2013 Dependence of copper concentration on the properties of Cu_2ZnSnS_4 thin films prepared by electrochemical method *Int. J. Electrochem. Sci.* **8** 359–68
[74] Mkawia E M, Ibrahim K, Ali M K M, Farrukh M A, Mohamed A S and Allam N K 2014 Effect of complexing agents on the electrodeposition of Cu–Zn–Sn metal precursors and corresponding Cu_2ZnSnS_4-based solar cells *J. Electroanal. Chem.* **735** 129–35
[75] Mkawi E M, Ibrahim K, Ali M K M, Farrukh M A and Allam N K 2014 Influence of precursor thin films stacking order on the properties of Cu_2ZnSnS_4 thin films fabricated by electrochemical deposition method *Superlattices Microstruct.* **76** 339–48
[76] Shiyani T, Raval D, Patel M, Mukhopadhyay I and Ray A 2016 Effect of initial bath condition and post-annealing on co-electrodeposition of Cu_2ZnSnS_4 *Mater. Chem. Phys.* **171** 63–72

[77] Shi J *et al* 2024 Multinary alloying for facilitated cation exchange and suppressed defect formation in kesterite solar cells with above 14% certified efficiency *Nat. Energy* **9** 1095–104

[78] Zhou Q *et al* 2024 Tailoring addition sequence of metal ions in precursor solution drives highly efficient kesterite solar cells *Adv. Funct. Mater.* **34** 2313301

[79] Chen X *et al* 2024 Achieving high open-circuit voltage in efficient kesterite solar cells via lanthanide europium ion induced carrier lifetime enhancement *Nano Energy* **124** 109448

[80] Zhao Y, Zhao J, Chen X, Cathelinaud M, Chen S, Ma H, Fan P, Zhang X, Su Z and Liang G 2024 Suppressing surface and bulk effect enables high efficiency solution-processed kesterite solar cells *Chem. Eng. J.* **479** 147739

[81] Xu B, Qin X, Lu X, Liu Y, Chen Y, Peng H, Yang P, Chu J and Sun L 2021 Realization of 11.5% efficiency $Cu_2ZnSn(S,Se)_4$ thin-film solar cells by manipulating the phase structure of precursor films *Sol. RRL* **5** 2100216

[82] Liu Y, Hu C, Qi Y, Zhou W, Kou D, Zhou Z, Han L, Meng Y, Yuan S and Wu S 2022 Li/Ag co-doping synergistically boosts the efficiency of kesterite solar cells through effective Sn_{Zn} defect passivation *Adv. Mater. Interfaces* **9** 2201677

[83] Cao L *et al* 2024 Passivating grain boundaries via graphene additive for efficient kesterite solar cells *Nano Micro Small* **20** 2304866

[84] Campbell S, Qu Y, Major J D, Lagarde D, Labbé C, Maiello P, Barrioz V, Beattie N S and Zoppi G 2019 Direct evidence of causality between chemical purity and band-edge potential fluctuations in nanoparticle ink-based $Cu_2ZnSn(S,Se)_4$ solar cells *J. Phys. D: Appl. Phys.* **52** 135102

[85] Xu B *et al* 2022 Positive role of inhibiting CZTSSe decomposition on intrinsic defects and interface recombination of 12.03% efficient kesterite solar cells *Sol. RRL* **6** 2200256

[86] Li X, Xinghuan X, Liao H, Yang S, Li X, Qiulian Q, Liu X, Zhao Y and Wang S 2022 Preparation of band-gap-grading $Cu_2ZnSn(S,Se)_4$ thin-film solar cells by post-sulfo-selenization treatment *J. Mater. Chem.* C **10** 15638–46

[87] Zhao Y, Chen S, Ishaq M, Cathelinaud M, Yan C, Ma H, Fan P, Zhang X, Su Z and Liang G 2024 Controllable double gradient bandgap strategy enables high efficiency solution-processed kesterite solar cells *Adv. Funct. Mater.* **34** 2311992

[88] Zhao Y *et al* 2022 Over 12% efficient kesterite solar cell via back interface engineering *J. Energy Chem.* **75** 321–9

[89] Long B, Cheng S, Zheng Q, Yu J and Jia H 2016 Effects of sulfurization time and H_2S concentration on electrical properties of Cu_2ZnSnS_4 films prepared by sol–gel method *Mater. Res. Bull.* **73** 140–4

[90] Alitia R, Putthisigamany Y, Chelvanathan P and Ristova M 2024 Spin-coated CZTS films prepared by two different precursor mixing regimes, at room temperature and at 150 °C *Heliyon* **10** e25354

[91] Otgontamir N, Enkhbat T, Enkhbayar E, Song S, Kim S Y, Hong T E and Kim J 2023 High efficiency kesterite solar cells through a dual treatment approach: improving the quality of both absorber bulk and heterojunction interface *Adv. Energy Mater.* **13** 2302941

[92] Courel M, Vigil-Galán O, Jiménez-Olarte D, Espíndola-Rodríguez M and Saucedo E 2014 Trap and recombination centers study in sprayed Cu_2ZnSnS_4 thin films *J. Appl. Phys.* **116** 134503

[93] Courel M, Valencia-Resendiz E, Pulgarín-Agudelo F A and Vigil-Galán O 2016 Determination of minority carrier diffusion length of sprayed-Cu_2ZnSnS_4 thin films *Solid-State Electron.* **118** 1–3

[94] Courel M, Valencia-Resendiz E, Andrade-Arvizu J A, Saucedo E and Vigil-Galán O 2017 Towards understanding poor performances in spray-deposited Cu_2ZnSnS_4 thin film solar cells *Sol. Energy Mater. Sol. Cells* **159** 151–8

[95] Courel M, Andrade-Arvizu J A, Guillén-Cervantes A, Nicolás-Marín M M, Pulgarín-Agudelo F A and Vigil-Galán O 2017 Optimization of physical properties of spray-deposited Cu_2ZnSnS_4 thin f ilms for solar cell applications *Mater. Des.* **114** 515–20

[96] Courel M, Picquart M, Arce-Plaza A, Pulgarín-Agudelo F A, González-Castillo J R, De Los Santos I M and Vigil-Galán O 2018 Study on the impact of stoichiometric and optimal compositional ratios on physical properties of Cu_2ZnSnS_4 thin films deposited by spray pyrolysis *Mater. Res. Express* **5** 015513

[97] Lee T, Sharif M H, Enkhbayar E, Enkhbat T, Salahuddin Mina M and Kim J 2022 Defect passivation for kesterite CZTSSe solar cells via *in situ* Al_2O_3 incorporation into the bulk CZTSSe absorber *Sol. RRL* **6** 2100862

[98] Enkhbat T, Enkhbayar E, Otgontamir N, Sharif M H, Mina M S, Kim S Y and Kim J 2023 High efficiency CZTSSe solar cells enabled by dual Ag-passivation approach via aqueous solution process *J. Energy Chem.* **77** 239–46

[99] Cong J *et al* 2024 Unveiling the role of Ge in CZTSSe solar cells by advanced micro-to-atom scale characterizations *Adv. Sci.* **11** 2305938

[100] Tseberlidis G, Gobbo C, Trifiletti V, Di Palma V and Binetti S 2024 Cd-free kesterite solar cells: state-of-the-art and perspectives *Sustain. Mater. Technol.* **41** e01003

[101] Fu J *et al* 2024 A critical review of solution-process engineering for kesterite thin-film solar cells: current strategies and prospects *J. Mater. Chem.* A **12** 545–66

[102] Wang T, Sui Y, Ma M, Zhao N, Miao C, Wang Z, Yang L, Wang F and Yao B 2023 Sb doping strategy to promote growth and suppress defects in solution-processed CZTSSe solar cells for improved optoelectronic performance *ACS Appl. Nano Mater.* **6** 18426–36

[103] Xianglin X, Su Z, Venkataraj S, Batabyal S K and Wong L H 2016 8.6% Efficiency CZTSSe solar cell with atomic layer deposited Zn-Sn-O buffer layer *Sol. Energy Mater. Sol. Cells* **157** 101–7

[104] Park J *et al* 2018 The role of hydrogen from ALD-Al_2O_3 in kesterite Cu_2ZnSnS_4 solar cells: grain surface passivation *Adv. Energy Mater.* **8** 1701940

[105] Almache-Hernández R *et al* 2021 Hole transport layer based on atomic layer deposited V_2O_x films: paving the road to semi-transparent CZTSe solar cells *Sol. Energy* **226** 64–71

[106] Yu Cho J Y, Jang J S, Karade V C, Nandi R, Pawar P S, Seok T-J, Moon W, Park T J, Kim J H and Heo J 2022 Atomic-layer-deposited ZnSnO buffer layers for kesterite solar cells: impact of Zn/(Zn+Sn) ratio on device performance *J. Alloys Compd.* **895** 162651

[107] Ren Y, Richter M, Keller J, Redinger A, Unold T, Donzel-Gargand O, Scragg J J S and Björkman C P 2017 Investigation of the SnS/Cu_2ZnSnS_4 Interfaces in kesterite thin-film solar cells *ACS Energy Lett.* **2** 976–81

[108] Gao S, Jiang Z, Wu L, Ao J, Zeng Y, Sun Y and Zhang Y 2018 Interfaces of high-efficiency kesterite $Cu_2ZnSnS(e)_4$ thin film solar cells *Chin. Phys.* B **27** 018803

[109] Saha S 2020 A status review on $Cu_2ZnSn(S,Se)_4$-based thin-film solar cells *Int. J. Photoenergy* **2020** 1–13

[110] Fonoll-Rubio R *et al* 2021 Insights into interface and bulk defects in a high efficiency kesterite-based device *Energy Environ. Sci.* **14** 507–23

[111] Pakštas V, Grincienė G, Selskis A, Balakauskas S, Talaikis M, Bruc L, Curmei N, Niaura G and Franckevičius M 2022 Improvement of CZTSSe film quality and superstrate solar cell performance through optimized post-deposition annealing *Sci. Rep.* **12** 16170
[112] Hao X, Sun K, Yan C, Liu F, Huang J, Aobo P and Green M 2016 Large Voc improvement and 9.2% efficient pure sulfide Cu_2ZnSnS_4 solar cells by heterojunction interface engineering *2016 IEEE 43rd Photovoltaic Specialists Conf. (PVSC)* (https://doi.org/10.1109/PVSC.2016.7750017)
[113] Grenet L, Suzon M A A, Emieux F and Roux F 2018 Analysis of failure modes in kesterite solar cells *ACS Appl. Energy Mater.* **1** 2103–13
[114] Nisika N, Kaur K and Kumar M 2020 Progress and prospects of CZTSSe/CdS interface engineering to combat high open-circuit voltage deficit of kesterite photovoltaics: a critical review *J. Mater. Chem.* A **8** 21547–84
[115] Neuwirth M, Zhou H, Schnabel T, Ahlswede E, Kalt H and Hetterich M 2016 A multiple-selenization process for enhanced reproducibility of $Cu_2ZnSn(S,Se)_4$ solar cells *Appl. Phys. Lett.* **109** 233903
[116] Guo J, Mao Y, Jianping A, Han Y, Cao C, Liu F, Jinlian B, Wang S and Zhang Y 2022 Microenvironment created by $SnSe_2$ vapor and pre-selenization to stabilize the surface and back contact in kesterite solar cells *Nano Micro Small* **18** 2203354
[117] Yixiong J *et al* 2024 An ITO-free kesterite solar cell *Nano Micro Small* **20** 2307242
[118] Mingrui H, Yan C, Jianjun L, Suryawanshi M P, Kim J, Green M A and Hao X 2021 Kesterite solar cells: insights into current strategies and challenges advanced science *Adv. Sci.* **8** 2004313
[119] Kim G Y, Son D-H, Thi Thu Nguyen T, Yoon S, Kwon M, Jeon C-W, Kim D-H, Kang J-K and Jo W 2016 Enhancement of photo-conversion efficiency in $Cu_2ZnSn(S,Se)_4$ thin-film solar cells by control of ZnS precursor-layer thickness *Prog. Photovolt., Res. Appl.* **24** 292–306
[120] Campbell S *et al* 2022 Recovery mechanisms in aged kesterite solar cells *ACS Appl. Energy Mater.* **5** 5404–14
[121] Wang A, He M, Green M A, Sun K and Hao X 2023 A critical review on the progress of kesterite solar cells: current strategies and insights *Adv. Energy Mater.* **13** 2203046
[122] Zhou Y, Xiang C, Dai Q, Xiang S, Li R, Gong Y, Zhu Q, Yan W, Huang W and Xin H 2023 11.4% efficiency kesterite solar cells on transparent electrode *Adv. Energy Mater.* **13** 2300253
[123] Zhao Y, Chen S, Zhenghua S, Luo J, Zhang X and Liang G 2023 Research progress of kesterite solar cells *Chin. Sci. Bull.* **68** 4662–73
[124] Zhao W, Pan D and Liu S 2016 Kesterite $Cu_2Zn(Sn,Ge)(S,Se)_4$ thin film with controlled Ge-doping for photovoltaic application *Nanoscale* **8** 10160–5
[125] Antunez P D, Bishop D M, Lee Y S, Gokmen T, Gunawan O, Gershon T S, Todorov T K, Singh S and Haight R 2017 Back contact engineering for increased performance in kesterite solar cells *Adv. Energy Mater.* **7** 1602585
[126] Sun Y, Qiu P, Yu W, Li J, Guo H, Wu L, Luo H, Meng R, Zhang Y and Liu S 2021 N-type surface design for p-type CZTSSe thin film to attain high efficiency *Adv. Mater.* **33** 2104330
[127] Naylor M C *et al* 2022 Ex situ Ge-doping of CZTS nanocrystals and CZTSSe solar absorber films *Faraday Discuss.* **239** 70–84
[128] Yang Y, Kang X, Huang L and Pan D 2016 Tuning the band gap of $Cu_2ZnSn(S,Se)_4$ thin films via lithium alloying *ACS Appl. Mater. Interfaces* **8** 5308–13
[129] Yang K-J *et al* 2016 A band-gap-graded CZTSSe solar cell with 12.3% efficiency *J. Mater. Chem.* A **4** 10151–8
[130] Ross N, Larsen J, Grini S, Vines L and Platzer-Björkman C 2017 Practical limitations to selenium annealing of compound co-sputtered Cu_2ZnSnS_4 as a route to achieving sulfur-selenium graded solar cell absorbers *Thin Solid Films* **623** 110–5
[131] Mohammadnejad S and Parashkouh A B 2017 CZTSSe solar cell efficiency improvement using a new band-gap grading model in absorber layer *Appl. Phys.* A **123** 758
[132] Grini S, Ross N, Persson C, Platzer-Björkman C and Vines L 2018 Low temperature incorporation of selenium in Cu_2ZnSnS_4: diffusion and nucleation *Thin Solid Films* **665** 159–63
[133] Ross N, Grini S, Rudisch K, Vines L and Platzer-Björkman C 2018 Selenium inclusion in $Cu_2ZnSn(S,Se)_4$ solar cell absorber precursors for optimized grain growth *IEEE J. Photovolt.* **8** 1132–41
[134] Andrade-Arvizu J, Izquierdo-Roca V, Becerril-Romero I, Vidal-Fuentes P, Fonoll-Rubio R, Sánchez Y, Placidi M, Calvo-Barrio L, Vigil-Galán O and Saucedo E 2019 Is it possible to develop complex S–Se graded band gap profiles in kesterite-based solar cells? *ACS Appl. Mater. Interfaces* **11** 32945–56
[135] Andrade-Arvizu J *et al* 2020 Rear band gap grading strategies on Sn–Ge-alloyed kesterite solar cells *ACS Appl. Energy Mater.* **3** 10362–75
[136] Ahmad F, Lakhtakia A, Anderson T H and Monk P B 2020 Towards highly efficient thin-film solar cells with a graded-bandgap CZTSSe layer *J. Phys. Energy* **2** 025004
[137] Guo H, Meng R, Wang G, Wang S, Wu L, Li J, Wang Z, Dong J, Hao X and Zhang Y 2022 Band-gap-graded $Cu_2ZnSn(S,Se)_4$ drives highly efficient solar cells *Energy Environ. Sci.* **15** 693–704
[138] Sharma I, Pawar P S, Yadav R K, Nandi R and Heo J 2022 Review on bandgap engineering in metal-chalcogenide absorber layer via grading: a trend in thin-film solar cells *Sol. Energy* **246** 152–80
[139] Andrade-Arvizu J *et al* 2022 Controlling the anionic ratio and gradient in kesterite technology *ACS Appl. Mater. Interfaces* **14** 1177–86
[140] Tseberlidis G, Trifiletti V, Vitiello E, Husien A H, Frioni L, Da Lisca M, Alvarez J, Acciarri M and Binetti S O 2022 Band-gap tuning induced by germanium introduction in solution-processed kesterite thin films *ACS Omega* **7** 23445–56
[141] Patel M and Ray A 2012 Enhancement of output performance of Cu_2ZnSnS_4 thin film solar cells—a numerical simulation approach and comparison to experiments *Physica* B **407** 4391–7
[142] Gokmen T, Gunawan O and Mitzi D B 2014 Semi-empirical device model for $Cu_2ZnSn(S,Se)_4$ solar cells *Appl. Phys. Lett.* **105** 033903
[143] Moore J E, Hages C J, Agrawal R, Lundstrom M S and Gray J L 2016 The importance of band tail recombination on current collection and open-circuit voltage in CZTSSe solar cells *Appl. Phys. Lett.* **109** 021102
[144] Hages C J, Carter N J and Agrawal R 2016 Generalized quantum efficiency analysis for non-ideal solar cells: case of $Cu_2ZnSnSe_4$ *J. Appl. Phys.* **119** 014505
[145] Simya O K, Mahaboobbatcha A and Balachander K 2015 A comparative study on the performance of Kesterite based thin film solar cells using SCAPS simulation program *Superlattices Microstruct.* **82** 248–61
[146] Frisk C, Ericson T, Li S-Y, Szaniawski P, Olsson J and Platzer-Björkman C 2016 Combining strong interface

recombination with bandgap narrowing and short diffusion length in Cu_2ZnSnS_4 device modeling *Sol. Energy Mater. Sol. Cells* **144** 364–70
[147] Meher S R, Balakrishnan L and Alex Z C 2016 Analysis of Cu_2ZnSnS_4/CdS based photovoltaic cell: a numerical simulation approach *Superlattices Microstruct.* **100** 703–22
[148] Kanevcen A, Repins I and Wei S-H 2015 Impact of bulk properties and local secondary phases on the $Cu_2(Zn,Sn)Se_4$ solar cells open-circuit voltage *Sol. Energy Mater. Sol. Cells* **133** 119–25
[149] Minbashi M, Ghobadi A, Yazdani E, Ahmadkhan Kordbacheh A and Hajjiah A 2020 Efficiency enhancement of CZTSSe solar cells via screening the absorber layer by examining of different possible defects *Sci. Rep.* **10** 21813
[150] Platzer-Björkman C *et al* 2019 Back and front contacts in kesterite solar cells: state-of-the-art and open questions *J. Phys.* **1** 044005
[151] Grenet L, Emieux F, Andrade-Arvizu J, De Vito E, Lorin G, Sánchez Y, Saucedo E and Roux F 2020 Sputtered ZnSnO buffer layers for kesterite solar cells *ACS Appl. Energy Mater.* **3** 1883–91
[152] Houshmand M, Esmaili H, Zandi M H and Gorji N E 2015 Degradation and device physics modeling of TiO_2/CZTS ultrathin film photovoltaics *Mater. Lett.* **157** 123–6
[153] Nisika N, Kaur K, Arora K, Chowdhury A H, Bahrami B, Qiao Q and Kumar M 2019 Energy level alignment and nanoscale investigation of A-TiO_2/Cu-Zn-Sn-S interface for alternative electron transport layer in earth abundant Cu-Zn-Sn-S solar cells *J. Appl. Phys.* **126** 193104
[154] Rahman M A 2021 Enhancing the photovoltaic performance of Cd-Free Cu_2ZnSnS_4 heterojunction solar cells using SnS HTL and TiO_2 ETL *Sol. Energy* **215** 64–76
[155] Bencherif H, Dehimi L, Mahsar N, Kouriche E and Pezzimenti F 2022 Modeling and optimization of CZTS kesterite solar cells using TiO_2 as efficient electron transport layer *Mater. Sci. Eng.* B **276** 115574
[156] Tseberlidis G, Di Palma V, Trifiletti V, Frioni L, Valentini M, Malerba C, Mittiga A, Acciarri M and Binetti S O 2023 Titania as buffer layer for Cd-free kesterite solar cells *ACS Mater. Lett.* **5** 219–24
[157] Yang S, Xue Y and Bai X 2024 Simulation study on the performance of Cu_2ZnSnS_4 thin-film solar cells by CdS-free buffer layer $Zn_{1-x}Mg_xO$ *MRS Adv.* **9** 1219–25
[158] Jhuma F A, Shaily M Z and Rashid M J 2019 Towards high-efficiency CZTS solar cell through buffer layer optimization *Mater. Renew. Sustain. Energy* **8** 6
[159] Wu X, Hao L, Wei Z, Wu Y, Ma X, Cheng Z, Wu J, Qi Y, Meng X and Su J 2022 Numerical simulations on CZTSSe-based solar cells with GaSe as an alternative buffer layer using SCAPS-1D *ECS J. Solid State Sci. Technol.* **11** 113004
[160] Kogler W *et al* 2020 Hybrid chemical bath deposition-CdS/sputter-Zn(O,S) alternative buffer for $Cu_2ZnSn(S,Se)_4$ based solar cells *J. Appl. Phys.* **127** 165301
[161] Campbell S, Zoppi G, Bowen L, Maiello P, Barrioz V, Beattie N S and Qu Y 2023 Enhanced carrier collection in Cd/In-based dual buffers in kesterite thin-film solar cells from nanoparticle inks *ACS Appl. Energy Mater.* **6** 10883–96
[162] Hernández-Calderón V, Vigil-Galán O, Guc M, Carrillo-Osuna A, Ramírez-Velasco S, Sánchez-Rodríguez F J, Vidal-Fuentes P, Giraldo S, Saucedo E and Sánchez Y 2020 CdS/ZnS bilayer thin films used as buffer layer in 10%-efficient $Cu_2ZnSnSe_4$ solar cells *ACS Appl. Energy Mater.* **3** 6815–23
[163] Sravani L, Routray S, Courel M and Pradhan K P 2021 Loss mechanisms in CZTS and CZTSe Kesterite thin-film solar cells: understanding the complexity of defect density *Sol. Energy* **227** 56–66
[164] Sravani L, Routray S, Pradhan K P and Piedrahita M C 2021 Kesterite thin-film solar cell: role of grain boundaries and defects in copper–zinc–tin–sulfide and copper–zinc–tin–selenide *Phys. Status Solidi* a **218** 2100039
[165] Yousefi M, Minbashi M, Monfared Z, Memarian N and Hajjiah A 2020 Improving the efficiency of CZTSSe solar cells by engineering the lattice defects in the absorber layer *Sol. Energy* **208** 884–93
[166] Saha U, Biswas A and Alam M K 2021 Efficiency enhancement of CZTSe solar cell using CdS(n)/$(Ag_xCu_{1-x})_2ZnSnSe_4$ (p) /$Cu_2ZnSnSe_4$ (p+) structure *Sol. Energy* **221** 314–22
[167] Kumar A and Thakur A D 2018 Role of contact work function, back surface field, and conduction band offset in Cu_2ZnSnS_4 solar cell *Jpn. J. Appl. Phys.* **57** 08RC05
[168] Maklavani S E and Mohammadnejad S 2020 Reduction of interface recombination current for higher performance of p^+-$CZTS_xSe_{(1-x)}$/p-CZTS/n-CdS thin-film solar cells using Kesterite intermediate layers *Sol. Energy* **204** 489–500
[169] Mansouri E, Abderrezek M and Benzetta A E 2024 Thin-film CZTSSe solar cells efficiency improvement through BSF SnS layer and concentrator applications *Energy Sources* A **46** 2024–39
[170] Padhy S, Mannu R and Singh U P 2021 Graded band gap structure of kesterite material using bilayer of CZTS and CZTSe for enhanced performance: a numerical approach *Sol. Energy* **216** 601–9
[171] Lahoual M, Bourennane M and Aidaoui L 2024 Numerical study of graded CZT(S,Se) solar cell with 2D transition metal dichalcogenide tungsten disulfide (WS_2) as a buffer layer *Phys. Status Solidi* a **221** 2400250
[172] Wang Y, Wang J, Li H, Zhao A, Li B, Bi J and Li W 2021 wxAMPS theoretical study of the bandgap structure of CZTS thin film to improve the device performance *Optoelectron. Lett.* **17** 475–81
[173] Saha U and Alam M K 2017 Proposition and computational analysis of a kesterite/kesterite tandem solar cell with enhanced efficiency *RSC Adv.* **7** 4806–14
[174] Ferhati H and Djeffal F 2019 An efficient analytical model for tandem solar cells *Mater. Res. Express* **6** 076424
[175] Kumar A 2021 Theoretical analysis of CZTS/CZTSSe tandem solar cell *Opt. Quantum Electron.* **53** 528
[176] Mora-Herrera D and Pal M 2022 Boosting the efficiency of Cd-free kesterite/kesterite tandem solar cell: a numerical simulation approach *Physica* E **138** 115056
[177] Ghalmi L, Bensmaine S, Elbar M, Chala S and Merzouk H 2022 Simulation study of CZTS/CZTSe tandem solar cell by using SCAPS-1D software *J. Nano Electron. Phys.* **14** 06033
[178] Arbouz H 2022 Modeling of a tandem solar cell structure based on CZTS and CZTSe absorber materials *Int. J. Comput. Exp. Sci. Eng.* **8** 14–8
[179] Bibi B, Farhadi B, Rahman W U and Liu A 2024 Numerical modeling and performance analysis of a novel Cd-free all-Kesterite tandem solar cell using SCAPS-1D *Next Mater.* **2** 100068
[180] Gohri S, Madan J, Pandey R and Sharma R 2023 Design and analysis of lead-free perovskite-CZTSSe based tandem solar cell *Opt. Quantum Electron.* **55** 171
[181] Maoucha A, Djeffal F, Ferhati H and AbdelMalek F 2023 Eco-friendly perovskite/CZTSSe tandem cell exceeding 28% efficiency through current matching and bandgap

optimization: a numerical investigation *Eur. Phys. J. Plus* **138** 620
[182] Wang D, Yao S, Zhong Y, Peng L, Shi T, Chen J, Liu X and Lin J 2022 Optoelectronic simulation of a four-terminal all-inorganic $CsPbI_3$/CZTSSe tandem solar cell with high power conversion efficiency *Phys. Chem. Chem. Phys.* **24** 22746–55
[183] Rudzikas M, Pakalka S, Donėlienė J and Šetkus A 2023 Exploring the potential of pure germanium kesterite for a 2T kesterite/silicon tandem solar cell: a simulation study *Materials* **16** 6107
[184] Al-Hattab M, Oublal E, Younes Chrafih Y, Moudou L, Bajjou O, Sahal M and Rahmani K 2023 Novel simulation and efficiency enhancement of eco-friendly Cu_2FeSnS_4/c-silicon tandem solar device *Silicon* **15** 7311–9
[185] Courel M and Vigil-Galán O 2018 Different approaches for thin film solar cell simulation *Advanced Ceramic and Metallic Coating and Thin Film Materials for Energy and Environmental Applications* ed J Zhang and Y G Jung (Springer)
[186] Courel M, Andrade-Arvizu J A and Vigil-Galán O 2015 Loss mechanisms influence on Cu_2ZnSnS_4/CdS-based thin film solar cell performance *Solid-State Electron.* **111** 243–50
[187] Courel M, Andrade-Arvizu J A and Vigil-Galán O 2014 Towards a CdS/Cu_2ZnSnS_4 solar cell efficiency improvement: a theoretical approach *Appl. Phys. Lett.* **105** 233501
[188] Courel M, Andrade-Arvizu J A and Vigil-Galán O 2016 The role of buffer/kesterite interface recombination and minority carrier lifetime on kesterite thin film solar cells *Mater. Res. Express* **3** 095501
[189] Jiménez T, Seuret-Jiménez D, Vigil-Galán O, Basurto-Pensado M A and Courel M 2018 $Sb_2(S_{1-x}Se_x)_3$ solar cells: the impact of radiative and non-radiative loss mechanisms *J. Phys. D: Appl. Phys.* **51** 435501
[190] Courel M, Pulgarín-Agudelo F A, Andrade-Arvizu J A and Vigil-Galán O 2016 Open-circuit voltage enhancement in CdS/$Cu_2ZnSnSe_4$-based thin film solar cells: a metal–insulator–semiconductor (MIS) performance *Sol. Energy Mater. Sol. Cells* **149** 204–12
[191] Courel M, Jiménez T, Arce-Plaza A, Seuret-Jiménez D, Morán-Lázaro J P and Sánchez-Rodríguez F J 2019 A theoretical study on Sb_2S_3 solar cells: the path to overcome the efficiency barrier of 8% *Sol. Energy Mater. Sol. Cells* **201** 110123
[192] Courel M, Jimenez T, De Los Santos I M, Morán-Lázaro J P, Ojeda Martinez M, Pérez L M, Laroze D, Feddi E and Sánchez-Rodríguez F J 2022 Impact of loss mechanisms through defects on $Sb_2(S_{1-x}Se_x)_3$/CdS solar cells with p-n structure *Eur. Phys. J. Plus* **137** 396
[193] Chen S, Walsh A, Gong X and Wei S-H 2013 Classification of lattice defects in the kesterite Cu_2ZnSnS_4 and $Cu_2ZnSnSe_4$ earth-abundant solar cell absorbers *Adv. Mater.* **25** 1522–39
[194] Varley J B and Lordi V 2013 Electrical properties of point defects in CdS and ZnS *Appl. Phys. Lett.* **103** 102103
[195] Hurkx G A M, Klaassen D B M and Knuvers M P G 1992 A new recombination model for device simulation including tunneling *IEEE Trans. Electron Devices* **39** 331–8
[196] Hurkx G A M, de Graaff H C, Kloosterman W J and Knuvers M P G 1992 A new analytical diode model including tunneling and avalanche breakdown *IEEE Trans. Electron Devices* **39** 2090–8
[197] Sanchez Y, Neuschitzer M, Dimitrievska M, Espindola-Rodriguez M, Lopez Garcia J, IzquierdoRoca V, Vigil-Galán O and Saucedo E 2014 High V_{OC} $Cu_2ZnSnSe_4$/CdS: cu based solar cell: evidences of a metal-insulator-semiconductor (MIS) type hetero-junction *Proc. 40th IEEE Photovoltaic Specialist Conf. (PVSC)* pp 0417–20
[198] Vigil-Galán O, Arias-Carbajal A, Mendoza-Pérez R, Santana-Rodríguez G, Sastre-Hernández J, Alonso J C, Moreno-García E, Contreras-Puente G and Morales-Acevedo A 2005 Improving the efficiency of CdS/CdTe solar cells by varying the thiourea/$CdCl_2$ ratio in the CdS chemical bath *Semicond. Sci. Technol.* **20** 819–22
[199] Ohno T R *et al* 2001 Microscopic characterization of polycrystalline APCVD CdTe thin film PV devices *Mater. Res. Symp. Proc.* **668** H6.5
[200] Karpov V G, Shvydka D and Roussillon Y 2005 Physics of CdTe photovoltaics: from front to back *Mater. Res. Soc. Symp. Proc.* **865** F10.1.1–12
[201] Zhao W, Zhou W and Miao X 2012 Numerical simulation of CZTS thin film solar cell *2012 7th IEEE Int. Conf. on Nano/Micro Engineered and Molecular Systems (NEMS)* (IEEE) pp 502–5
[202] Cherouana A and Labbani R 2017 Study of CZTS and CZTSSe solar cells for buffer layers selection *Appl. Surf. Sci.* **424** 251–5
[203] Saha U and Alam M K 2017 Proposition of an environment friendly triple junction solar cell based on earth abundant CBTSSe/CZTS/ACZTSe materials *Phys. Status Solidi* **12** 1700335
[204] Khattak Y H, Baig F, Ullah S, Marí B, Beg S and Ullah H 2018 Enhancement of the conversion efficiency of thin film kesterite solar cell *J. Renew. Sustain. Energy* **10** 033501
[205] Haghighi M, Minbashi M, Taghavinia N, Kim D-H, Mahdavi S M and Kordbacheh A A 2018 A modeling study on utilizing SnS_2 as the buffer layer of CZT(S, Se) solar cells *Sol. Energy* **167** 165–71
[206] Gupta G K and Dixit A 2018 Theoretical studies of single and tandem $Cu_2ZnSn(S/Se)_4$ junction solar cells for enhanced efficiency *Opt. Mater.* **82** 11–20
[207] Ferhati H and Djeffal F 2018 Graded band-gap engineering for increased efficiency in CZTS solar cells *Opt. Mater.* **76** 393–9
[208] Saha U and Alam M K 2018 Boosting the efficiency of single junction kesterite solar cell using Ag mixed Cu_2ZnSnS_4 active layer *RSC Adv.* **8** 4905–13
[209] Wang D, Wu J, Liu X, Wu L, Ao J, Liu W, Sun Y and Zhang Y 2019 Formation of the front-gradient bandgap in the Ag doped CZTSe thin films and solar cells *J. Energy Chem.* **35** 188–96
[210] Hood S N, Walsh A, Persson C, Iordanidou K, Huang D, Kumar M, Jehl Z, Courel M, Lauwaert J and Lee S 2019 Status of materials and device modelling for kesterite solar cells *J. Phys.* **1** 042004
[211] Maklavani S E and Mohammadnejad S 2020 Enhancing the open-circuit voltage and efficiency of CZTS thin-film solar cells via band-offset engineering *Opt. Quantum Electron.* **52** 72
[212] Amiri S and Dehghani S 2020 Design of highly efficient CZTS/CZTSe tandem solar cells *J. Electron. Mater.* **49** 2164–72
[213] Et-taya L, Ouslimane T and Benami A 2020 Numerical analysis of earth-abundant $Cu_2ZnSn(S_xSe_{1-x})_4$ solar cells based on Spectroscopic Ellipsometry results by using SCAPS-1D *Sol. Energy* **201** 827–35
[214] Ghobadi A, Yousefi M, Minbashi M, Kordbacheh A H A, Abdolvahab A H and Gorji N E 2020 Simulating the effect of adding BSF layers on $Cu_2BaSnSSe_3$ thin film solar cells *Opt. Mater.* **107** 109927

[215] Bibi B, Farhadi B, Rahman W U and Liu A 2021 A novel design of CTZS/Si tandem solar cell: a numerical approach *J. Comput. Electron.* **20** 1769–78

[216] Benzetta A E, Abderrezek M and Djeghlal M E 2021 Numerical study of CZTS/CZTSSe tandem thin film solar cell using SCAPS-1D *Int. J. Light Electron Opt.* **242** 167320

[217] Mora-Herrera D, Pal M and Santos-Cruz J 2021 Theoretical modelling and device structure engineering of kesterite solar cells to boost the conversion efficiency over 20% *Sol. Energy* **220** 316–30

[218] Bouarissa A, Gueddim A, Bouarissa N and Maghraoui-Meherezi H 2021 Modeling of ZnO/MoS_2/CZTS photovoltaic solar cell through window, buffer and absorber layers optimization *Mater. Sci. Eng.* B **263** 114816

[219] Rana M S, Islam M M and Julkarnain M 2021 Enhancement in efficiency of CZTS solar cell by using CZTSe BSF layer *Sol. Energy* **226** 272–87

[220] Prabhu S, Pandey S K and Chakrabarti S 2021 Theoretical investigations of band alignments and SnSe BSF layer for low-cost, non-toxic, high-efficiency CZTSSe solar cell *Sol. Energy* **226** 288–96

[221] Moustafa M, Al Zoubi T and Yasin S 2021 Numerical analysis of the role of p-$MoSe_2$ interfacial layer in CZTSe thin-film solar cells using SCAPS simulation *Optik* **247** 167885

[222] Kumar A 2021 Impact of selenium composition variation in CZTS solar cell *Optik* **234** 166421

[223] Srivastava A, Piyush Dua T R L and Tripathy S K 2021 Numerical simulations on CZTS/CZTSe based solar cell with ZnSe as an alternative buffer layer using SCAPS-1D *Mater. Today Proc.* **43** 3735–9

[224] Joseph Mebelson T and Elampari K 2021 A study of electrical and optical characteristics of CZTSe solar cell using Silvaco Atlas *Mater. Today Proc.* **46** 2540–3

[225] Bibi B, Farhadi B, Khan Asghar H M N U H, Rahman W U and Liu A 2022 Effect and optimization of the Zn_3P_2 back surface field on the efficiency of CZTS/CZTSSe tandem solar cell: a computational approach *J. Appl. Phys.* **56** 025502

[226] Mishra S K, Padhy S and Singh U P 2022 Silver incorporated bilayer Kesterite solar cell for enhanced device performance: a numerical study *Sol. Energy* **233** 1–10

[227] Mazumder S and Senthilkumar K 2022 Device study and optimization of CZTS/ZnS based solar cell with CuI hole transport layer for different conduction band offset *Sol. Energy* **237** 414–31

[228] Mazumder S, Mazumder P and Senthilkumar K 2022 Device modeling and study of AZO/i-ZnO/ZnS/CZTS-bilayer solar cell for different series and shunt resistances *Sol. Energy* **245** 46–57

[229] Pansuriya T, Malani R and Kheraj V 2022 Investigations on the effect of buffer layer on CMTS based thin film solar cell using SCAPS 1-D *Opt. Mater.* **126** 112150

[230] Rachidy C *et al* 2022 Enhancing CZTS solar cell parameters using CZTSe BSF layer and non toxic SnS_2/In_2S_3 buffer layer *Mater. Today Proc.* **66** 26–36

[231] Bencherif H 2022 Towards a high efficient Cd-free double CZTS layers kesterite solar cell using an optimized interface band alignment *Sol. Energy* **238** 114–25

[232] Moustafa M, Al Zoubi T and Yasin S 2022 Exploration of CZTS-based solar using the ZrS_2 as a novel buffer layer by SCAPS simulation *Opt. Mater.* **124** 112001

[233] Srivastava A, Tripathy S K, Lenka T R and Goyal V 2022 Numerical simulations of novel quaternary chalcogenide $Ag_2MgSn(S/Se)_4$ based thin film solar cells using SCAPS 1-D *Sol. Energy* **239** 337–49

[234] El Hamdaoui J, El-Yadri M, Lakaal K, Kria M, Courel M, Ojeda M, Pérez L M, Laroze D and Feddi E 2022 Ab initio study on electronic and optical properties of Cu_2NiGeS_4 for photovoltaic applications *Sol. Energy* **237** 333–9

[235] Kumar P G N, Chandrasekar P, Routray S, Courel M and Massoud Y 2022 Understanding performance limitation of Cu_2CdSnS_4 as photoactive layer: physics of defect states and recombination mechanisms *IEEE Sens. J.* **22** 20381

[236] Boubakeur M, Aissat A, Chenini L, Ben Arbia M, Maaref H and Vilcot J P 2023 Optimization of $CdZn_yS_{1-y}$ buffer layer properties for a $ZnO/CZTS_xSe_{1-x}$/Mo solar cell to enhance conversion efficiency *J. Electron. Mater.* **52** 284–92

[237] Charghandeh R and Abbasi A 2023 Effect of In(O,S) buffer layer on the band alignment and the performance of CZT(S,Se) thin film solar cells *Mater. Today Commun.* **37** 107299

[238] Kannan P K and Anandkumar M 2023 A theoretical investigation to boost the efficiency of CZTS solar cells using SCAPS-1D *Optik* **288** 171214

[239] El Hamdaoui J, Lakaal K, Mazkad D, Beraich M, El Fatimy A, Courel M, Perezg L M, Díaz P, Laroze D and Feddi E 2023 First principles study on electronic and optical properties of Cu_2CoGeS_4 for photovoltaic conversion and photocatalytic applications *Mater. Res. Bull.* **164** 112235

[240] El Ouarie N, El Hamdaoui J, Sahoo G S, Rodriguez-Osorio K G, Courel M, Zazoui M, Pérez L M, Laroze D and Feddi E 2023 Modeling of highly efficient CNGS based kesterite solar cell: a DFT study along with SCAPS-1D analysis *Sol. Energy* **263** 111929

[241] Dakua P K, Panda D K, Kashyap S, Laidouci A and Sadanand 2024 Simulation and numerical modeling of high-efficiency CZTS solar cells with a BSF layer *Int. J. Numer. Modelling* **37** e3188

[242] Ali M R, Khan T M, Nurjahan-Ara and Al Ahmed S R 2025 Numerical simulation to optimize the photovoltaic performances of Cu_2ZnSnS_4 solar cell with Cu_2NiSnS_4 as hole transport layer *J. Phys. Chem. Solids* **197** 112448

[243] Miller D A B, Chemla D S, Damen T C, Gossard A C, Wiegmann W, Wood T H and Burrus C A 1985 Electric field dependence of optical absorption near the band gap of quantum-well structures *Phys. Rev.* B **32** 1043

[244] Mazzer M *et al* 2006 Progress in quantum well solar cells *Thin Solid Films* **511–512** 76–83

[245] Anderson N G 1995 Ideal theory of quantum well solar cells *J. Appl. Phys.* **78** 1850–61

[246] Chandrasekar P, Palaniswamy S and Routray S 2021 Exploiting high-density earth-abundant kesterite quantum wells for next-generation PV technology *IEEE Trans. Electron Devices* **68** 5511–7

[247] Ekins-Daukes N, Adams J, Ballard I, Barnham K, Browne B, Connolly J, Tibbits T, Hill G and Roberts J 2009 Physics of quantum well solar cells *Proc. SPIE* **7211** 119–29

[248] Nelson J, Paxman M, Barnham K, Roberts J and Button C 1993 Steady-state carrier escape from single quantum Wells *IEEE J. Quantum Electron.* **29** 1460–8

[249] Barnham K and Duggan G 1990 A new approach to high-efficiency multi-band-gap solar cells *J. Appl. Phys.* **67** 3490–3

[250] Barnham K, Ballard I, Connolly J, Ekins-Daukes N, Kluftinger B, Nelson J and Rohr C 2002 Quantum well solar cells *Physica* E **14** 27–36

[251] Bushnell D, Tibbits T, Barnha K, Connolly J, Mazzer M, Ekins-Daukes N, Roberts J, Hill G and Airey R 2005 Effect of well number on the performance of quantum-well solar cells *J. Appl. Phys.* **97** 124908

[252] Jani O and Honsberg C 2006 Absorption and transport via tunneling in quantum-well solar cells *Sol. Energy Mater. Sol. Cells* **90** 3464–70

[253] Farrow R F 1995 *Molecular Beam Epitaxy: Applications to Key Materials* (Elsevier)

[254] Henini M 1996 *III–Vs Rev.* **9** 33–6

[255] Suzuki Y, Kikuchi T, Kawabe M and Okada Y 1999 Atomic hydrogen-assisted molecular beam epitaxy for the fabrication of multi-quantum-well solar cells *J. Appl. Phys.* **86** 5858–61

[256] Okada Y, Seki S, Takeda T and Kawabe M 2002 Control of dark currents in multi-quantum well solar cells fabricated by atomic H-assisted molecular beam epitaxy *J. Cryst. Growth* **237** 1515–8

[257] Aho A, Polojarvi V, Korpijarvi V-M, Salmi J, Tukiainen A, Laukkanen P and Guina M 2014 Composition dependent growth dynamics in molecular beam epitaxy of GaInNAs solar cells *Sol. Energy Mater. Sol. Cells* **124** 150–8

[258] Miyoshi M, Tsutsumi T, Kabata T, Mori T and Egawa T 2017 Effect of well layer thickness on quantum and energy conversion efficiencies for InGaN/GaN multiple quantum well solar cells *Solid-State Electron.* **129** 29–34

[259] Mukhtarova A, Valdueza-Felip S, Durand C, Pan Q, Grenet L, Peyrade D, Bougerol C, Chikhaoui W, Monroy E and Eymery J 2013 InGaN/GaN multiple-quantum well heterostructures for solar cells grown by MOVPE: case studies *Phys. Status Solidi* c **10** 350–4

[260] Irvine S, Barrioz V, Lamb D, Jones E and Rowlands-Jones R 2008 MOCVD of thin film photovoltaic solar cells—next-generation production technology? *J. Cryst. Growth* **310** 5198–203

[261] Schmieder K J, Yakes M K, Bailey C G, Pulwin Z, Lumb M P, Hirst L C, Gonzalez M, Hubbard S M, Ebert C and Walters R J 2014 Analysis of gaas solar cells at high mocvd growth rates *2014 IEEE 40th Photovoltaic Specialist Conf. (PVSC)* pp 2130–3

[262] Miyoshi M, Ohta M, Mori T and Egawa T 2018 A comparative study of InGaN/GaN multiple-quantum-well solar cells grown on sapphire and AlN template by metalorganic chemical vapor deposition *Phys. Status Solidi* a **215** 1700323

[263] Schulte K L, Simon J, Young M R and Ptak A J 2018 Improvement of short-circuit current density in GaInP solar cells grown by dynamic hydride vapor phase epitaxy *IEEE J. Photovolt.* **8** 1616–20

[264] Simon J, Schulte K L, Young D L, Haegel N M and Ptak A J 2016 GaAs solar cells grown by hydride vapor-phase epitaxy and the development of GaInP cladding layers *IEEE J. Photovolt.* **6** 191–5

[265] Simon J, Schulte K L, Jain N, Johnston S, Young M, Young M R, Young D L and Ptak A J 2016 Upright and inverted single-junction GaAs solar cells grown by hydride vapor phase epitaxy *IEEE J. Photovolt.* **7** 157–61

[266] Supplie O *et al* 2018 Metalorganic vapor phase epitaxy of III–V-on-silicon: experiment and theory *Prog. Cryst. Growth Charact. Mater.* **64** 103–32

[267] Irvine S and Capper P 2019 *Metalorganic Vapor Phase Epitaxy (MOVPE): Growth, Materials Properties, and Applications* (Wiley) (https://doi.org/10.1002/9781119313021)

[268] Magnanini R, Tarricone L, Parisini A, Longo M and Gombia E 2008 Investigation of GaAs/InGaP superlattices for quantum well solar cells *Thin Solid Films* **516** 6734–8

[269] Kalyuzhnyy N A *et al* 2016 Increasing the quantum efficiency of InAs/GaAs QD arrays for solar cells grown by MOVPE without using strain-balance technology *Prog. Photovolt.* **24** 1261–71

[270] Mitzi D B, Gunawan O, Todorov T K, Wang K and Guha S 2011 The path towards a high-performance solution-processed kesterite solar cell *Sol. Energy Mater. Sol. Cells* **95** 1421–36

[271] Arul N S, Yun D Y, Lee D U and Kim T W 2013 Strong quantum confinement effects in kesterite Cu_2ZnSnS_4 nanospheres for organic optoelectronic cells *Nanoscale* **5** 11940–3

[272] Courel M 2019 An approach towards the promotion of Kesterite solar cell efficiency: the use of nanostructures *Appl. Phys. Lett.* **115** 123901

[273] Sravani L, Routray S and Pradhan K 2020 Toward quantum efficiency enhancement of kesterite nanostructured absorber: a prospective of carrier quantization effect *Appl. Phys. Lett.* **117** 133901

[274] Sahoo G S, Routray S, Pradhan K and Mishra G 2021 Electrical, optical, and reliability. Analysis of QD-embedded kesterite solar cell *IEEE Trans. Electron Devices* **68** 5518–24

[275] Prabhu S, Pandey S K and Chakrabarti S 2022 Innovative structural engineering of sustainable and environment-friendly Cu_2ZnSnS_4 solar cell for over 20% conversion efficiency *Int. J. Energy Res.* **46** 15300–8

[276] Rodríguez-Osorio K G *et al* 2023 Analytical modeling and optimization of $Cu_2ZnSn(S,Se)_4$ solar cells with the use of quantum wells under the radiative limit *Nanomaterials* **13** 2058

[277] Xu J, Yang X, Yang Q-D, Wong T-L and Lee C-S 2012 Cu_2ZnSnS_4 hierarchical microspheres as an effective counter electrode material for quantum dot sensitized solar cells *J. Phys. Chem.* C **116** 19718–23

[278] Cao Y, Xiao Y, Jung J-Y, Um H-D, Jee S-W, Choi H M, Bang J H and Lee J-H 2013 Highly electrocatalytic $Cu_2ZnSn(S_{1-x}Se_x)_4$ counter electrodes for quantum-dot-sensitized solar cells *ACS Appl. Mater. Interfaces* **5** 479–84

[279] Gu X, Zhang S, Qiang Y, Zhao Y and Zhu L 2014 Synthesis of Cu_2ZnSnS_4 nanoparticles for applications as counter electrodes of CdS quantum dot-sensitized solar cells *J. Electron. Mater.* **43** 2709–14

[280] Mahajan S, Stathatos E, Huse N, Birajdar R, Kalarakis A and Sharma R 2018 Low cost nanostructure kesterite CZTS thin films for solar cells application *Mater. Lett.* **210** 92–96

[281] He M, Kou D, Zhou W, Zhou Z, Meng Y and Wu S 2019 Se-assisted performance enhancement of $Cu_2ZnSn(S,Se)_4$ quantum-dot sensitized solar cells via a simple yet versatile synthesis *Inorg. Chem.* **58** 13285–92

[282] Das S, Alam I, Raiguru J, Subramanyam B and Mahanandia P 2019 A facile method to synthesize CZTS quantum dots for solar cell applications *Physica* E **105** 19–24

[283] Das S, Sa K, Alam I and Mahanandia P 2019 Enhancement of photocurrent in Cu_2ZnSnS_4 quantum dot-anchored multi-walled carbon nanotube for solar cell application *J. Mater. Sci.* **54** 8542–55

[284] Zhou Z-J, Deng Y-Q, Zhang P-P, Kou D-X, Zhou W-H, Meng Y-N, Yuan S-J and Wu S-X 2019 Cu_2ZnSnS_4 quantum dots as hole transport material for enhanced charge extraction and stability in all-inorganic $CsPbBr_3$ perovskite solar cells *Sol. RRL* **3** 1800354

[285] Das S, Mahakul P C and Mahanandia P 2020 High efficient hybrid bulk hetero junction thin-film solar cell embedded with kesterite Cu_2ZnSnS_4 quantum dots *Superlattices Microstruct.* **148** 106719

[286] Das S and Mahanandia P 2022 Improved PCE of solution processed kesterite Ag_2ZnSnS_4 quantum dot photovoltaic cell *Mater. Chem. Phys.* **281** 125878

[287] Das S, Alam I and Mahanandia P 2022 Cu_2ZnSnS_4 QDs anchored 2-D few-layer graphene bridge enhanced photo

induced charge carrier transport behavior for high efficient kesterite photovoltaic cell *Opt. Mater.* **132** 112775
[288] Palanisamy C, Routray S and Palaniswamy S 2023 Diversity analysis of defect distribution and carriers quantization in Cu_2ZnSnS_4/$Cu_2ZnSn(S,Se)_4$ kesterite quantum well solar cell *ECS J. Solid State Sci. Technol.* **12** 055009
[289] Chandrasekar P, Routray S, Palaniswamy S and Massoud Y 2023 Environmentally benign nanostructured kesterite binate quantum dot well (BQDW) solar cell: a proposal towards high efficiency *IEEE Trans. Nanotechnol.* **22** 473–80
[290] Chris A B, Routray S and Massoud Y 2023 Nanostructure-based CZGS/CZGSe multiple quantum wells could sense wider solar spectrum to enhance light-harvesting efficiency *IEEE Sens. J.* **23** 18125–32
[291] Giraldo S *et al* 2019 Study and optimization of alternative MBE-deposited metallic precursors for highly efficient kesterite CZTSe:Ge solar cells *Prog. Photovolt., Res. Appl.* **27** 779–88
[292] Cure Y, Pouget S, Reita V and Boukari H 2017 $Cu_2ZnSnSe_4$ thin films grown by molecular beam epitaxy *Scr. Mater.* **130** 200–4
[293] Song N, Young M, Liu F, Erslev P, Wilson S, Harvey S P, Teeter G, Huang Y, Hao X and Green M A 2015 Epitaxial Cu_2ZnSnS_4 thin film on Si (111) 4° substrate *Appl. Phys. Lett.* **106** 252102
[294] Harvey S P, Perkins C, Young M, Moutinho H, Wilson S and Teeter G Heteroepitaxial growth of CZTS *2014 IEEE 40th Photovoltaic Specialist Conf. (PVSC)* (https://doi.org/10.1109/PVSC.2014.6925396)
[295] Harvey S P, Wilson S, Moutinho H, Norman A G and Teeter G 2017 Low-temperature surface preparation and epitaxial growth of ZnS and Cu_2ZnSnS_4 on ZnS(1 1 0) and GaP(1 0 0) *J. Cryst. Growth* **478** 89–95
[296] Shimamune Y, Jimbo K, Nishida G, Murayama M, Takeuchi A and Katagiri H 2018 Effect of annealing in sulfur flux on Cu_2ZnSnS_4 formation by using molecular beam epitaxy system *Jpn. J. Appl. Phys.* **57** 08RC10
[297] Nishida G, Murayama M, Takeuchi A, Shimamune Y, Jimbo K and Katagiri H 2018 Suppression of $Cu_{2-x}S$ formation in Cu_2ZnSnS_4 by tin incorporation using molecular beam epitaxy system *Jpn. J. Appl. Phys.* **57** 08RC03